Helwan University
Faculty of Engineering
Civil Engineering Department
Mattaria-Cairo

**HELWAN
UNIVERSITY**

"Shear Behaviour OF High Strength R.C. Beams With Fibers Added TO Concrete Mix."

A Thesis

Submitted to the Faculty of Engineering Helwan University for the
Fulfillment of the Requirement of M.Sc. Degree in Civil Engineering

Prepared by

Eng. Ahmed Mahmoud Yosri Ahmed
B.Sc. in Civil Engineering,

Supervisors

Asc.Prof. Dr. Nasr Zenhom,
Asc.Professor of concrete structures
Faculty of Engineering, EL-Mattaria, Helwan University

Asc. Prof Dr. Mostafa Abd- Elmegied
Asc. Prof of concrete structures
Faculty of Engineering, EL-Mattaria,
Helwan University.

Asc. Prof Dr. Ata El-Kareim Shoaib
Asc.Prof of concrete structures
Faculty of Engineering- EL-Mattaria,
Helwan University.

2014

ABSTRACT

The objective of this thesis is to investigate experimentally the behavior of high strength steel fiber reinforced concrete beams in shear, for predicting the shear strengths of these structural members.

In the experimental program, the volume fraction of fiber and the shear span to depth ratio of the specimens are considered in order to determine the effect of these variables on the specimen strength.

The studied parameters included volume fraction of fibers (0, 0.25%, 0.5%, and 0.75%) by weight, and shear span to depth ratios (1.5, 1.7, and 2.2). The elastic behavior of tested beams at flexural zone was also investigated.

Experimental results indicated that the shear strength of tested beams was significantly increased as the volume fraction of steel fibers increased. The number of the cracks increased by using discrete steel fibers and became finer. Moreover, the crack propagation and modes of failure may be changed by using discrete steel fibers. Finally, the discrete steel fibers increase ductility and failure loads of the tested beams.

Experimental results indicated also that the shear strength of tested beams was significantly increased as the shear span to depth ratio decreased.

Modification of an existing formula, proposed for the prediction of beam shear strengths, and the incorporation of a term to account for the contribution from the fibers to the specimen strength, yielded results which correspond very closely to those obtained experimentally and in other research programs.

ACKNOWLEDGMENT

I would like to thank ALLAH for blessings that ALLAH granted to me all the way till I finished this research, and all through my life.

I want to express this profound gratitude and deep appreciation to the supervisors and thank them for great effort for solving all problems during the research and for direct supervision and valuable advice and encouragement during the course.

In addition, I would like to my friends and consulting engineering laboratories officials for their help and advice during this research. Finally,I make all the meanings of love, gratitude and appreciation to my family (my Father, my mother, my sister and my brother) their love and encouragement me and whatever I do for them not fulfilled their right and all what I hope is a pleasing ALLAH then my father and mother.

CONTENTS

CHAPTER 1: INTRODUCTION

CHAPTER 2: LITERATURE REVIEW

CHAPTER 3: EXPERIMENTAL PROGRAM

CHAPTER 4: TEST RESULTS AND ANALYSIS

CHAPTER 5: THEORETICAL ANALYSIS

CHAPTER6: SUMMARY, CONCLUSIONS, AND RECOMMENDATIONS

LIST OF TABLES

CHAPTER 2: LITERATURE REVIEW

CHAPTER 3: EXPERIMENTAL PROGRAM

CHAPTER 4: TEST RESULTS AND ANALYSIS

CHAPTER 5: THEORETICAL ANALYSIS

LIST OF FIGURES

CHAPTER 2: LITERATURE REVIEW

CHAPTER 3: EXPERIMENTAL PROGRAM

CHAPTER 4: TEST RESULTS AND ANALYSIS

Chapter One

INTRODUCTION

1.1 General Overview

The constructions of ever longer span bridges, taller buildings, deeper offshore structures, and other mega-structures are calling for construction materials with increasingly improved properties particularly strength, stiffness, toughness, ductility, and durability. In some instances, simultaneous improvement in a combination of properties will needed. Such properties are composite parts of what are often called high performance materials or advanced materials to differ ate them from the conventional.

The use of high performance materials, when considered as an alternative in design, is generally not necessary throughout the structure. In most cases, only a small part of the structure may be affected. Some examples include the beam-column connections in earthquake resistant frames, selected plastic hinge or fuse locations in seismic structures, the lower sections of shear walls or the lower columns in high rise buildings, the disturbed regions near the anchorages at the end of prestressed concrete girders, the high bending and punching shear zones around columns in two-way slab systems, tie-back anchors, and numerous structural members subjected to combined loadings.

Examples where advanced materials were used to improve structural performance are abundant, particularly in aerospace applications. In Civil Engineering, the most prominent example is the use of high strength concrete in the columns of high-rise buildings and in offshore structures. Different building structures, such as beamless reinforced concrete slabs, footings of

foundation, shear in beams, have a brittle failure mode and versatile complex stress behavior. This failure occurs when tensile strength exceeds limit values.

This failure is usually very sudden due to brittle behavior of plain concrete in tension.

High-strength concrete generally has the advantages, over normal strength concrete, of providing:

1. Increased stiffness,
2. Reduced axial shortening of members and therefore reduced problems concerning.
3. The maintenance of horizontally supported surfaces.
4. Construction time saving, as strength development occurs at an early age.
5. Possibility of creating new types of structural supporting systems-an area that requires further research, economic advantages - the ability to remove formwork rapidly, the increased availability of floor area as member sizes can be reduced and decreased foundation costs as the overall weight of the structure can be reduced.

Other advantages, such as reduced prestressing losses (due to a reduced coefficient of creep) and a reduction in the quantity of reinforcement required, can also be incurred. It should be noted that the properties of core samples, removed from structural members after seven years of service, have indicated that the properties of **HSC** remain excellent over time.

1.2 Objectives and Scope of the Research Program

The main objectives of this research are to:

1. Study the behavior of high strength reinforced concrete mixed with discrete steel fiber in shear.
2. Study the mode of failure and cracks patterns with different parameters.

3. Study the effect of span to depth ratio on shear strength of H.S.C beams with discrete steel fiber.

4. Discussion and analysis of experimental results.

Scope of the research program:

In order to satisfy these objectives, it is necessary to divide the research into an experimental and a theoretical program.

The aims of the experimental program are to investigate the influence on the shear behavior of **H.S.R.C** beams when the following properties are varied:

1. The volume fraction of fibers (V_f).

2. The shear span to depth ratio (a/d).

The experimental program allows for an effective investigation of some of the factors influencing the shear strength of these specimens. In the theoretical program, the results of these experiments, will be applied to try to obtain a predictive equation will enable the shear strength of steel fiber reinforced HSC beams to be quantified successfully.

1.3 Organization of thesis

This thesis divides into six main sections:

Chapter 2 provides a brief review and discussion of the literature associated with this field of study,

Chapter 3 outlines the experimental program,

Chapter 4 provides the observations and results from this program, and contains a discussion of the results (Result's analysis),

Chapter 5 theoretical study,

Chapter 6 summaries the overall conclusions of this study.

Chapter Two

LITRATURE REVIEW

2.1 Introduction

This Chapter mainly addresses the issues in the shear of high strength concrete. The Chapter starts with the definition of HSC, its historical development and extensive use across the world, the shear strength of high strength concrete beams has been explained on the basis of experimental research and empirical relationship developed by different researchers in last two decades. Then definition of high strength fiber reinforced concrete (HSFRC), its historical development, and the shear strength of (HSFRC) using steel fiber will be discussed. lastly, the Provisions of international building codes for the shear design of high strength steel fiber reinforced concrete have been presented.

2.2 High Strength Concrete

The definition of High Strength Concrete (HSC) has been changing with time due to advancement in the concrete and material technology.

At times the compressive strength of 40 MPa was considered as high strength, however with improved mixed design, ultra high range water reducers (Super-plasticizers), and mineral admixtures, concretes with compressive strength above 100 MPa are easily obtained in the field**. (ACI-318 committee) [1]** Revealed that in the 1960's, 52 MPa (7500 psi) concrete was considered high-strength concrete and in the 1970's, 62 MPa (9000psi) concrete was considered as HSC.

The committee also recognized that the definition of the high-strength concrete varies on a geographical basis. In regions where 62 MPa (9000 psi)

concrete is already being produced commercially, high-strength concrete might be in the range of 83 to 103 MPa (12,000 to 15,000psi).

The High Strength Concrete has been successfully used in the construction of prestressed bridges in the world such as Braker Lane Bridge, built in Austin, Texas, USA in 1990, with concrete strengths ranging from 75.8 MPa to 96.5 MPa at 28 days. The Red River Cable-Stayed Bridge Guangxi, China (65 MPa), Normandy Bridge, France (60 MPa) and Portneuf Bridge Quebec, Canada (60 MPa) **[Bickley and Mitechlles, 2001] [2].**

Applications of high strength concrete:

- To put the concrete into service at much earlier age, for example opening the pavement at 3-days.
- To build high-rise buildings by reducing column sizes and increasing available space.
- To build the super structures of long-span bridges and to enhance the durability of bridge decks.
- To satisfy the specific needs of special applications such as durability, modulus of elasticity, and flexural strength. Some of these applications include dams, grandstand roofs, marine foundation parking garages, and heavy-duty industrial floors.

High-strength concrete is often used in structures not because of its strength, but because of other engineering properties that come with higher strength, such as increased static modulus of elasticity (stiffness), decreased permeability to injurious materials, or high abrasion resistance.

In bridge structures, high-strength concrete is used to achieve one or a combination of the following mechanical attributes:

- increase span length
- increase girder spacing
- Decrease section depth.

The decreased permeability of high-strength concrete presents opportunities for improving durability and increasing service life.

The use of lightweight high-strength concrete provided the advantages of reduced weight and increased strength **(Zia et al., 1997)** [3]**.**

2.3 Shear Strength of R.C Beams

The shear stress acts parallel or tangential to the section of a material. When a simple beam is subjected to bending, the fibers above the neutral axis are in compression and the fibers located below the neutral axis are in tension.

A concrete beam with longitudinal steel when subjected to external loads will develop diagonal tensile stresses, which will tend to produce cracks.

These cracks are vertical at the centre of the span and will become inclined as they reach the support of the beam. The stress that causes the inclined cracks in the beam is called diagonal tension stresses **(Jose M.A, 2002)** [4].

The shear stress (v*)* in a homogenous elastic beam is given as:

$$v = \frac{V.Q}{I.b}$$

Where, V = Shear force at section under consideration.

Q = Static moment about the neutral axis of that portion of cross section lying between a line through point in question parallel to neutral axis and nearest face of the beam.

I = Moment of Inertia of the cross section about neutral axis.

b = Width of the beam at a given point.

(Hennebique and Ritter) at the end of the 19th century [5] were the pioneers in the study of stirrups and shear. **In 1964 (kepfer,H) [6] stated** the simple or multiple truss system model where the concrete is the compressed strut and stirrups or bent-up bars are the tensile member.

Later (**Kupfer, 1964**) **[6]** proposed a variable strut inclination (even smaller than 45 degrees within following limits: 0.25< tgα <1.00with α = inclination of the compressive strut to the axis of the member).

Moreover, (**Collins and Vecchio**) **in 1986[7]** developed the modified compression field theory for reinforced concrete elements. Nowadays, fibers are working to find the best procedure for shear design based on earlier experiences with MC78, MC90 as well as MC2010.

The majority of the analytical models, introduced here before, have to be re-arranged when steel fibers are added in concrete matrix, because they considerably influence shear behavior as well as the shear capacity.

At any rate, along these decades, year by year, different experiments done by researchers all over the word, have tried to predict the shear capacity of members with and without transverse reinforcement.

2.4 Mode of Failures of Concrete Beams in Shear

Various failure modes in RC beams are shown in Figure 2.1.a in the region of flexural failure, cracks are mainly vertical in the middle third of the beam span and perpendicular to the lines of principal stress. These cracks result from a very small shear stress *v* and a dominant flexural stress *f, which* results in an almost horizontal principal stress *ft (max).*

Diagonal tension failure happens, if the strength of the beam in diagonal tension is lower than its strength in flexure. The shear span-to-depth ratio is of intermediate magnitude for diagonal failure, varying between 2.5 and 5.5 for the case of concentrated loading.

Such beams can be considered of intermediate slenderness. Cracking starts with the development of a few fine vertical flexural cracks at mid span, followed by the destruction of the bond between the reinforcing steel and the surrounding concrete at the support. Thereafter, without ample warning of impending failure, two or three diagonal cracks develop at about 1½d to 2*d* distance from the face of the support in the case of reinforced concrete beams,

and usually at about a quarter of the span in the case of pre-stressed concrete beams. As they stabilize, one of the diagonal cracks widens into a principal diagonal tension crack and extends to the top compression fibers of the beam, as seen in Figure 2.1.b **(Jose,2000) [8].**

In beams having shear span to depth ratio less than 2.5, a few fine flexural cracks start to develop at mid span and stop propagating as destruction of the bond occurs between the longitudinal bars and the surrounding concrete at the support region.

Thereafter, an inclined crack steeper than in the diagonal tension case suddenly develops and proceeds to propagate toward the neutral axis. The rate of its progress is reduced with the crushing of the concrete in the top compression fibers and a redistribution of stresses within the top region occurs. Sudden failure takes place as the principal inclined crack dynamically joins the crushed concrete zone, as illustrated in Figure 2.1.c. This type of failure can be considered relatively less brittle than the diagonal tension failure due to the stress redistribution. Yet it is, in fact, a brittle type of failure with limited warning, and such as design should be avoided completely. This failure is often called as compression failure or web shear failure.
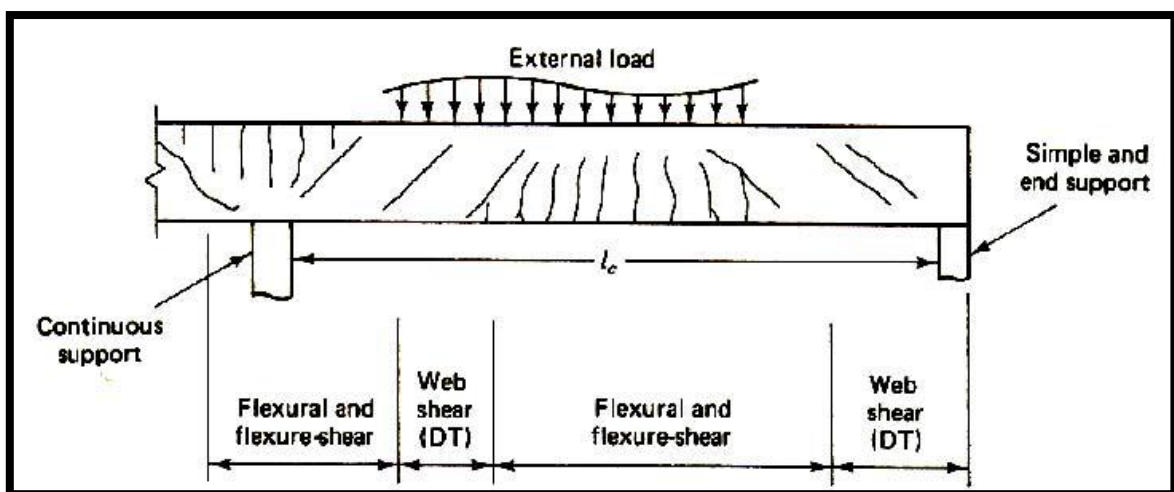
Fig (2.1.a).
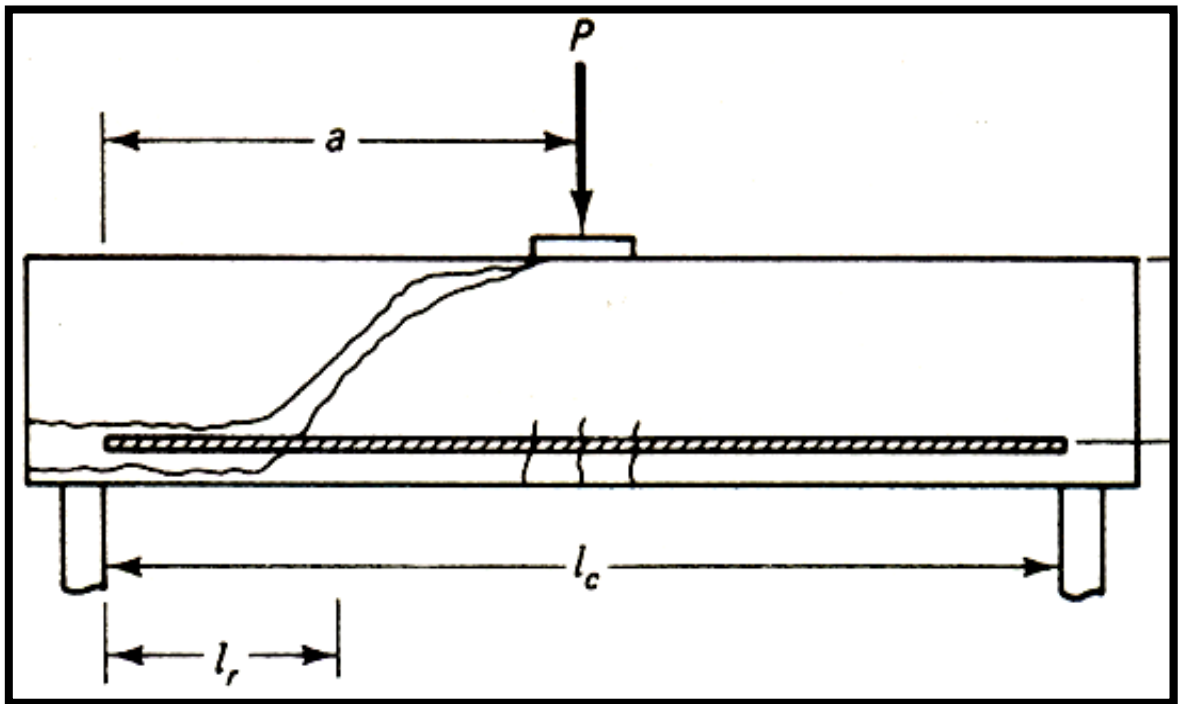
Fig (2.1.b).
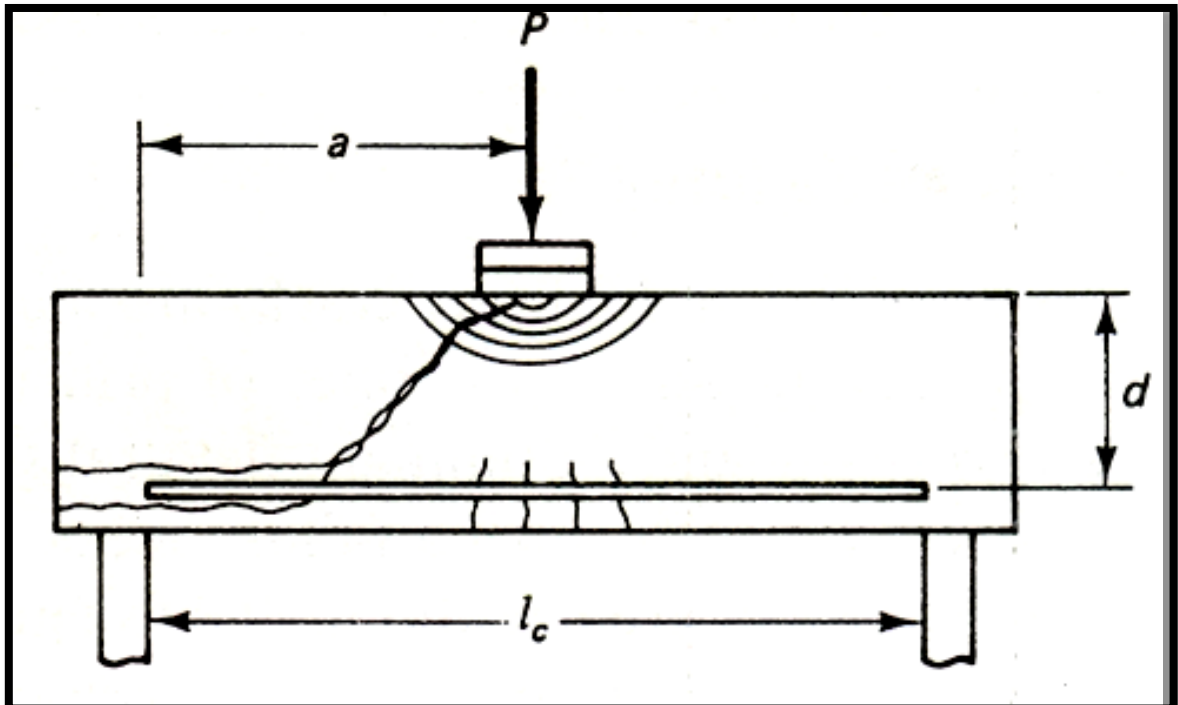
Fig (2.1.c).

Figure 2.1 Types of cracks expected in the reinforced concrete beams (Jose, 2000).

   The joint committee ASCE-ACI-426 in 1973 and later in 1998[9] reported the following five mechanisms for resisting the shear in reinforced concrete sections **(NCHRB, 2005) [10];**

1. Shear in the un-cracked concrete zone in cracked concrete member:

   The un-cracked compression zone offers some resistance to the shearbut for slender beams with no axial force; this part is very negligible due to small depth of compression zone.

2. Residual tensile stresses:

   When concrete is cracked and loaded in uni-axial tension, it can transmit tensile stresses until crack widths reach 0.06 mm to 0.16 mm, which adds to the shear capacity of the concrete.

   When the crack opening is small, the resistance provided by residual tensile stresses is significant. However, in a large member, the contribution of crack tip tensile stresses to shear resistance is less significant due to the large crack widths that occur before failure in such members.

3. Interface shear transfer:

   The contribution of interface shear transfer to shear strength is a function of the crack width and aggregate size. Thus, the magnitude decreases as the crack width increases and as the aggregate size decreases.

   Consequently, this component is also called "aggregate -interlock" denoted by V_a. However, it is now considered more appropriate to use the terminology "interface shear transfer "or "friction".

4. Dowel action:

   When a crack forms across longitudinal bars, the dowelling action V_d, of the longitudinal bars provides a resisting shear force, which depends on the amount of concrete cover beneath the longitudinal bars and the

degree to which vertical displacements of those bars at the inclined crack are restrained by transverse reinforcement.

5. Shear reinforcement:

This forms the main part of the shear capacity of the beams wit web reinforcement and is typically modeled with 45-degree truss model.

For beams with transverse reinforcement, the basic model to explain the mechanism for carrying the shear was proposed by **Ritter (1899) [11].**

The load was assumed to flow down the concrete diagonal struts and then lifted to the compression chord by transverse tension ties on its way to support

2.5 Factors Affecting Shear Strength of Concrete Beams

One of the major reasons for limited understanding of the shear behavior and diagonal failure of the RC beams is greater number of parameters involved in the problem**. Kani (1967) [12]** identified the following parameters affecting the diagonal cracking of RC beams.

1. Grade of steel (tensile strength of longitudinal steel).
2. Compressive strength of Concrete.
3. Cross section and shape of beams (web width, depth etc.)
4. Shear arm or shear span.
5. Types, arrangements, quantity and location of web reinforcement
6. Types of loadings.
7. Types of beams supports (Simply supported or continuous).
8. Pre-stress forces and its point of application etc.

The shear of high strength concrete RC structure is comprised of two main parts:

1. (V_c) The nominal concrete contribution includes, in an undefined way, the contributions of the still un-cracked concrete at the head of a hypothetical diagonal crack, the resistance provided by aggregate

interlock along the diagonal crack face, and the dowel resistance provided by the main reinforcing steel.

2. (*Vs*): The shear resistance provided by the stirrups.

In high strength concrete, the diagonal tension cracks are expected to have smooth plane, due to very high strength of concrete matrix. This leads to crushing of aggregates and as result, the aggregate interlocking is not playing significant role in resisting the shear.

There is a consensus amongst the researchers, that the aggregates interlocking decreases, when the compressive strength of RC concrete increases, due to peculiar failure of the HSC (**Cladera and Mari, 2005**) **[13].** The decrease of aggregates interlocking may lead to reduction in the shear strength of HSC.

The research of (**Ahmed *et al.* 1986**) [14] have shown that the current design methods are not conservative for HSC particularly for larger shear to depth ratio (Slender beams a/d >3.0) and relatively low longitudinal steel ratio.

(**Duthin and Carino 1996**) **[15]** Further pointed out that most of the current shear design techniques either do not acknowledge the loss in the aggregate interlock mechanism in high strength concrete or simply do not account for the influence of adding shear reinforcement to other shear transfer mechanisms.

(**Johnson and Ramirez 1989**) **[16]**, reported that for a constant low shear reinforcement, the overall reserve shear strength after diagonal cracking diminishes with increase in the compressive strength of concrete.

They further proposed the following expression for the shear strength of HSRC beams with transverse reinforcement.

$$\boldsymbol{v_{uc}} = \boldsymbol{\xi} \{ \, \mathbf{0.97} \, \boldsymbol{\rho}^{\mathbf{0.46}}. \boldsymbol{fc}^{\frac{1}{2}} + \mathbf{0.2} \, \boldsymbol{\rho}^{\mathbf{0.91}}. \boldsymbol{fc}'^{\mathbf{0.38}} . \left(\frac{\boldsymbol{a}}{\boldsymbol{d}}\right)^{-\mathbf{2.33}} + \{ \mathbf{1.75} \, \boldsymbol{I_b} \, \boldsymbol{\rho_v} \boldsymbol{f_{yv}} \}$$

ρ_v: Steel ratio of web reinforcement.

f_{yv}: Yield stress of web reinforcement.

The factor I_b is given by the equation:

$$I_b = \frac{0.97\,\rho^{0.46}\,fc\prime^{1/2}}{0.97\,\rho^{0.46}\,fc\prime^{1/2} + 0.2\,\rho^{0.91}\,fc\prime^{0.38}\,.(a/d)^{-2.33}}$$

To check whether the shear failure is due to beam action or arch action, the author further proposed a critical value as

$$(a/d)_c = 0.57\,\frac{\rho^{0.19}\,f_{y1}^{0.41}}{f_c^{\prime\,0.05}}$$

Hence $I_b = 0.57$ which means that for

      1). a/d < (a/d)c I_b<0.57, arch action prevails.

      2). a/d > (a/d)c I_b>0.57, beam action prevails.

They also proposed an expression for minimum web reinforcement of HSRC beams to avoid brittle failure of the beams, which is given as follows;

$$A_{wmin} = \frac{f_{ctm}}{7.5}\,\frac{b_w\,s}{f_y}\ \textbf{Mpa}$$

Here, f_{ctm} stands for tensile strength of HSC, which is given as;

$$\boldsymbol{f_{ctm} = 0.3\,\sqrt[3]{f_c^2}}\ \textbf{Mpa if}\, fc < 60\ MPa$$

fc is specified compressive strength of concrete.

$$\boldsymbol{f_{ctm} = 0.58\,\sqrt[2]{f_c}}\ \ \textbf{MPa if}\, fc > 60\ MPa$$

They also concluded that the limitation of 2% longitudinal steel for HSRC beams with web reinforcement is also not justified.

2.6 Fiber Reinforced Concrete

Is a concrete containing dispersed fibers, the concept of discrete reinforcement finds its root in 1874 when A. Berard patented it for the first time (**Balaguru et al., 1992**) [17]. Compared to the conventional reinforcement, the fibre reinforcement is:

- Distributed throughout across section (whereas bars are only   place where needed).

- Relatively short and closely spaced (while bars are continuous and not as closely spaced).

- Not comparable, in term of area, to the one of the bars.

As stated before, the addition of fibers to plain concrete totally changes the post-cracking behavior leading to a softening branch after the peak load.

Moreover, the fibers bridging the cracks contribute to increase the strength, the failure strain and the toughness of the composite.

The toughness is significantly increased obtaining, thus, a versatile construction material but fiber reinforced concrete becomes more and more attractive when it is able to totally replace transversal reinforcements that are one of the more labor-cost activities necessary for concrete structures. This technology also improves the durability of concrete structures.

The fiber reinforced concrete is not a recent concept, but, due to the lack of national and international standards, it is not used in significant structural applications.

Nowadays it is mainly used in non-structural elements like:

- Slabs and pavements in which fibers are added as secondary reinforcement and with the aim of withstanding the crack induced by the humidity and the temperature variation (crack for which the conventional reinforcement is not effective);

- Tunnel linings, precast piles (that have to be hammered in the ground), and blast resistance structures that have to carry high load or deformation;

- Thin sheets or elements with complicated shape where the conventional reinforcement cannot be used and, in any case, due to the thin concrete cover, it will be difficult to preserve from corrosion.

In most of the applications, the function of the fibers does not consist into increasing the strength (although an increase of tensile strength is consequence) but just to control and delay both widening cracks and the behavior of the concrete after the crack of the matrix. In a simple view, the elements involved in the system FRC are three: the concrete, the bond and the fibers.

The moderate addition of fibers has no effect on the mechanical material properties of plain concrete before cracking unless the fiber dosage exceeds around 80 kg/m3 **(Technical Report No. 63) [18].** In consequence, the addition of fibers does not change the compression strength after 28 days that is the main characteristic used to classify concrete.

However, fiber addition causes a less brittle failure; this is due to the fact that compression failure of concrete is related to its tension failure, since tensile stresses cause growth of the pre-existing micro cracks in the concrete (and tanks to the fiber bridging the stresses continue to increase).

2.6.1 Length of Fibers

The fiber lengthl_f, is the distance between the outer ends of the fiber. The developed length of the fiberl_d, is the length of the axis line of the fiber. The length of the fiber should be measured according to specific reference codes.

2.6.2 Equivalent Diameter

The equivalent diameter, d_f, is the diameter of a circle with an area equal to the mean cross sectional area of the fiber.

- For circular cross sections with a diameter greater than 0.3 mm, the equivalent diameter of the fiber shall be measured with a micrometer, in two directions, approximately at right angles, with accuracy in accordance to specific reference codes. The equivalent diameter is given by the mean value of the two diameters.

- For fibers with a diameter less than 0.3 mm, the diameter shall be measured with optical devices, with accuracy in accordance to specific reference codes.

- For elliptical sections, the equivalent diameter shall be evaluated starting from the measuring of the two axes, using a micrometer with accuracy in accordance to specific reference codes. The equivalent diameter is given by the mean length of the two axes.

- For rectangular sections, the width, b_f, and the thickness, h_f, shall be measured in accordance to specific reference codes. The equivalent diameter is given by:

$$df = \sqrt{\frac{4.bf.hf}{\pi}}$$

- Alternatively, and in particular for fibers with irregular sections, the equivalent diameter can be evaluated with the following formula:

$$df = \sqrt{\frac{4.m}{\pi.ld.\rho f}}$$

Being *m* the mass, *l*d the developed length and ρ_f the fiber density.

Nevertheless, the addition of fibers changes the consistence. The mutation depends upon the aspect ratio of the fibers that is defined as the ratio of its length *l*f to its diameter d_f (when cross section is not circular, diameter is substituted by equivalent diameter).

It is physically difficult to include fibers with an aspect ratio of more than 50 because concrete contains about 70 % by volume of aggregate particles, which, obviously, cannot be penetrated by fibers.

Longer fibers of smaller diameter will be more efficient in the hardened FRC, but will make the fresh FRC more difficult to cast. This explains why the

mix design of FRC often requires additives for obtaining the consistence needed.

Another important factor that could not be ignored is the maximum aggregate size; every time that a concrete matrix is designed, particular attention should be paid to the determination of this parameter that influences the phenomenon of interlock.

The bond between the matrix and the fibers influences the performances of the FRC. The value of the bond strength for a straight round steel fiber rarely exceeds four MPa, but, with mechanical deformation of the fiber or devices (anchors), the bond slip can be avoided during the fiber failure.

It is difficult to predict the behavior of the fiber; this is because it depends on both fiber shape and concrete strength. Therefore it is not possible to give a generalized "bond strength" which could be used in numerical calculations. The only certainty in the fiber behavior is that the fiber bond lies between fiber slip and fiber failure.

2.6.3 Types of Fibers

As shown in Table (2.1), there are many different types of fibers in commerce with different properties. On the whole, steel fibers remain the most used fibers (50 % of total tonnage used), followed by polypropylene (20 %), glass (5 %) and other fibers (25 %) **(Benthia, 2008)** [19].

Table (2.1) Properties of Fibers Used As Reinforcement in Concrete (Banthia, 2008).

Fibre type	Tensile strength (MPa)	Tensile modulus (GPa)	Tensile strain (%) min max		Fiber diameter (µm)	Alkali stability (relative)
Asbestos	600÷3600	69÷150	0.1	0.3	0.02÷3	excellent
Carbon	590÷4800	28÷520	1	2	7÷18	excellent
Aramid	2700	62÷130	3	4	11÷12	good
Polypropylene	200÷700	0.5÷9.8	10	15	10÷150	excellent
Polyamide	700÷1000	3.9÷6	10	15	10÷50	-
Polyester	800÷1300	up to 15	8	20	10÷50	-
Rayon	450÷1100	up to 11	7	15	10÷50	fair
Polyvinyl Alcohol	800÷1500	29÷40	6	10	14÷600	good
Polyacrylonitrile	850-1000	17÷18	9	19		good
Polyethylene	400	2÷4	100	400	40	excellent
Polyethylene pulp (oriented)	400	2÷4	100	400	1-20	excellent
High Density Polyethylene	2585	117	2.2	38		excellent
Carbon steel	3000	200	1	2	50÷85	excellent
Stainless steel	3000	200	1	2	50÷85	excellent
AR-Glass	1700	72	2	12÷20		good

The type of fibers to be used depends mainly upon the application of the FRC. Asbestos fibers have been used for a long time in pipes and corrugated or flat roofing sheets. Glass fibers find their application as reinforcing materials in automotive and naval industries or like cladding materials. Vegetable fibers have been used in low cost buildings. Synthetic fibers like polyethylene (PE), polypropylene (PP), acrylics (PAN), polyvinyl acetate (PVA), polyester (PES)

and carbon are incorporated in the cement matrix mainly for reducing plastic shrinkage cracking and for increasing the resistance to fire spalling.

At any rate, the most interesting fibers in the building materials sector are those made out of metal. They improve the toughness and reduce the crack widths. Surely, along the years, thanks to the new technology, their shape is changed and today modern steel fibers have higher slenderness and more geometry that is complex.

2.6.3.1 Steel Fibers

In particular, metallic fibers are made of either carbon steel or stainless steel and their tensile strength varies from 200 to 2600 MPa.

ACI Committee 544 [20]showed that; for conventionally mixed steel fiber reinforced concrete (SFRC), high aspect ratio fibers are more effective in improving the post-peak performance because of their high resistance to pullout from the matrix. A detrimental effect of using high aspect ratio fibers is the potential for balling of the fibers during mixing. Techniques for retaining high pullout resistance while reducing fiber aspect ratio include enlarging or hooking the ends of the fibers, roughening their surface texture, or crimping to produce a wavy rather than straight fiber profile.

The European Standard EN 14889-1:2006 (CEN, 2006) [21]says that steel fibers are straight or deformed pieced of cold-drawn steel wire, straight or deformed cut sheet fibers, melt extracted fibers, shaved cold drawn wire fibers and fibers milled from steel block which are suitable to be homogeneously mixed into concrete or mortar.

Moreover, in that norm, steel fibers are divided into five general groups and are defined in accordance with the basic material used for the production of the fibers according to:

   - Group I, cold-drawn wire;

   - Group II, cut sheet;

   - Group III, melt extracted;

- Group IV, shaved cold drawn wire;

- Group V, milled from blocks.

There are also many other classifications made by other standard bodies that consider different fibers features. The Japanese Society of Civil Engineers (JSCE) has classified steel fibers according to the shape of their cross-section:

- Type 1: Square section;

- Type 2: Circular section;

- Type 3: Crescent section.

ASTM A 820 provides a classification for four general types of steel fibers based upon the product used in their manufacture:

- Type I—Cold-drawn wire;

- Type II—Cut sheet;

- Type III—Melt-extracted;

- Type IV—other fibers.

For steel fibers, three different variables are used for controlling the fibers performance:

1. The aspect ratio;

2. The fiber shape and surface deformation (including anchorages that increase their performance) and

3. The surface treatments (**Lofgren, 2008**) [22].

For fibers, in order to be effective in cementations matrices, it has been found (by both experiments and analytical studies) that they should have the following properties:

(1) A tensile strength significantly higher than the matrix (from two to three orders of magnitude);

 (2) A bond strength with the matrix preferably of the same order as, or higher, than the tensile strength of the matrix;

 (3) An elastic modulus in tension significantly higher than that of the matrix (at least three times) and

(4) Enough ductility so that the fiber does not fracture due to its abrasion or bending.

In addition, the Poisson ratio (ν) and the coefficient of thermal expansion (α) should preferably be of the same order of magnitude for both fiber and matrix (**lofgren, 2008**) [22].

A great variety of fiber shapes and lengths are available depending on the manufacturing process.

The cross-section of an individual fiber could be circular, rectangular, irregular, flat or any substantially polygonal shape.

Mechanical deformation along their length can improve the bond strength producing smooth, indented, deformed, crimped, coiled and twisted fibers. In addition, different shaped ends could improve the bond strength (end paddles, end-buttons, end-hooks or other anchorages).

Steel fibers can also have coatings like zinc (for improving corrosion resistance) or brass (for improving bond characteristics).

Fiber length ranges from 10 to 60 mm with equivalent diameters between 0.5 and 1.2 mm (0.15-0.40 mm thickness and 0.25-0.90 mm in width) and an aspect ratio less than 100 (typically ranging from 40 to 80).

While the straight fiber is only anchored in the matrix by friction and chemical adhesion, all other fibers, which have a deformation along their axis, develop greater bond properties.

In order to utilize the usually high tensile strength of fibers it is important that fibers are well anchored in the concrete matrix.

(**Minelli, 2005**) **[23] Indicated that** crimped fibers show a better workability compared to straight or other forms of fibers for a similar fiber aspect ratio

The orientation and the distribution of fibers are worth mentioning. They play an important role for the mechanical performance of the FRC. Body random orientation is characterized by equi-probable and unlimited (free)

distribution of short fibers throughout the body of the concrete (in three dimensional space). Plane random orientation occurs in thin walled elements (flat sheets, plate, thin walls, etc.).

The smaller the cross-section is, the more restricted the possibilities of free orientation of the fibers and a three dimensional bulk are.

The mechanical behavior must include the orientation of the fiber in order to quantify the fibers bridging the crack. For this purpose, it is common to define the fiber efficiency factor as the efficiency of bridging, in terms of the amount of fibers bridging crack, with respect to orientation effects.

The fiber content in a mixture, when steel fibers are used, usually varies between 0.25 and 2 % by volume, i.e. from 20 to 160 kg/m3. Normally lowest percentage is used in slabs on grade while the upper value is used for structurally more complicated applications.

Nowadays, it is believed that a proper characterization of fibers should be undertaken by considering the post-cracking behavior itself rather than the geometry and the amount of fibers provided in the matrix. In fact, the same amount of fibers in different types of concrete give quite different.
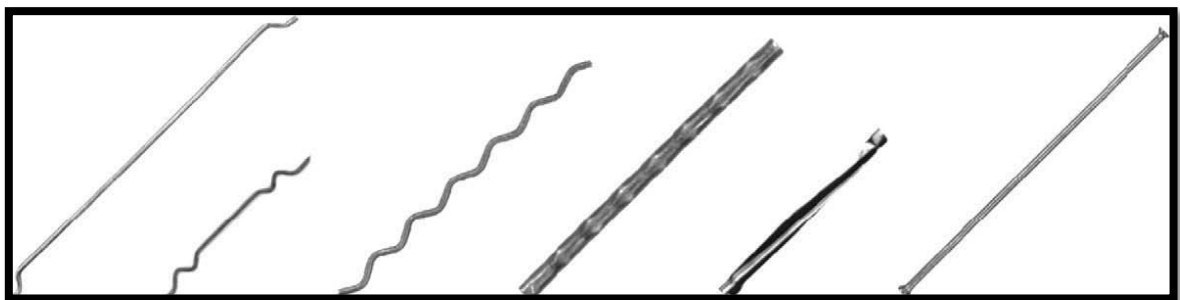
Fig (2.2) Different types of steel fibers.

2.6.3.2 Developing Technology for Steel Fibers:

ACI Committee 544[20] presented that SFRC technology has grown over the last three decades into a mature industry. However, improvements are continually being made by industry to optimize fibers to suit applications.

A current need is to consolidate the available knowledge for SFRC and to incorporate it into applicable design codes.

A developing technology in SFRC is a material called SIFCON (Slurry Infiltrated Fiber Concrete). It is produced by filling an empty mold with loose steel fibers (about 10 percent by volume) and filling the voids with high strength cement- based slurry. The resulting composite exhibits high strength and ductility, with the versatility to be shaped by forms or molds

2.6.3.4 Modes of Failure

When beams are tested under a load up to the failure it is essential to record the mode in which the beam fails observing the crack path and position at failure. The types and formation of cracks depend on both the span-to-depth ratio of the beam and the load.

These variables influence the moment and shear along the length of the beam. For a simply supported beam under uniformly distributed load or concentrated load at the mid-span, without pre-stressing, three types of cracks are identified (**Amlan et al, 2011**) **[24]:**

- Flexural cracks: these cracks are located near the mid-span; they start from the bottom of the section and propagate vertically upwards.

- Web shear cracks: these cracks are located near the neutral axis and close to the support, they propagate inclined to the beam axis.

- Flexure shear cracks: these cracks start at the bottom of the beam due to flexure and propagate inclined due to both flexure and shear.

Beams with low span-to-depth ratio or inadequate shear reinforcement often present a shear failure. A failure due to shear is sudden if compared to a failure due to flexure, cracks are more localized and most of them are located above and along the inclined line joining the support with the point at which the load is applied. The following five modes of failure due to shear are identified:

a) Diagonal tension failure: in this mode, an inclined crack propagates rapidly due to inadequate shear reinforcement.

b) Shear compression failure: there is crushing of the concrete near the compression flange above the tip of the inclined crack.

c) Shear tension failure: due to inadequate anchorage of the longitudinal bars, the diagonal cracks propagate horizontally along the bars.

d) Arch rib failure: for deep beams, the web may buckle and subsequently crush. There can be anchorage failure or failure of the bearing.

e) Web crushing failure: the concrete in the web crushes owing to inadequate web thickness.

The modes are shown through sketches in Figure (2.3).
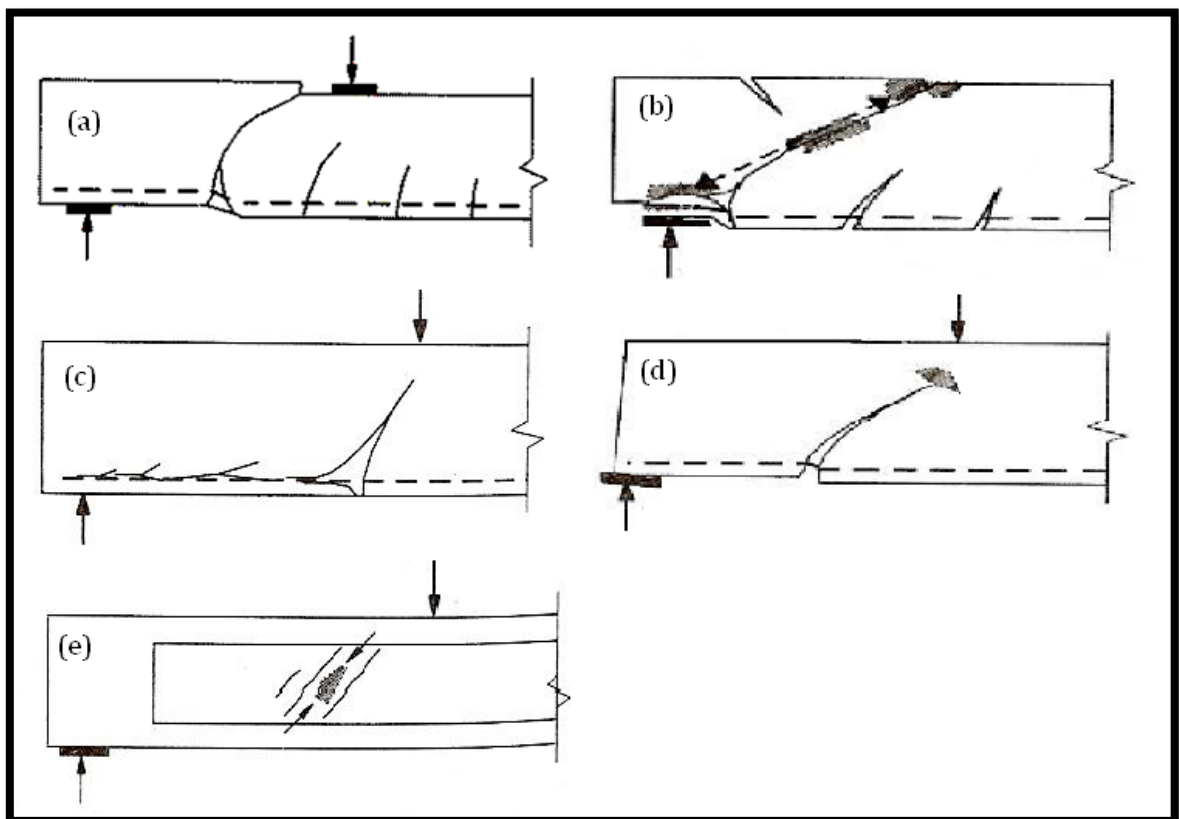
Figure (2.3) Modes of failure: (a) diagonal tension failure, (b) shear compression failure,(c) Shear tension failure, (d) arch rib failure and (e) web crushing failure (Amlan et al,2011*).*

The occurrence of a mode of failure depends on the span-to-depth ratio, loading, cross-section of the beam, amount and anchorage of reinforcement as well as the concrete strength. The flexural failure, opposite to the shear one, is characterized by crack that appear progressively, allowing the beam to reach significant ductility (Figure 2.4)
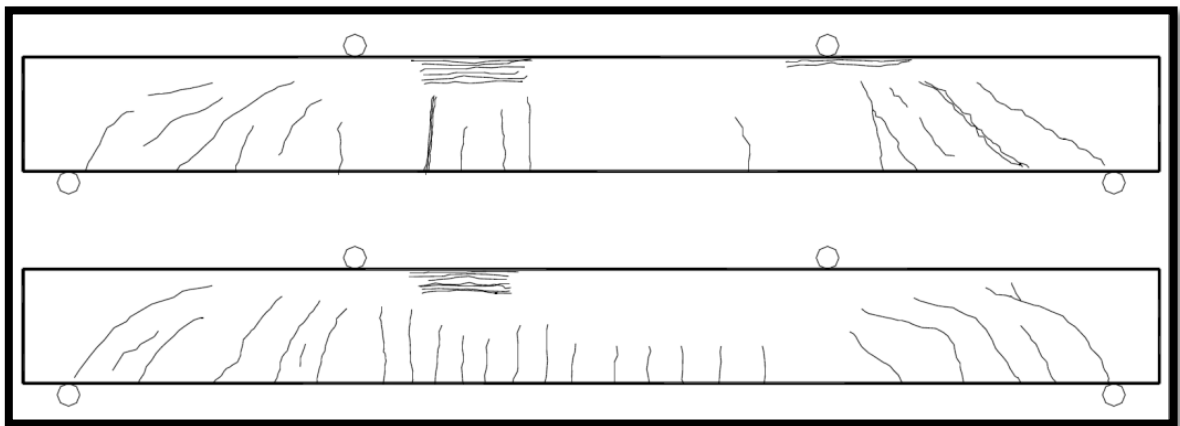
Figure (2.4) Crack patterns at flexural ultimate condition **(Chucchiara et al., 2003) [25]**

2.7 Shear Strength of High Strength Steel Fiber Reinforced Concrete Beams

High strength concrete is a brittle material, and the higher the strength of concrete the lower its ductility. This inverse relation between strength and ductility is a serious drawback for the use of higher-strength concrete, and a compromise between these two characteristics of concrete can be obtained by adding discontinuous steel fibers.

Addition of steel fibers to concrete makes it more homogeneous and isotropic and transforms it from a brittle to a more ductile material.

Steel fibers have some advantages over vertical stirrups or bent-up flexural steel. First, the fiber spacing is much closer than the practical spacing of stirrups, since the former is randomly and more or less uniformly distributed throughout the concrete volume. Secondly, the first crack and the ultimate tensile strength of concrete are increased by the presence of steel fibers.

This results in an increase of the load necessary to produce shear cracking as well as the ultimate shear resistance of the beams. Thirdly, stirrups require a high labor input for cutting, bending and fixing and in thin webs, they can be impractical and difficult to fix. Lastly, in relatively shallow beams, the necessary development length of the stirrups may not be available because of the short distance between the mid-depth and the compression face of the member, and therefore the use of stirrups may not be economical.

The methods recommended in codes of practice for calculating the ultimate shear strength of ordinary beams cannot be used for fiber concrete beams because of the different properties of the plain and fiber concretes.

Considerable amount of experimental data are available on the shear strength of steel fiber mortar and concrete rectangular beams. Predictive equations for shear strength of fiber-reinforced concrete beams have also been suggested by some previous investigators. Some of these equations are generally based on tests of a particular type of steel fiber. The need for a generalized shear strength equation is therefore obvious if steel fibers are to be used in actual structural members.

Sharma (1986) [26] tested seven beams with steel fiber reinforcement, of which 4 also contained stirrups. The fibers had deformed ends. Based on these tests and those by **Batson et al (1972a) and Williamson and Knab (1975) [27],** he proposed the following equation for predicting the average shear stress vd in the SFRC beams. (In the equation that follows, a typographical error in Sharma's 1986 paper has been corrected.)

$$v_{cf} = \frac{2}{3} f'_t \left(\frac{d}{a}\right)^{0.25}$$

where f'_t is the tensile strength of concrete obtained from results of indirect tension tests of 6 x 12 in. (150 x 300 mm) cylinders, and *d/a* is the effective depth to shear- span ratio. Straight, crimped, and deformed-end fibers were included in the analysis and the average ratio of experimental to

calculated shear stress was 1.03 with a mean deviation of 7.6 percent. The influence of different fiber types and quantities is considered through their influence on the parameter f'_t .

The proposed design approach follows the method of ACI 318 for calculating the contribution of stirrups to the shear capacity, to which is added the resisting force of the concrete calculated from the shear stress given by above eq.

J. Son1, B. Beak1, C. Choi2 [28] investigated the behavior of steel fiber reinforced normal strength concrete subjected to predominant shear. This study aims to effect on shear strength, about steel fiber in Ultra High Performance Concrete through experiment, also steel fiber is how to effects at the strength and ductility of Ultra High Performance Concrete. Investigate shear equation of UHPC through comparing previous proposal, how to effects steel fiber on shear strength equation of UHPC.

In this study, steel fiber effect on the shear strength in UHPC. It is difficult estimation of shear strength, common approach in the area of high strength. So, study the impact of each factor what configure UHPC will.

From this investigation, the conclusions can be followed.

(1) Initial shear strength 3 times increase to the effect of steel fiber.

(2) 200MPa specimen (BS-200-2.0) is 15% increase shear strength than compressive strength 100MPa (BS-100-2.0).

(3) Steel fiber contained specimen (BS-200-2.0) is 140% increase shear strength than without fiber specimen (BS-200-0).

(4) Flexural failure induction is more effective when steel fiber contain.

(5) Steel fiber contained concrete was increase the ductility at ultimate strength.

(6) It is difficult to express UHPC shear strength using previously proposal equations.

More research is needed for factors that are influencing the shear. (Steel fiber, strength of concrete, shear span ratio).

Divya S Nair, Dr. Ruby Abraham, and Dr.Lovely K M M.Tech[29] presents the details of an experimental investigation to determine the shear carrying capacity of high strength fiber reinforced concrete beam (HSFRC). M60 grade concrete was designed as per ACI method and the aspect ratio of the fibers were taken as 40 for the present investigation and volume fraction varied from 0 to 1%. Specimens of size 100×150×1200mm were prepared and tested under 2 point loading.

The test results show that the addition of fibers in high strength concrete increases the load carrying capacity and also the ductility. The available equations in the literature for calculating the shear strength were studied in detail. The existing equation proposed by Shin was modified. The comparison between computed values and experimentally obtained values is shown to validate the proposed model.

 Test result shows that by adding fibers the hardened property of the concrete was increased. Only slight variation was found in the compressive strength due to the addition of fibers but increase in flexural strength was about 40% when the fiber content was increased from 0% to 1%. In addition, there was a significant increase in split cylinder strength.

Table (2.2) Properties of Steel Fiber (Divya S Nair Dr. Ruby Abraham Dr.Lovely K M M.Tech) [30]

Length (mm)	20
Diameter (mm)	0.5
Aspect ratio(l/d)	40
Ultimate Stress	412 N/mm2

Table (2.3) Hardened Properties of Concrete

Property	CB	FB$_{0.25\%}$	FB$_{0.50\%}$	FB$_{0.75\%}$	FB$_{1.0\%}$
Cube compressive strength	79.25	80.70	81.20	81.96	82.3
Cylinder strength	63.90	65.40	67.24	67.42	68.67
Modulus of elasticity	6.96×1^4	8.23×1^4	8.54×10^4	8.63×10^4	8.643×1^4
Split tensile strength	3.11	3.54	3.82	4.53	4.95
Flexural strength	4.37	4.54	5.85	6.86	7.23

In the present study, 15 beam specimens of size $100 \times 150 \times 1200$ mm were prepared. The volume fraction of fibers used was 0.25%, 0.5%, 0.75% and 1% (FB 0.25%, FB0.5percentage, FB0.75percentage and FB1percentage). For each volume fraction, three specimens were cast. Three control specimens without fibers were also prepared. The required materials were thoroughly mixed in a drum type mixer machine and the super plasticizer (SP) was added along with 50% of the water. Since the workability was reduced with the addition of steel fibers, the dosage of SP was adjusted to obtain a constant workability of compaction factor of 0.9.

After 24 hours of casting, specimens were remolded and kept for water curing. After 28 days of curing specimens were taken out and kept ready for testing. Results:

Table (2.4) shows the test result of first crack load (by visual inspection) and ultimate load. It can be observed that as the fiber content increases the first crack load increases gradually and specimen with 1% fiber, the first crack load increased by 52.7%. Similarly, ultimate load also increased due to the addition of fibers and at 1% fiber, the increase was about 60%.

Table (2.4) ULTIMATE LOAD, FIRST CRACK LOAD

Designation of beam specimen	First crack load(KN)	Ultimate load (KN)
CB	34	41
FB0.25%	40	52
FB0.5%	44	59
FB0.75%	52	78
FB1%	72	102

All the specimens exhibited linear behavior initially and as the load increases specimens with higher percentage of fibers exhibited non-linear behavior. It can be observed that as the fiber content increases the stiffness of the specimen increases.

The specimen with fiber content 0 to 0.75% failed in shear and the specimens with 1% fiber content it was observed that the failure was due to the combined action of flexural crack and shear crack.

Energy absorption capacity of all the specimens was calculated as area under load deflection curve. It can be observed that as fiber content increased, the energy absorption capacity increased and for 1% fiber, an increase of 75.5% was found. This can be attributed to the effect of fibers in bridging the crack and hence enhancement in energy absorption capacity.

Table (2.5) Energy Absorption Capacity of SFRP

Beam Specification Energy absorption capacity (N-mm)	Energy absorption capacity (N-mm)
CB	1.76×10^6
FB0.25%	3.2×10^6
FB0.5%	4.1×10^6
FB0.75%	5.8×10^6
FB1%	7.2×10^6

Divya S Nair, Dr. Ruby Abraham, and Dr.Lovely K M M.Tech [29] show that

- The addition of fibers in high strength concrete increases the first crack load and ultimate load. For 1% volume fiber the ultimate load increased by 60%. Inclusion of steel fibers in the concrete mix improves the shear strength of RC beams and tends to change the mode of failure from brittle shear to ductile flexure.

- The ultimate shear strength of HSFRC beams can reasonably predicted by the modified equation suggested.

Remigijus Šalna, Gediminas Marčiukaitis [30] analyses the influence of steel fiber volume and shear span ratio on the strength of fiber reinforced concrete elements in various states of stress. 36 beams with three different shear spans (*a/h* = 1, 1.5, and 2 %) and three different fiber volumes (1, 1.5, and 2 %) were tested to examine how these factors influence the behavior of such elements.

Test results suggest that steel fiber volume and shear span can increase load capacity, plasticity and cracking. Experimental research showed that steel fiber volume has different influence at different shear span ratios. Regression

analysis of experimental data was carried out and empirical approach showing different effect of these factors was proposed. Furthermore, test results were compared with different theoretical and empirical approaches of other authors.

Nine beams have been tested by **D.H. Lim, B.H. OhA [31]** to investigate the influence of fiber reinforcement on the mechanical behavior of reinforced concrete beams in shear. The major test variables are the volume fraction of steel fibers and the ratios of stirrups to the required shear reinforcement. The test results show that the first crack shear strength increases significantly as fiber content increases and the improvement in ultimate shear strength is also achieved. The present study indicates that fiber reinforcement can reduce the amount of shear stirrups required and that the combination of fibers and stirrups may meet strength and ductility requirements. The volume fraction of steel fibers were varied from 0% to 2% and the ratios of stirrups from 0% to 100% of the required shear reinforcement, The beams were tested under four-point loading condition and the load was applied to the test beams as two equal concentrated loads by means of steel spreader beam.

D.H. Lim, B.H. OhA, showed that the compressive strength increased by about 25% when fibers were introduced into the concrete by up to 2% by volume, the increase in flexural strength was about 55% when the fiber content was increased to from 0% to 2%. One other more important characteristic in flexural behavior is that the fiber reinforced concrete showed remarkable ductility and energy absorption capacity.

D.H. Lim, B.H. OhA, represented that *One* predominant effect of steel fibers is to increase the shear cracking strength. Generally, the shear cracking strength of fiber reinforced concrete is higher than that of conventional reinforced concrete. Fig. 7 shows the variation of shear cracking strength with fiber contents. It can be seen that the inclusion of fiber increases shear-cracking strength significantly. This indicates that it is more effective to increase the shear cracking strength and ductility through the addition of more steel fibers.

It can be seen that by **D.H. Lim, B.H. OhA,** experimental work that fiber reinforced concrete beams exhibited similar improvements in ultimate shear strength compared with the companion beams without fibers. Fiber contents of up to 2% employed in the beams, showed small improvement in ultimate shear strength. However, mentioned earlier, as the volume of fiber increases, improvements in shear cracking strength is significant compared with companion beams without fibers and with only stirrups.

From these test results, it can be concluded that through the addition of fiber reinforcement, we can reduce the amount of shear stirrups required. An optimum combination of steel fibers and shear stirrups may be arrived at the required strength and ductility. It is possible that 50–75% of conventional stirrups, together with 1% of fiber volume contents may be an optimum for the beam tested.

Review of Ashour [32] The results of this research indicated the same general relationships between the a/ d ratio and the mode of failure. The tests indicated a marked improvement in the post-peak behavior of the specimens, with a significant increase in the ductility.

The effect of the fibers on beam ductility became more pronounced as the a/d ratio increased, and this supports the idea that the fibers are more effective in contributing to the beam transfer mechanism, than to the arch mechanism.

Most significantly, the results confirmed those noted by **Valle [45]**, in that it was observed that the addition of fibers to the specimens caused a noticeable increase in the shear strength.

Two formulae (in MPa) were also proposed for the prediction of the shear capacity of HSFRC beams:

$$v_c = \left(0.7\sqrt{f_c'} + 7F \right)\frac{d}{a} + 17.2\, \rho\, \frac{d}{a} \quad \text{a/d} \leq 2.5$$

$$v_c = \left(2.11\sqrt[3]{f'_c} + 7F\right)(\rho\, d/a)^{0.333} \quad \text{a/d} > 2.5$$

$$F = \left(\frac{l}{d}\right) v_f\, d_f \quad \text{And} \quad d_f \text{ is the fiber effectiveness}$$

In 1987, two researchers, Narayanan and Darwish [33], postulated their formula that, in the following years, has been one of the most used and has later been shown to be one of the best alternatives through comparison with published data**.**

Their purpose was to investigate the behavior of steel fiber reinforced concrete beams subjected to predominant shear. After their investigation, they presented the semi-empirical equations that are tools to be used for design purposes.

These predictive equations are suggested for evaluating

(1) The cracking shear strength and

(2) The ultimate shear strength of fiber reinforced concrete beams.

In the paper mentioned above, they established that the inclusion of steel fibers in RC beams results in a substantial increase in their shear strength (e.g., when 1 % volume fraction of fibers was used, an increase of up to 170 % in the ultimate shear strength was observed).

The test program consisted on fabricating 49 beams having identical rectangular cross section of 85 x 150 mm, and testing them under four symmetrically placed concentrated loads.

Four clear spans and four shear spans were employed. Three different types of beam were tested:

(1) Beams without web reinforcement,

(2) Beams with conventional stirrups and,

(3) Beams containing crimped steel fibers as web reinforcement.

Test result showed that the first-crack shear strength f_{cr} increased significantly due to the crack-arresting mechanism of the fibers. Even for a fiber volume fraction of 1 %, which was the optimum percentage, the ultimate

shear strength improvements were of the same order as those obtained from conventional stirrups.

They recognized that the shear force *V* withstood by a beam could have the following form:

$$V = V_a + V_b + V_c + V_d$$

Where V_a is the vertical component of the interlocking force, which results from interlocking of aggregate particles across a crack; V_b is the vertical component of the fiber pull-out forces along the inclined crack; V_c is the shearing force across the compression zone and V_d is the transverse force induced in the main flexural reinforcement by dowel action.

However, it should be noted that the above four shear forces are not necessarily additive when failure is imminent. In the formula hereinafter shown, the contribution of the aggregate interlocking has been ignored (this assumption gives a safe prediction).
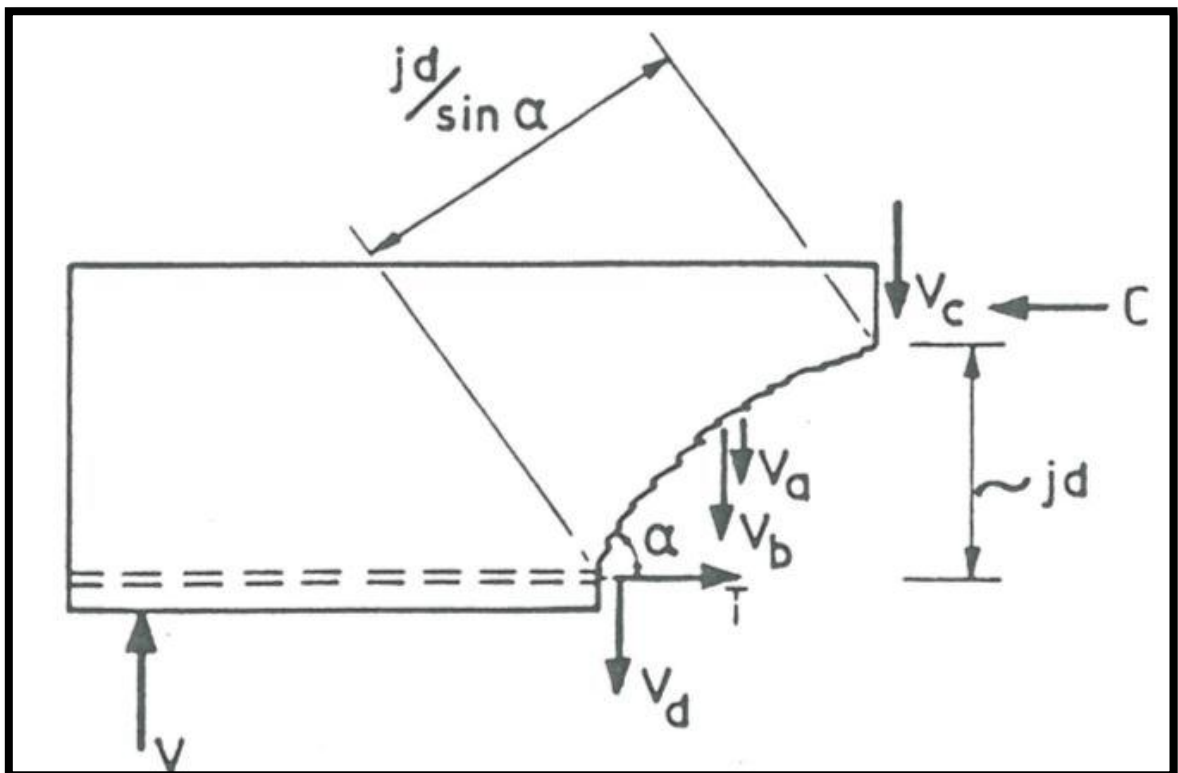
Figure (2.5) free body diagram of part of the shear span of a simple supported beam fiber reinforced concrete beam (Narayanan et al., 1987) [33].

Fiber factor F given by $F = \left(\frac{l}{d}\right) v_f \, d_f$

Where $\frac{l}{d}$ is the fiber aspect-ratio, v_f is the fibre volume fraction and d_f is the bond factor that accounts for differing fiber bond characteristics; based on a large series of pull-out tests, d_f was assigned a relative value of 0.5 for round fibres, 0.75 for crimped fibers and 1.0 for indented fibers.

$$V = 0.41.\tau.F + e.A'.f_{spfc} + e.B'.\rho.\frac{d}{a}$$

Where τ is the average fibre matrix interfacial bond stress. With steel fibers in cementitious composites, the fiber matrix interfacial bond is mainly a combination of adhesion and friction and mechanical interlocking. The available investigations on the fiber bond resistance have shown a large scatter of test results (Narayanan et al., 1987). However, the indirect methods adopted by **Swamy, Mangat and Rao (1974) [34]** seem to be more realistic, and the value of 4.15 N/mm2. Suggested by them for the ultimate bond stress τ was adopted in the Narayanan &Darwish study. (τ=4.15 Mpa).

f_{spfc}: the split cylinder strength.

$$f_{spfc} = \frac{f_{cuf}}{(20-\sqrt{F})} + 0.7 + \sqrt{F} \quad \text{Mpa}$$

Where f_{cuf} is the cube strength of fiber concrete.

The term e is a non-dimensional factor that takes into account the effect of arch action and is given by:

$$e=1 \text{ when } \frac{a}{d} > 2.8$$

$$e=2.8\frac{d}{a} \text{ when } \frac{a}{d} < 2.8$$

A' is a non-dimensional constant having a value of 0.24.

B' is a dimensional constant having the value of 80 N/mm2.

The last and third term, considers the dowel action provided by the amount of longitudinal tensile reinforcement ρ= As/bd with the shear span ratio a/d.

RILEM TC 162-TDF (2003) [35] The RILEM Design Method is based on **the European pre-standard ENV 1993-1-1 (Euro code 2) [36].** This method calculates the shear capacity V as consisting of 3 separate contributions:

$$V = V_c + V_w + V_f$$

This is the equation given in the first draft of **EC 2 (1993) [36]** with the addition of the term for the contribution of the fibers V_f. However, the shear resistance of the plain concrete V_c is taken from the second draft of the EC 2 (2001) with the partial safety factor $\gamma_c = 1.5$.

$$v_c = \left\{ \frac{0.18}{\gamma c} k. \left(100\rho. f_{fck}\right)^{\frac{1}{3}} + 0.15\sigma_{cp} \right\}. b_w d$$

Where $k = 1 + \sqrt{\frac{200}{d}} \leq 2$, $v_f = k_f k_1 \tau_{fd} b_w d$, $\tau_{fd} = 0.12. f_{Rk4}$,

$k_f = 1 + n. \left(\frac{h_f}{b_w}\right)\left(\frac{h_f}{d}\right)$ and $k_f \leq 1.5$ and $k_1 = 1 + \sqrt{\frac{200}{d}} \leq 2$

f_{fck}: Characteristics cylinder compressive strength [N/mm²]

b: Width of the beam [mm]

d : Effective depth of the beam [mm]

k_f: Factor for taking into account the contribution of the flanges in T-section it is equal to one for rectangular sections

h_f : The height of the flange

b_f: The width of the flange

b_w : The width of the web

$$n = \frac{b_f - b_w}{h_f} \leq 3$$

$$f_{Rk4} = \frac{3. F_{R,4}. L}{2. b. h_{sp}^2} = 1.0 \text{ N/mm}^2$$

Shin et al. (1994) [37].This paper reports the results of an investigation on the strength and ductility of fiber reinforced high strength concrete beams (with concrete compression strength equal to 80 MPa) with and without steel fiber reinforcement, the diagonal cracking strength as well as the nominal shear strength of the beams were determined. 22 beam specimens were tested under monotonically increasing loads applied at mid-span. The major test parameters included the volumetric ratio of steel fibers, the shear-span-to depth ratio, the amount of longitudinal reinforcement and the amount of shear reinforcement.

Empirical equations are suggested for evaluating the nominal shear strength of SFR high-strength concrete beams

For beam with a/d <3

$$v_n = 0.22\ f_{sp} + 217\rho.\frac{d}{a} + 0.834.\,v_b$$

Ding et al. (2011) [38]. This paper presents the results of an experimental research program on the shear behavior of steel fiber reinforced SCC beams.

The major aims of this program are to evaluate the possibility of replacing stirrups by steel fibers, to study the hybrid effect of steel fibers and stirrups on the mechanical behavior of beams, and to analyze the influence of steel fibers in the failure mode and shear strength. The beams studied in the test program had a cross section of 200 mm x 300 mm and 2400 mm length.

They were tested on a span of 2100 mm having two stirrups ratio and two fiber contents. They were nine beams, but only 3 over these were suitable for the investigation carried in this work. Moreover, the authors investigated the validity of the existing semi-empirical equation for predicting the shear strength and they suggested a new formula.

$$v_{uf} = \xi \left[0.97\ \rho_s^{0.46} f_c'^{0.5} + 0.2\rho_s^{0.91} f_c'^{0.38} f_{yl}^{0.96} \left(\frac{a}{d}\right)^{-2.33} \right] + 1.75 I_b \rho_{st} f_{yst} + 0.5\tau v_f \frac{l_f}{d_f} ctg\alpha$$

ξ: factor tacking account size effect $= \dfrac{1}{\sqrt{1+\frac{d}{25d_a}}}$

d: depth, d_a : maximum agg.size.

f_c' : Compressive strength of cylinder $= 0.86f_{cu}$

$$I_b = \frac{0.97\,\rho_s^{0.46}\,f_c'^{0.5}}{.97\,\rho_s^{0.46}\,f_c'^{0.5} + 0.2\rho_s^{0.91}f_c'^{0.38}\,f_{yi}^{0.96}\left(\frac{a}{d}\right)^{-2.33}}$$

Lim et al. (1999) [39]. The purpose of this study was to explore the shear characteristics of reinforced concrete beams containing steel fibres. The tests reported in this article consist of nine beams reinforced with stirrups and steel fibers. The main aims of this study were to investigate

(1) The mechanical behavior of reinforced concrete beams containing steel fibers under shear.

(2) The potential use of fibers to replace the stirrups.

(3) The combinations of stirrups and steel fibers for improvements in ultimate and shear cracking strengths as well as ductility.

A method of predicting ultimate shear strength of beams, when reinforced with stirrups and steel fibers, is proposed.

Cucchiara et *al (2004) [25].* The aim of the paper consists of the evaluation of the improvement in the post-peak behavior due to the presence of fibers and in particular to the coupled effects of fibers and stirrups.

The load-deflection graphs recording the post-peak branch, allowing the conclusion that the inclusion of fibers can modify the brittle shear mechanism into a ductile flexural mechanism, thus allowing a larger dissipation of energy necessary especially in seismic resistant reinforced concrete framed structures.

The tests were carried out by considering two different values of shear span, different volume of fiber and stirrups, for two series of eight beams.

Kwak et al (2004) [41]. Twelve reinforced concrete beams were tested to failure to evaluate the influence of fiber-volume fraction, *a/d* and concrete compressive strength on beam strength and ductility.

The beams denoted by the letters FHB (fiber-reinforced, higher-strength concrete beams) were constructed with concrete having a compressive strength near 65 MPa while the one denoted by FNB2 had an average compressive strength of 31 MPa. No stirrups were included in the shear span, only behind the supports in order to preclude the possibility of anchorage failure of the longitudinal bars.

The authors' results demonstrated that the nominal stress at shear cracking and the ultimate shear strength increased with increasing concrete compressive strength, fiber volume, and decreasing shear span-depth ratio.

Moreover, the results of 139 tests of FRC beams without stirrups were used to evaluate existing and proposed empirical equation for estimating shear strength.

The evaluation indicated that the equation developed by **Narayanan and Darwish [33]** and the equation proposed herein provided the most accurate estimates of shear strength.

$$v_u = 3.7 . e . f_{spfc}^{\frac{2}{3}} . \left(\rho \, \frac{d}{a} \right)^{\frac{1}{3}} + 0.8 v_b$$

$$v_b = 0.41 \tau F$$

$$e = \begin{cases} 1 \, for \, \frac{a}{d} > 3.4 \\ 3.4 \frac{d}{a} \, for \, \frac{a}{d} \leq 3.4 \end{cases}$$

Kearsley et al (2004) [41]. The authors of this paper investigated the effect of stainless steel fibers by casting nine different series of beams.

Three beams in each series were cast, resulting in 27 beams. Out of nine series, one series was done in plain concrete without any shear reinforcement, three series were with fiber reinforcement and five series were with both fiber and conventional shear reinforcement. To evaluate the effect of the fibers, the equivalent flexural tensile strength of the SFR-concrete was determined

applying load in control of displacement on 150 x 150 x 750 beams in four point bending test (clear span equal to 600 mm).

The test values confirm that the stainless steel cast fibers are significantly less effective in providing post-cracked concrete strength than draw wire fibers.

It can be observed that the contribution of fibers to the ultimate shear strength depends essentially on the volume fraction of the fibers, on their geometric characteristics and on the fiber-matrix interfacial bond that determines the resistance to fiber pull-out.

ACI 318 [1] expresses the ultimate strength for HSC concrete in shear v_u by the following equation:

$$v_u = v_c + v_s$$

$$v_c = \left[0.158\sqrt{f_c'} + 17.24\rho\left(\frac{V_u.d}{M_u}\right)\right] b.d \quad \leq 0.29\sqrt{f_c'}\, b.d \quad Mpa$$

V_u , M_u : Shear force and moment at the critical section.

ρ : Longitudinal tension steel ratio.

ACI allows the following simplification assuming that the term $\frac{V_u.d}{M_u}$ is small;

$$v_c = 0.166\sqrt{f_c'} \quad \text{b.d} \quad Mpa$$

$$v_s = \frac{A_{sv}\, f_{ysv}d_v\,(\cot\theta_v + \cot\alpha)\,\sin\alpha}{S}$$

Where

A_{sv}: Area of shear reinforcement within spacing S.

f_{ysv}: Yield strength of shear reinforcement.

d_v : Lever arm resisting flexural moment (usually =0.9d).

θ_v : Angle of inclination (which varies between 30 and 60 degrees) of the diagonal compressive stress to the longitudinal axis of the beam.

α : Angle of inclined stirrups to the longitudinal axis of the beam.

(BS8110) [42] British Standard expresses the ultimate strength for HSC concrete in shear v_c by the following equation:

$$v_c = \frac{0.79}{\gamma_c} \left(100\rho \frac{f_{cu}}{25}\right)^{1/3} \left(\frac{400}{d}\right)^{1/4} b.d \quad \text{Mpa}$$

Euro Code2 (EC2) [36] expresses the ultimate strength for HSC concrete in shear v_c by the following equation:

$$v_c = 0.035 f_{ck}^{2/3} k(1.2 + 40\rho)b.d \quad \text{Mpa}$$

$$k = (1.6 - d) \; > 1$$

Chinese Code for Design of Concrete Structure, GB50010–2002 [43] expresses the ultimate strength for HSC concrete in shear v_c by the following equation:

$$V_u = \frac{1.75}{\lambda+1} f_t bd + f_{yst} \frac{A_{st}.d}{S} \quad \text{N}$$

$$v_u = \frac{V_u}{b.d} \quad \text{Mpa}$$

Where V_u is the shear load of the RC member, f_t is the tensile strength of the prism, λ is the shear span-to-depth ratio, and v_u is the shear strength of the RC member.

$$V_{uf} = \frac{1.75}{\lambda+1} f_t bd(1 + \beta_v \lambda_f) + f_{yst} \frac{A_{st}.d}{S} \quad \text{N}$$

$$v_{uf} = \frac{V_{uf}}{b.d} \quad \text{Mpa}$$

Where V_{uf} is the shear load of the fiber reinforced RC member, β_v is the influence coefficient of the steel fibers, λ_f is fiber factor, $\lambda_f = v_f l_f / d_f$, and v_{uf} is shear strength of fiber reinforced RC member.

Ultimate shear strength of High strength fiber Reinforced Concrete is given by **Li (1992) [44]** by the following equation:

$$v_c = 1.25 + 4.68(f_f - f_{sp}) \quad Mpa$$

f_{sp} : Split cylindrical strength;

f_f : Flexural strength of fibre concrete.

Most significantly, the results confirmed those noted by **Valle, M.O., Shear Transfer in Fiber Reinforced Concrete, M.S. Thesis, Department of Civil Engineering, Massachusetts Institute of Technology,**

1991[45]. observed that the addition of fibers to the specimens caused a noticeable increase in the shear strength.

Two formulae (in MPa) were also proposed for the prediction of the shear capacity of HSFRC beams :

$$v_c = (\ 0.7\sqrt{f_c'} + 7\text{F}\ )\frac{d}{a} + 17.2\rho\frac{d}{a}\ \text{Mpa}$$

$$v_c = (\ 2.11\sqrt[3]{f_c'} + 7\text{F}\ )\frac{d}{a} + \left(\rho\frac{d}{a}\right)^{0.333}\ \text{Mpa}$$

Evaluation according to Egyptian code (ECP-203) [46]:

Shear force is present in beams at sections where there is a change in bending moment along the span. An exact analysis of shear strength in reinforced concrete beam is quite complex. Several experimental studies have been conducted to understand the various modes of failure that could occur due to possible combination of shear and bending moment. Despite the great research efforts, however, there is still not a simple. In addition, many of the factors that influence the determination of the required minimum amount of shear reinforcement are not yet known.

The shear strength of R.C. beams depends on the strength of concrete, the percentage of the longitudinal reinforcement and the span-to-depth ratio or stiffness of the beam. From shear force, diagram find that the shear force is equal to support reaction that equal to haft of vertical load, and the theoretical shear force is equal to the force for allowable concrete shear strength, as in Eq. (1) plus the force from carrying shear strength by vertical stirrups as in Eq. (2):

$$q_{cu} = 0.214\sqrt{\frac{f_{cu}}{\gamma_c}}\ MPa\ \ \text{Eq (1)}$$

$$q_{sus} = \frac{A_{st}.f_y}{\gamma_s.b.s}\ \text{MPa} \qquad \text{Eq(2)}$$

Where f_{cu} is characteristic cube compressive strength of concrete in N/mm2, A_{st} is the area of stirrups, b is the section width, S is the spacing between stirrups. γ_c , γ_s is the material factor of safety of concrete and steel,

respectively and are taken equal unity in calculation. Then, the theoretical shear force can be calculated as the following equation:

$$v_{the} = [0.5q_{cu} + q_{sus}]xbd$$

Chapter Three

EXPERIMENTAL PROGRAM

3.1 Introduction

This chapter describes the experimental work performed through this study; beginning with specimens details, determination of the properties of used materials, preparing of mix design of specimens, the measurement devices, casting procedure, test setup, and finally test procedure, , in order to study shear strengthening of high strength concrete beams with added discrete steel fiber.

3.2 Objectives of the Research

1. Study the behavior of high strength reinforced concrete mixed with discrete steel fiber.

2. Study the effect of span to depth ratio on shear strength of HSRC beams with discrete steel fiber

3. Study the mode of failure and crack pattern for all specimens.

4. Discussion and analysis of experimental results.

3.3 Description of Test Specimens

Present study includes twelve specimens, divided to three groups, the first group of specimens contains four specimens which are identified as (A–0), (A–1), (A-2), and (A-3), the second group contains four specimens which are identified as (B-0), (B-1), (B-2) and (B-3), and third group also contains four specimens which are identified as (C-0), (C-1),(C-2), and(C-3). Each group has beams of constant span equal 1500 mm and rectangle cross section 250mm depth and 120mm width as listed in Table (3.1). The letter (A) indicate that shear span to depth ratio (a/d) is (1.5), the letter (B) indicate that shear span to

depth ratio (a/d) is (1.7), and the letter (C) indicate that shear span to depth ratio (a/d) is (2.2). Where (a) means the distance from applied concentrated load to support of beam, and (d), is the depth of beam as shown on figure (3.1). Using numbers (0), (1), (2), and (3) in the specimen's names indicate the volume of fraction of fiber in specimens by weight, are equal to (0%), (0.25%), (0.5%), and (0.75%) respectively.

Volume of fraction percentage can be defined as:

$$v_f = v_{sf} / v_c$$

Where v_{sf} Is the volume of steel fiber, and v_c is the volume of specimen.

The dimensions of the tested beams are shown in Fig (3.1), the tested beams represented about half scale models of prototype structural beam in building. They have Rec-section, consisted of 250 mm in thickness and 120 mm width and its supporting length was 1500 mm. Table (3.1) present beams dimension and details of reinforcement.
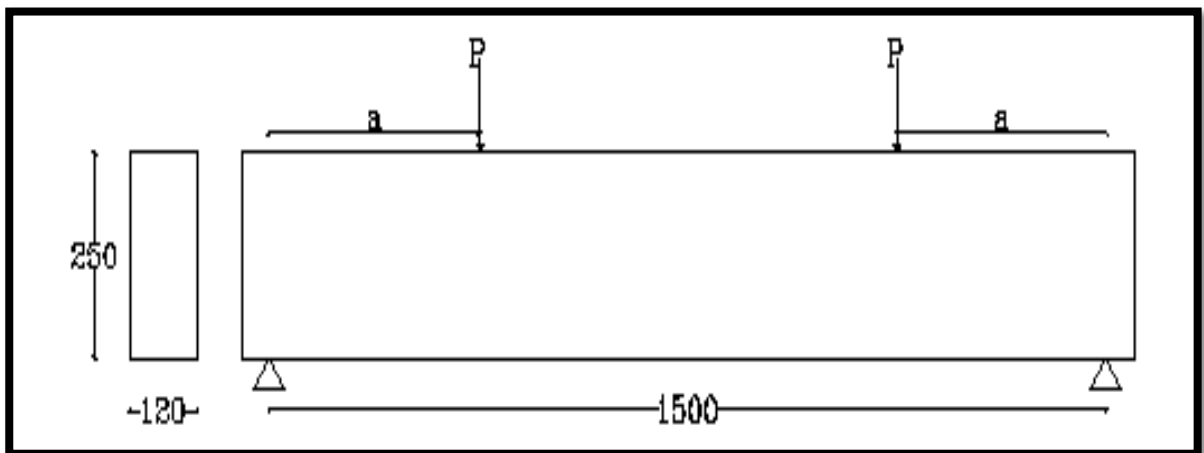
Fig (3.1). Beam Dimension

Table (3.1). Specimens Details.

GROUB No.	a/d	Dimension	Specimens	Fiber Content	Vertical Stirrups	Main Steel	Compres. St.
A	1.5	120x250	A-0	0%	7Φ8 / m	2D16	2D12mm
		120x250	A-1	0.25%	7Φ8 / m	2D16	2D12mm
		120x250	A-2	0.5%	7Φ8 / m	2D16	2D12mm
		120x250	A-3	0.75%	7Φ8 / m	2D16	2D12mm
B	1.7	120x250	B-0	0%	7Φ8 / m	2D16	2D12mm
		120x250	B-1	0.25%	7Φ8 / m	2D16	2D12mm
		120x250	B-2	0.5%	7Φ8 / m	2D16	2D12mm
		120x250	B-3	0.75%	7Φ8 / m	2D16	2D12mm
C	2.2	120x250	C-0	0%	7Φ8 / m	2D16	2D12mm
		120x250	C-1	0.25%	7Φ8 / m	2D16	2D12mm
		120x250	C-2	0.5%	7Φ8 / m	2D16	2D12mm
		120x250	C-3	0.75%	7Φ8 / m	2D16	2D12mm

3.4 Tests of Used Materials

This part presents a summary for the properties of used materials in this research. The used materials were tested in order to investigate their properties. A summery for the properties of the materials used and the mix design for the tested beams will be presented later on.

3.4.1 Coarse Aggregates

Coarse aggregate (Crushed Dolomite) was used in this research with maximum nominal aggregate size 40mm and fineness modulus 6.3. The used coarse aggregate was clean, free of impurities and with no organic compounds. Coarse aggregates tests carried out according to the Egyptian Standard Specifications. The characteristics of coarse aggregate are tabulated in Table (3.2).

Table (3.2). Coarse Aggregate Characteristics

Test	Results	Specification Limit
Specific Gravity	2.72	2.6 – 2.8
Unit Weight and voids	1.59	----------------
Materials Finer than Sieve no 200	1.82	Less than 2 %
Abrasion (Los Anglos)	19.26	Less than 25 %
Absorption	2.03	----------------
Crushing	23	Less than % 30
Impact	18.6	Less than 30 %

3.4.2 Fine Aggregates

Fine aggregate used in this research is natural sand composed of siliceous materials. The used fine aggregate was clean, free of impurities and with no organic compounds with fineness modulus 2.84. Fine aggregates tests also carried out according to the Egyptian Standard Specifications No. 1109 / 2002. The characteristics of fine aggregate are tabulated in Table (3.3).

Table (3.3). Fine Aggregate Characteristics

Test	Results	Specification Limit
Specific Gravity	2.61	-------------
Unit Weight and Voids	1.79	-------------
Materials Finer than Sieve no 200	2.60	Less than 4 %

3.4.3 Combined Aggregates

Coarse aggregate and fine aggregate were combined with ratio 0.68: 0.32. The grading of this mix obtained from sieve analysis test according to the Egyptian Standard Specifications No. 1109 / 2002. The max nominal aggregate

size is 20mm and fineness modulus is 4.93. The results of the test were tabulated in Table (3.4).

Table (3.4). Results of Sieve Analysis Test for Combined Aggregate

Sieve Size (mm)	Retained on Each Size (gm)	Total Retained	Total Retained %	Passing %
40	0	0	0	100
20	100	100	4	96
10	432	532	21.28	78.72
5	819	1351	54.04	45.96
2.5	186	1537	61.48	38.52
1.25	140	1677	67.08	32.92
0.65	496	2173	86.92	13.08
0.3	280	2453	98.12	1.88
0.16	38	2491	99.64	0.36
Pan	9	2500	100	0

3.4.4 Cement

The cement used in this research was ordinary Portland cement (OPC). Tests of cement were carried out according to the Egyptian code No. 373/1991. This type of cement is suitable for all ordinary construction work. It does not resist sulphate attack and it has medium rate of strength. It has resistance to dry shrinkage and crushing, but less resistance to chemical attack, thaw-freezing, and abrasion. The characteristics of used cement were tabulated in Table (3.5).

Table (3.5). Characteristics of Ordinary Portland cement

Properties		Test Results	Limits of the E.S.S
Fineness of cement, percentage of retained on the standard 0.09 mm sieve by weight		8 %	Not more than 10 %
Specific Gravity		3.15	
Expansion (mm)		1.2	Not more than 10
Initial Setting Time (hr's min's)		1 40	Not less than 45 min
Final Setting Time (hr's min's)		3 20	Not more than 10 hrs
Compression Strength (Kg/cm^2)	3 days	240	Not less than 185 kg/cm^2
	7 days	375	Not less than 265 kg/cm^2

3.4.5 Reinforcement Steel

The steel used in this research was high tensile steel (36/52) for longitudinal reinforcement. It have 3600 kg/cm^2 yield stress. The bars used for reinforcement were 12mm and 16 mm diameter deformed bars. Tests were carried out of the Egyptian standard specifications. Table (3.6) presents a summary of tests performed on the steel to determine its properties.

Table (3.6). Properties of Steel Used in the Experimental Work

Properties	Φ 12	Specification
Yield Stress (MPa)	380	360
Ultimate Stress (MPa)	615	520
Weight per meter Length	0.601	0.587-0.649
Ultimate Stress/ Yield Stress	1.5	1.05
Elongation	14	12

3.4.6 Proprieties of Steel Fiber Used

The steel fiber with length 60mm, diameter 0.75mm, aspect ratio 80, density 78.5KN/m^3, an ultimate tensile strength of 1100 MPa, and an ultimate tensile strain of 2.2% (based on the manufacturer) were used.

Fig (3.2). Fiber Shape

3.5 Mix Design and Preparing of Specimens

The mix proportions of the concrete used are given in Table (3.7). Mechanical-mixed concrete with replacement of 10 percent (by weight) of the cement by silica fume was used to produce high strength concrete.

The silica fume has 2.23 a specific gravity and 200000 cm²/gm surface area which is about 50 times finer than the used Portland cement. Due to the very high surface area of silica fume, there is a commensurate increase in water demand. To produce high-strength concrete water-cement ratio of about 0.30, high range water reducing admixture was used. Super plasticizer was added as admixture to reduce water ratio and to improve the workability of high-strength concrete during casting. Normal Portland cement product was used for all specimens. Coarse aggregate with maximum nominal size of 40 mm was used in order to ensure good compaction of concrete, for each test specimen, three150 x 150 x 150 mm cubes and two cylinders of 150mm diameter and 300mm height were prepared, the cubes were used to determine the compressive strength of concrete, and the cylinders were used to determine the splitting tensile strength of concrete.

Table (3.7). Mix Design

Constituent	Mix Proportioning
Cement	550 kg/m3
Fine aggregates	650 kg/m3
Coarse aggregates	1050 kg/m3
w/c ratio	0.3
water	165 litres
Silica fume % of cement	10%
Super plasticizer (L/100 kg of cement)	1.8
Average Cylinder Compressive strength (28 days) fc′	510 MPa

3.5.1 Quantity of Materials Needed

Table (3.8) give the volume of beams, which were used in preparing of all the test specimens. This table helping to estimate materials cost. The total volume of beams was 0.6 m³. This volume needed to approximately 330 kg of normal Portland cement, 33 kg of silica fume, 6 liter of super plasticizer, 390 kg of sand, 633 kg of coarse aggregate, and 40 kg of steel fibers.

Table (3.8). Quantity of Materials Needed

Material	Weight (kg)
Cement (kg)	330
Coarse aggregate (kg)	633
Fine aggregate (kg)	390
Water (kg)	99
Water /cement ratio (w/c %)	0.3
Super plasticizer (L/100 kg of cement)	1.75-1.8
Silica fume (% of cement)	10

3.5.2 Fabrication of Wooden Forms

The test specimens were cast monolithically in timber forms. One form has been made for each group of the specimens. The length of the form for the all groups was 1650 mm. The form was made of 25 mm thickness plywood, which was coated by a film of polyurethane to stiff the form and to proof it from water. After casting, the test specimens were covered with polyethylene sheets to prevent loss of moisture by evaporation; Fig (3.3) shows the arrangements and dimension of the wooden form. Test specimens were stripped off the forms on the second day after casting, and they were dispersed by water for an average one month.

Fig (3.3). Wooden Forms

3.5.3 Reinforcement Details of Specimens

Fig. (3.4) shows the reinforcement details of specimen (A–0) as an example for the reinforcement of the specimens .The main longitudinal reinforcement of the beam was the same in all test specimens. It was approximately 1.34 % of the cross-sectional area of the beam, it was 2 bars of 16 mm diameter deformed steel ,the secondary reinforcement was 2 bars of 12 mm diameter deformed steel, and For all specimens shear reinforcement (stirrups) was 7 ϕ 8 / m .All reinforcement bars were provided with adequate anchorage lengths at their ends. In all specimens the clear concrete cover was 25 mm.

Fig (3.4). Reinforcement Details of Beam

3.6 Measuring Device

3.6.1 Load Cell

Digital Load cell of capacity 550KN with accuracy of 0.1KN was adopted to measure the applied load. The value of loads was recorded from the monitor connected to the load cell.

3.6.2 Electrical Strain Gauges

Electrical strain gauges were used to measure strain in stirrups and steel reinforcement. The electrical strain gauges were of type PL-60-11-1L. The gauges had the following characteristic: gauge length 60mm, gauges resistance $120.3\pm0.5\Omega$, gauges factor $2.07\pm1\%$, temp. compensation for 11×10^{-6} and transverse sensitivity 0.7%. The strain gauges were connected to a strain meter device with accuracy 1×10^{-6}, and covered by a waterproof coating to protect them from water and damage during casting. Figure (3.5) and (3.6) show the strain gauges on stirrups, and steel reinforcement.
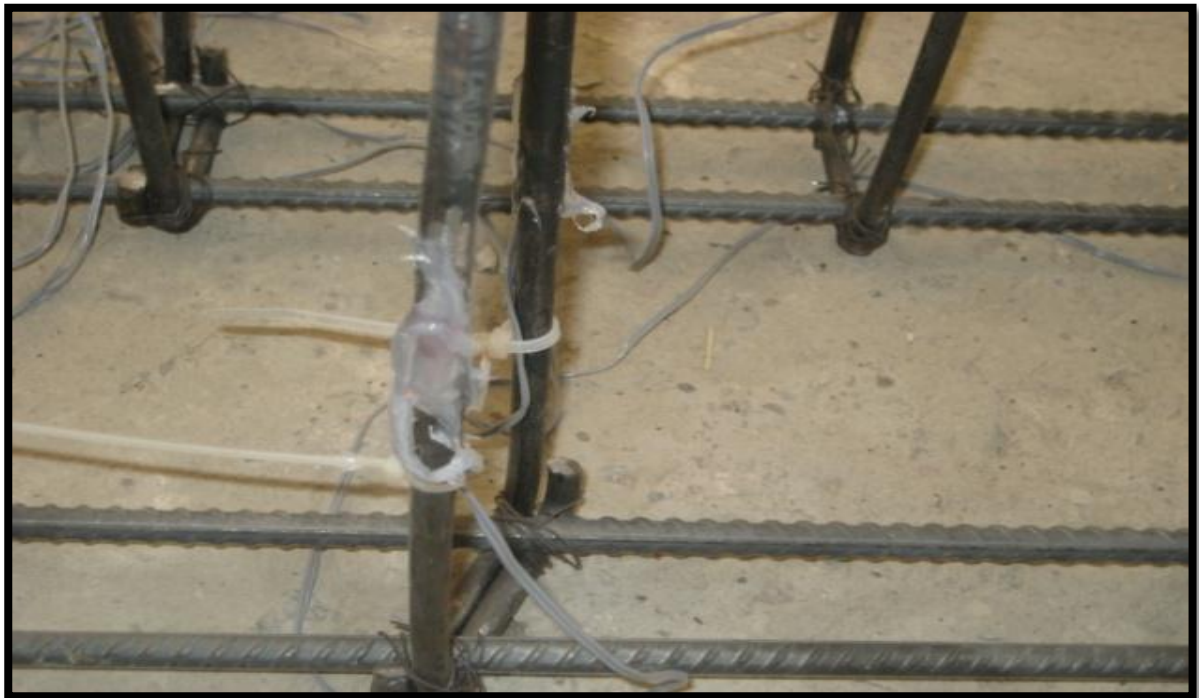
Fig (3.5). Strain Gauge for Stirrups

Fig (3.6). Strain Gage at Mid-Span of Beam

3.6.3 Deflection Measurements

Deflection was measured using three dial gauges, which were assembled at the edge of the test zone. The distance between the each dial gauges was 250 mm. These dial gauges have accuracy 0.01 mm.

3.7 Testing procedure

3.7.1 Preparation and Casting of Specimens

The rebar was first assembled into reinforcing cage using utilizing stirrups, and there were hold together with steel wire. The reinforcing cages placed inside formwork. The concrete was then prepared following the procedure outlined below:

1. The sand, cement, silica fume, and gravel were placed in rotating-drum mixer and mixed for 30 seconds,

2. At this stage, the water, and super plasticizer were then gradually added to the mixer,

3. If fibers were used, these were sprinkled into the mixer,

4. The mixing was then discontinued 5 minutes after step 2 had been completed.

The concrete was then placed in the formwork, in addition three test cubes, and twelve test cylinders were casting, and the specimens were then vibrated for 3 minutes. Curing stage began for one month from casting of specimens as shown on figure (3.7), and figure (3.8).

Fig (3.7). Casting the Standard Cubes and Cylinder

Fig (3.8). Specimens after Casting

3.7.2 Compression and Splitting Tensile Tests:

Twelve cubes each of 150x150x150, and eight cylinders each of 150mm diameter, and 300mm height, were prepared during casting processes, cubes were used for compression tests, and cylinders were used for compression tests and tensile tests. Prior to testing, the cylinders for compression tests were capped using hydro stone, in order to ensure an event contact surface with the loading platens of the testing machine. The compression test program consisted of three main stages:

1. Test cubes get average compressive strength for them. The young's modulus of cylinders were measured by placing two linear Voltage displacement Transducers (LVDT) on diametrically opposite sides of the cylinders being tested, and then loading the cylinders up to approximately 40% of the expected ultimate capacity, at displacement rate of 0.016 in/min.

2. The LVDT'S were then removed, and the cylinders reloaded at a displacement rate of 0.016 in/min. To enable the ultimate compressive strength f_c' to be determined.

In performing the splitting tensile tests, the cylinders were placed flat on their longitudinal axis, and loaded until the occurrence of vertical cracking, which was readily determined from the load-displacement plot, as loading occurred. **The results from these splitting tensile tests were not utilized in this experimental program**.

3.8 Compressive Strength

Table (3.9) represented compressive strength for specimens after 28 days from casting, after 7 days, six cubes and four cylinders of these specimens were tested and the remains specimen (six cubes and four cylinders) were tested after 28 days. Figures (3.9) and (3.10) represented the standard cubes and cylinders failure.

Fig (3.9). Standard Cube Failure Shape

Fig (3.10). Standard Cylinder Failure Shape

Table (3.9). Results of Testing Concrete Specimens Cubes and Cylinder

Specimens No.	Fiber Content	Average Compressive Strength (MPa)
0	0%	51
1	0.25%	53
2	0.50%	55.8
3	0.75%	68.9

3.9 Test Setup

The beam shear tests were performed using four points loading. The beams were tested after removal from water, to avoid the development of shrinkage cracks and a consequent reduction in the tensile strength of the specimens. Digital Load cell of capacity 550KN with accuracy of 0.1KN was adopted to measure the applied load. The value of loads was recorded from the monitor connected to the load cell. The beams were tested using an incremental loading procedure. The vertical displacement of the beams was recorded using three electric dial gauges. One at the middle of beams, the other at distance

equal to half of the beam depth from the support, and the third near support as shown on figure (3.11).
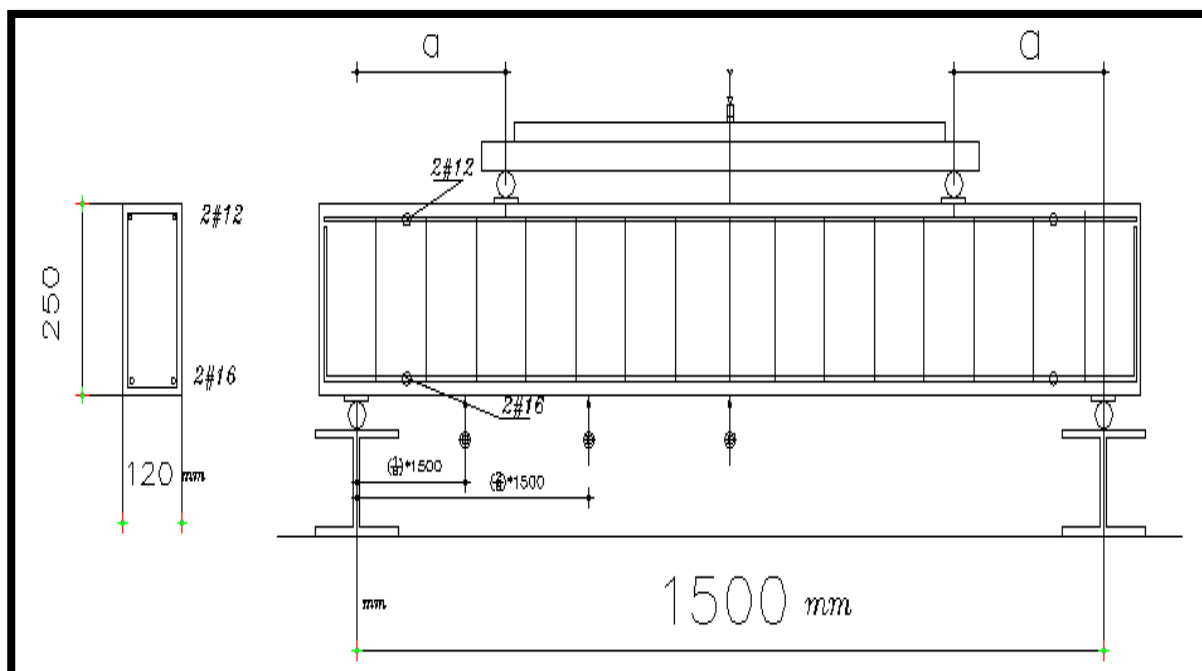

Fig (3.11). Specimen Details.

Figure (3.12) and (3.13) shows sample of specimens before testing, and the positions of dial gauges. During tests, the applied load was kept constant at each load stage for measuring and observing.
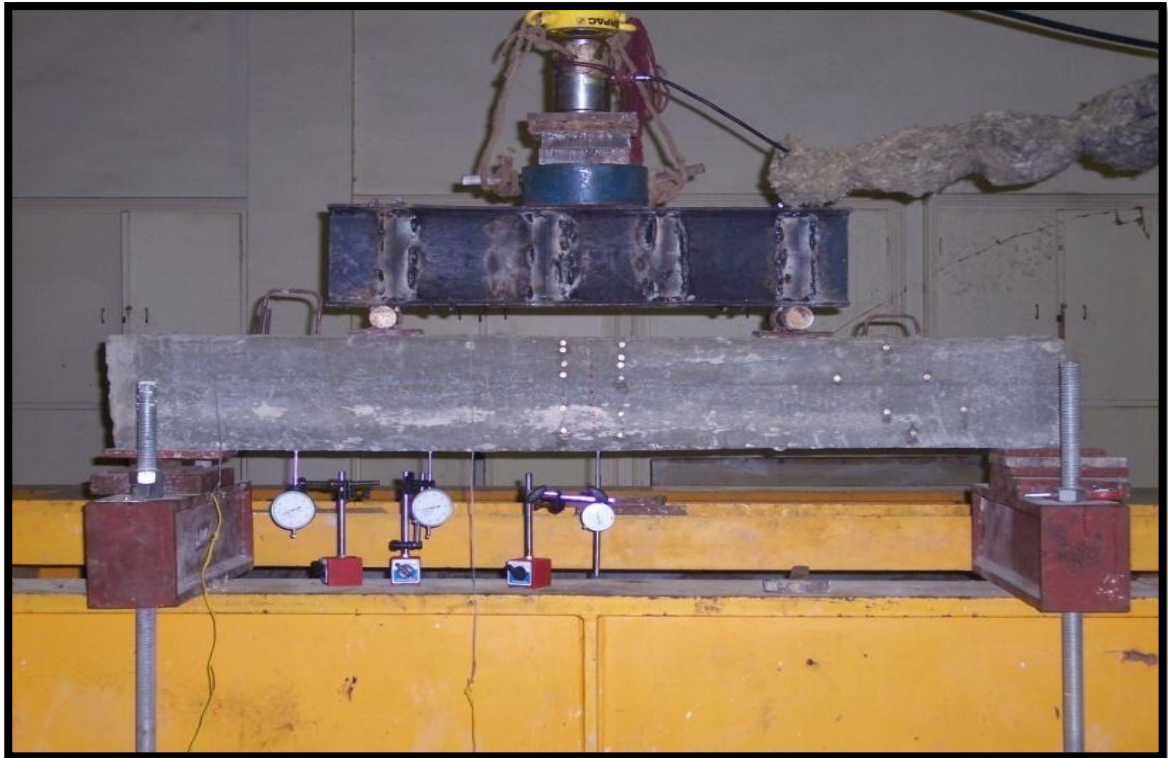
Fig (3.12). Specimen before Testing.
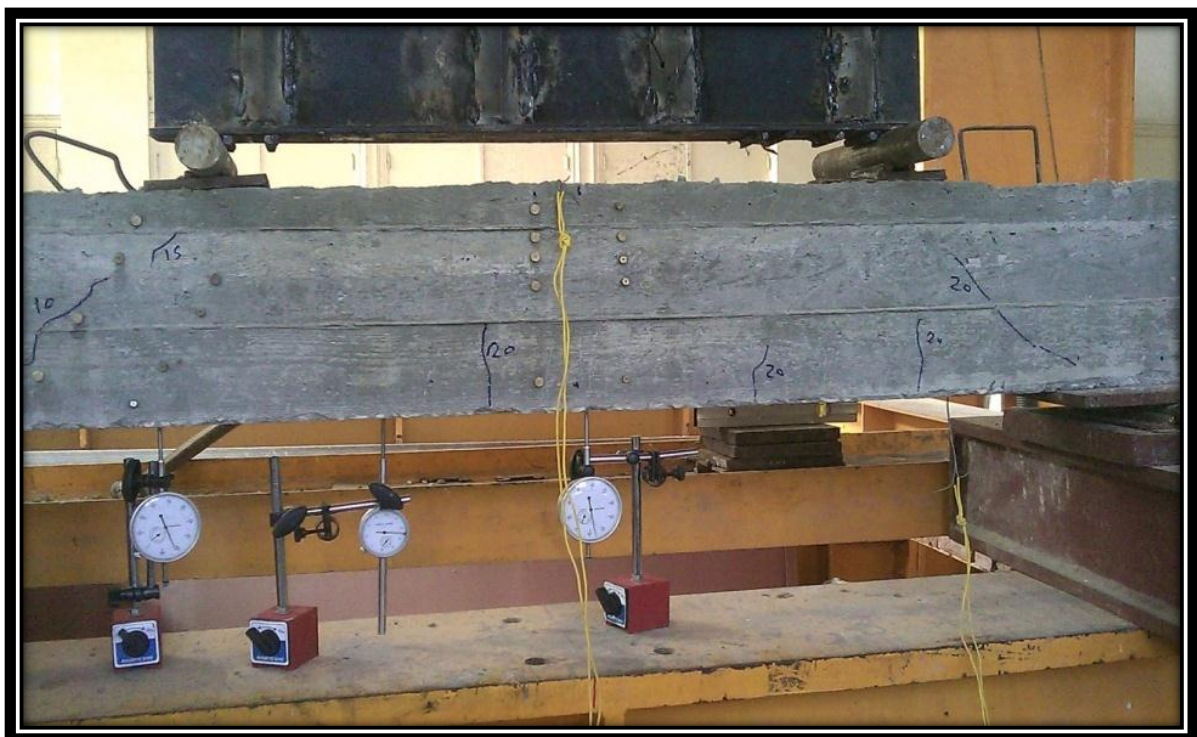
Fig (3.13). Specimen during Testing.

- Test results will be describe on the next chapter in details.

Chapter Four

TEST RESULTS AND ANALYSIS

4.1 Introduction

In spite of the fact that analytical modeling is less expensive and provides the capability to effectively, explore the influence of more parameters than experimental programs, experimental studies remain the most reliable and most efficient approach.

Experimental testing provides physical knowledge and information about the behavior of the experimental of test program. Moreover, test results are essential in calibrating and verifying analytical models.

In this chapter, the results obtained for all tested beams in the experimental program are presented, and analyzed. These results include behavior of tested beams, load-deflection for beams, deformed shape for beams, modes of failures, and shear strength of tested beams. The observed behavior of all the tested beams is also described in this chapter.

4.2 Behavior of Tested Beams

This section describes the most important results observed after testing of the specimens. The effect of changing shear span-depth ratio (a/d) are illustrated in tables and figures, the effect of changing volume fraction of steel fiber on shear resistance are presented on tables and figures.

4.2.1 GROUP A

4.2.1.1 Beam (A-0)

The beam has rectangular - section, of 250 mm in height and 120 mm width and its length was 1500 mm as mentioned before. The beam consisted of

two 16 mm bars used as tension reinforcements and vertical stirrups 7ɸ8/m. Shear span-to-depth ratio for this beam was (1.5). The behavior of this beam can be summarized as follows:

   a- First shear cracks were initiated at 118 KN.

   b- At a load of about 129 KN another shear cracks appeared.

   c- The flexural cracks not appeared in this specimen.

   d- Shear failure took place at a load of 145 KN; this failure was sudden and loud. The crack patterns and load-deflection diagram of this beam are shown respectively in Fig. (4.1) and Fig. (4.2).

   Fig (4.3) indicates the deformed shape of beam deflection along beam length at various values of loads 60 KN, 100 KN, and 145 KN.

Figure (4.1) Crack Patterns for specimen (A-0).

Figure (4.2) Load-Deflection Curve for Specimen (A-0).

Figure (4.3) Deformed Shape for Specimen No (A-0).

4.2.1.2 Beam (A-1)

The beam has rectangular - section, of 250 mm in height and 120 mm width and its length was 1500 mm as mentioned before. The beam consisted of two 16 mm bars used as tension reinforcements and vertical stirrups 7ϕ8/m.

Shear span-to-depth ratio for this beam was 1.5, with fiber content (0.25%) . The behavior of this beam can be summarized as follows:

a- First shear cracks were initiated at 145 KN.

b- At a load of about 150 KN flexural crack was appeared.

c- The first flexural shear crack initiated at a load of about 150 KN. At this stage propagation of the flexural crack was also observed.

d- Shear failure took place at a load of 165 KN. This failure was sudden and loud. The crack patterns and load-deflection diagram of this beam are shown in Fig. (4.4) and Fig. (4.5) respectively.

Fig (4.6) indicate the deformed shape of beam deflection along beam length at various values of loads 60 KN, 110 KN, and 140 KN.

Fig(4.4). Crack Patterns for specimen (A-1).
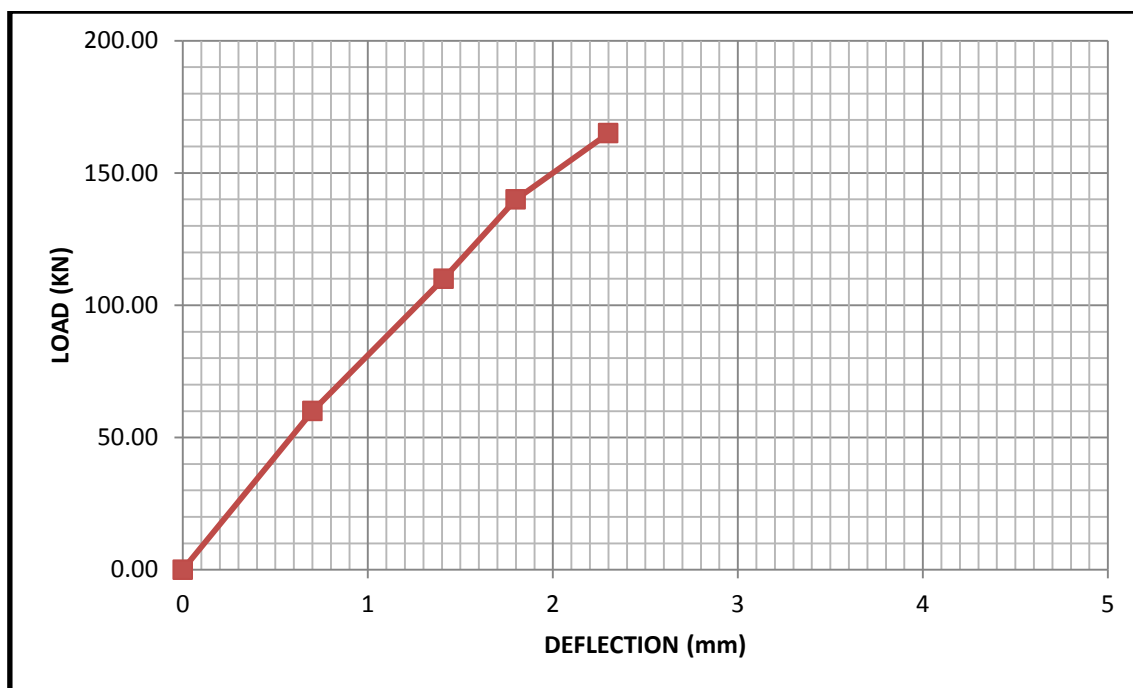
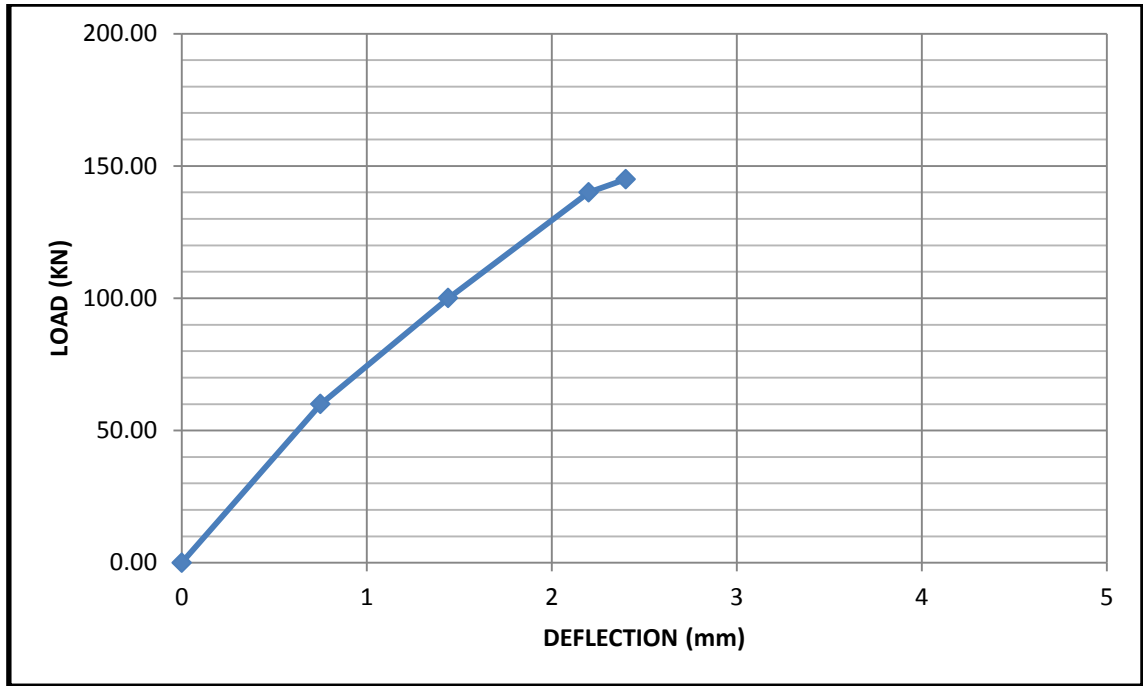Fig (4.5). Load-Deflection curve for specimen (A-1).
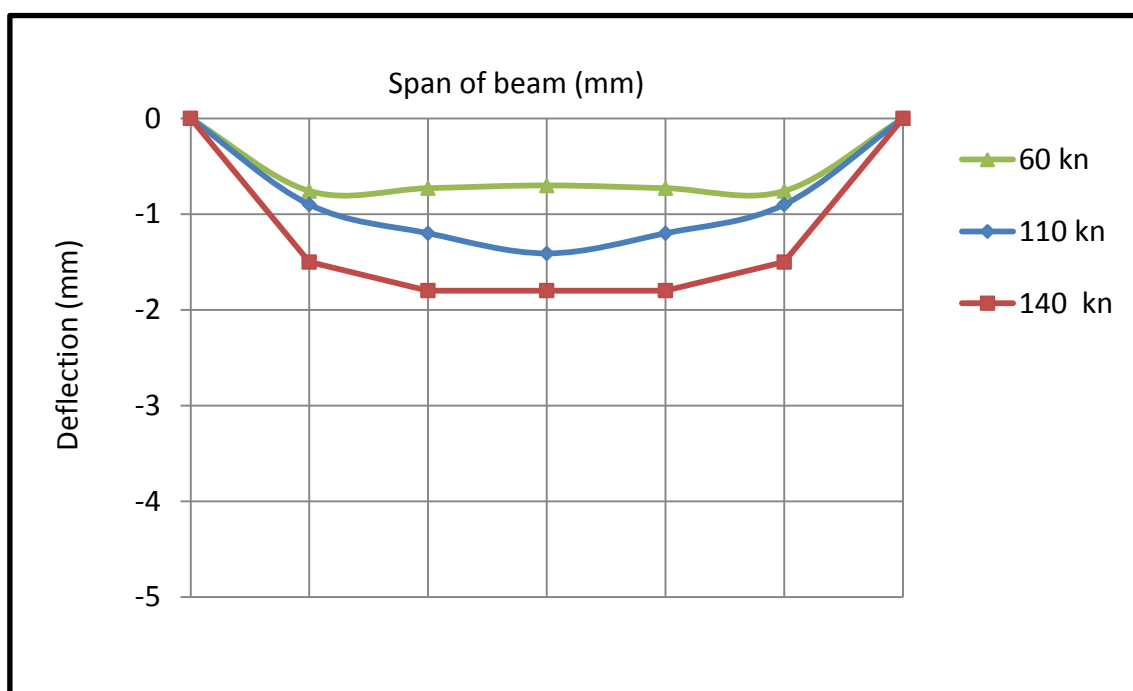
Fig (4.6). Deformed Shape for Specimen No. (A-1).

4.2.1.3 Beam (A-2)

The beam has rectangular - section, of 250 mm in height and 120 mm width and its length was 1500 mm as mentioned before.

The beam consisted of two 16 mm bars used as tension reinforcements and vertical stirrups 7ϕ8/m, Shear span-to-depth ratio for this beam was 1.5, with fiber content (0.5%). The behavior of this beam can be summarized as follows:

a- First shear cracks were initiated at 155 KN.

b- At a load of about 170 KN first flexural crack was initiated.

c- The shear crack propagated until a load of about 175 KN   which the second flexural shear crack initiated, at   thisstage propagation   of flexural crack, and also initiation of three minor   flexural   cracks   was also observed.

d- Shear failure took place at a load of 180 KN. This failure was sudden and loud. The crack patterns and load-deflection diagram of this beam are shown in Fig. 4.7 and Fig. 4.8 respectively.

Fig 4.9 indicate the deformed shape of beam deflection along beam length at various values of loads 60 KN, 90 KN, and 140 KN.
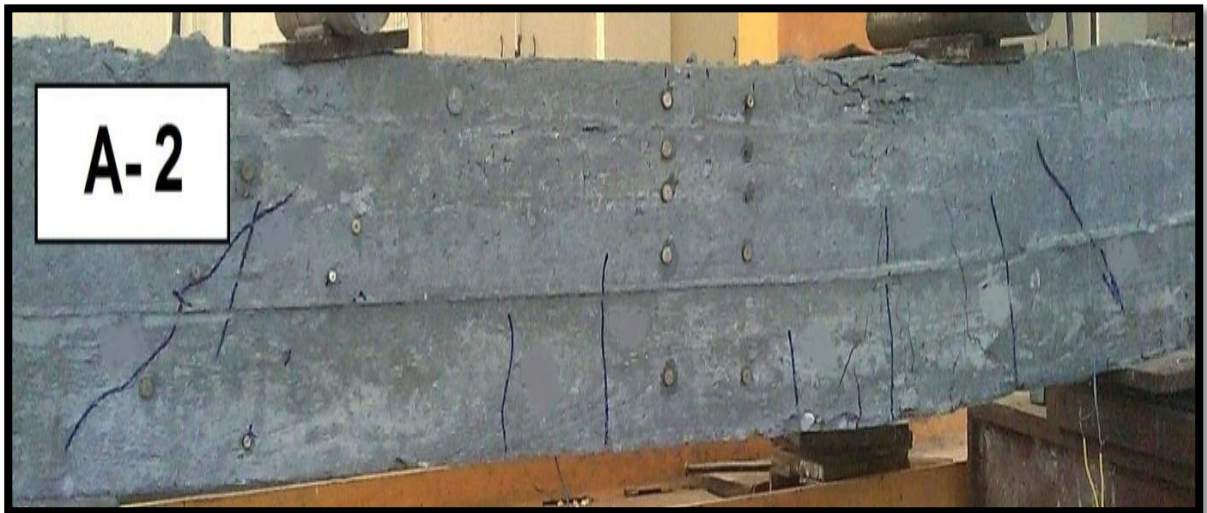
Fig (4.7). Crack Patterns for specimen (A-2).
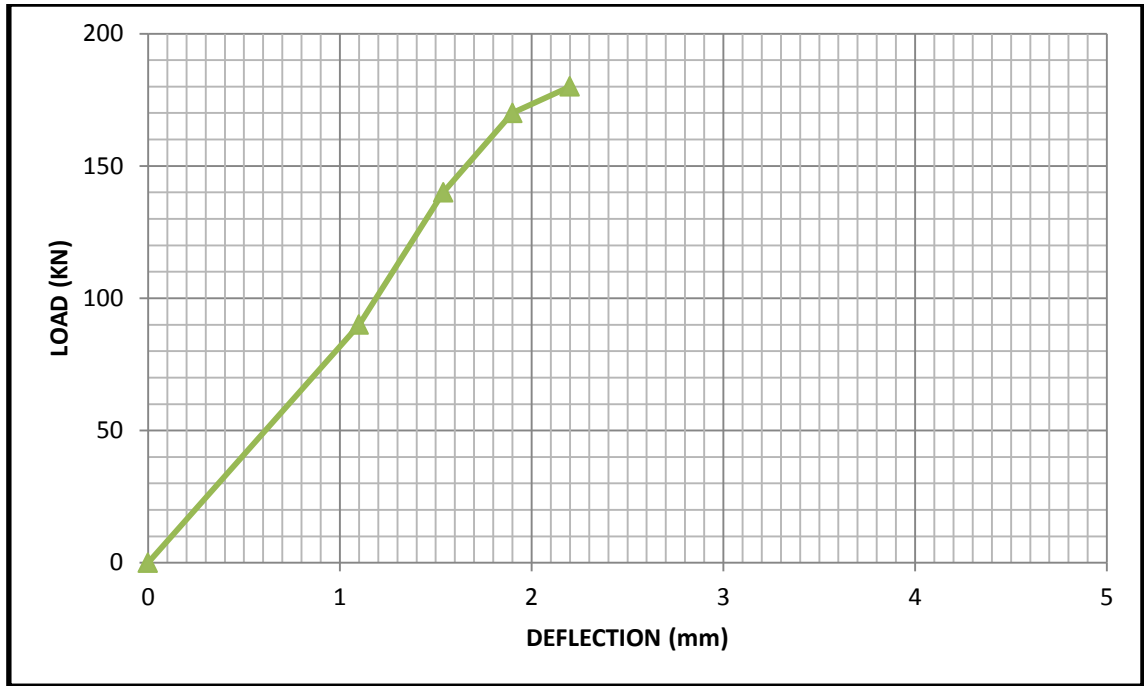
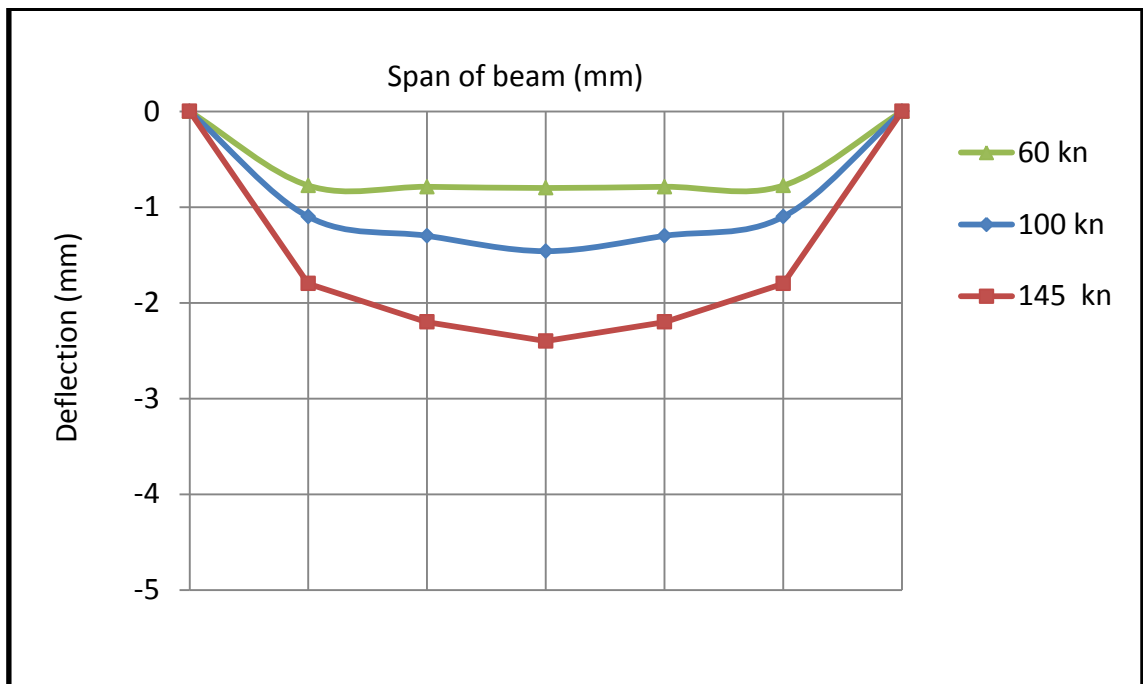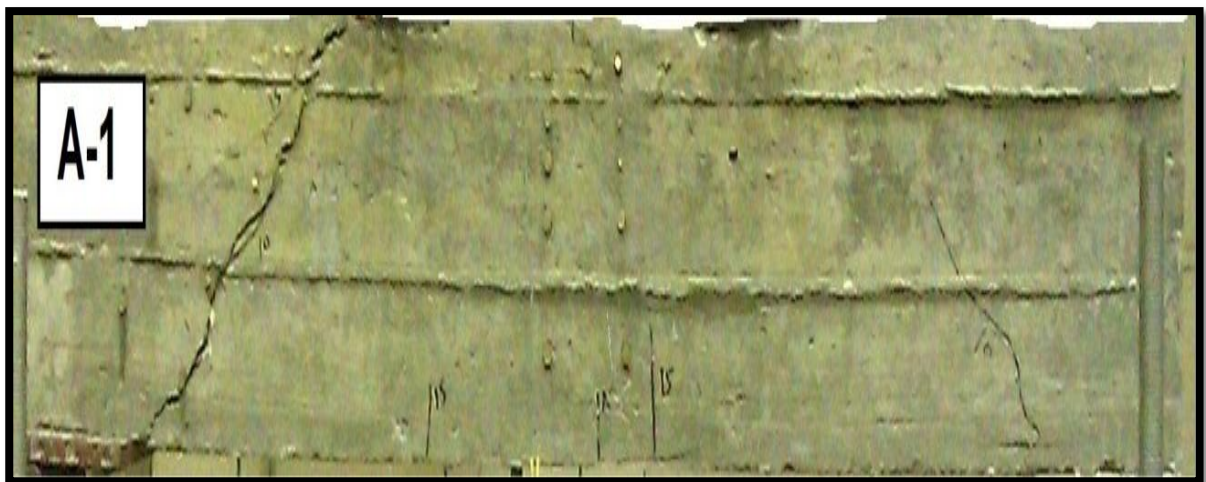Fig (4.8). Load-Deflection curve for specimen (A-2).
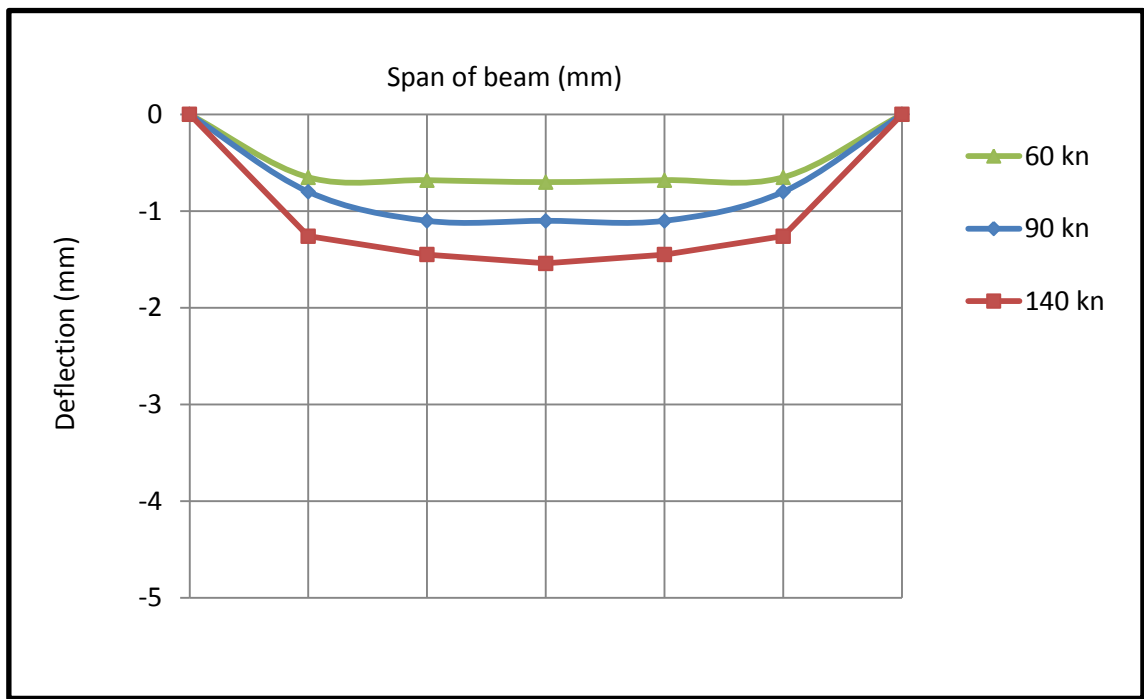
Fig (4.9). Deformed Shape for Specimen No (A-2).

4.2.1.4 Beam (A-3)

The beam has rectangular - section, of 250 mm in hight and 120 mm width and its length was 1500 mm as mentioned before. The beam consisted of

two 16 mm bars used as tension reinforcements and vertical stirrups 7ϕ8/m. Shear span-to-depth ratio for this beam was 1.5, with fiber content (0.75%). The behavior of this beam can be summarized as follows:

    a- First shear cracks were initiated at 165 KN.

    b- At a load of about 180 KN first flexural crack was initiated.

    c- The shear crack propagated until a load of about 195 KN   which the second flexural shear crack initiated, At this stage propagation   of flexural crack, and also initiation of three   minor flexural cracks was also observed.

    d- Shear failure took place at a load of 215 KN. This failure was sudden and loud. The crack patterns and load-deflection diagram of this beam are shown in Fig. 4.10 and Fig. 4.11 respectively.

    Fig 4.12 indicate the deformed shape of beam deflection along beam length at various values of loads 50 KN, 90 KN, and 140 KN.

Fig (4.10). Crack Patterns for specimen (A-3).
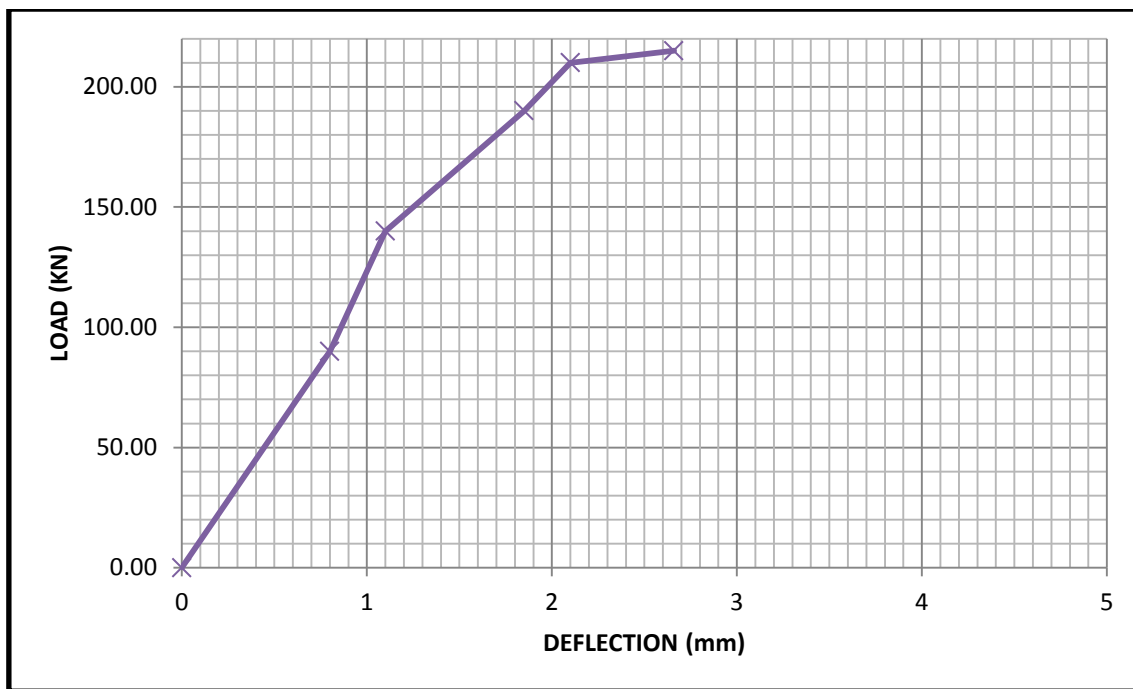
Fig (4.11). Load-Deflection Curve for Specimen (A-3).

Fig (4.12). Deformed Shape for Specimen No (A-3).

4.2.2 GROUP B

4.2.2.1 Beam (B-0)

The beam has rectangular - section, of 250 mm in hight and 120 mm width and its length was 1500 mm as mentioned before. The beam consisted of two 16 mm bars used as tension reinforcements and vertical stirrups 7ϕ8/m. Shear span-to-depth ratio for this beam was 1.7, fiber content of this specimen was (0%). The behavior of this beam can be summarized as follows:

a- First shear cracks were initiated at 130 KN.

b- At a load of about 132 KN another shear crack was appeared.

c- The flexural cracks not appeared in this specimen.

d- Shear failure took place at a load of 135 KN; this failure was sudden and loud. The crack patterns and load-deflection diagram of this beam are shown in Fig. 4.13 and Fig. 4.14 respectively.

Fig 4.15 indicates the deformed shape of beam deflection along beam length at various values of loads 50 KN, 100 KN, and 135 KN.


Fig (4.13). Crack Patterns for specimen (B-0).
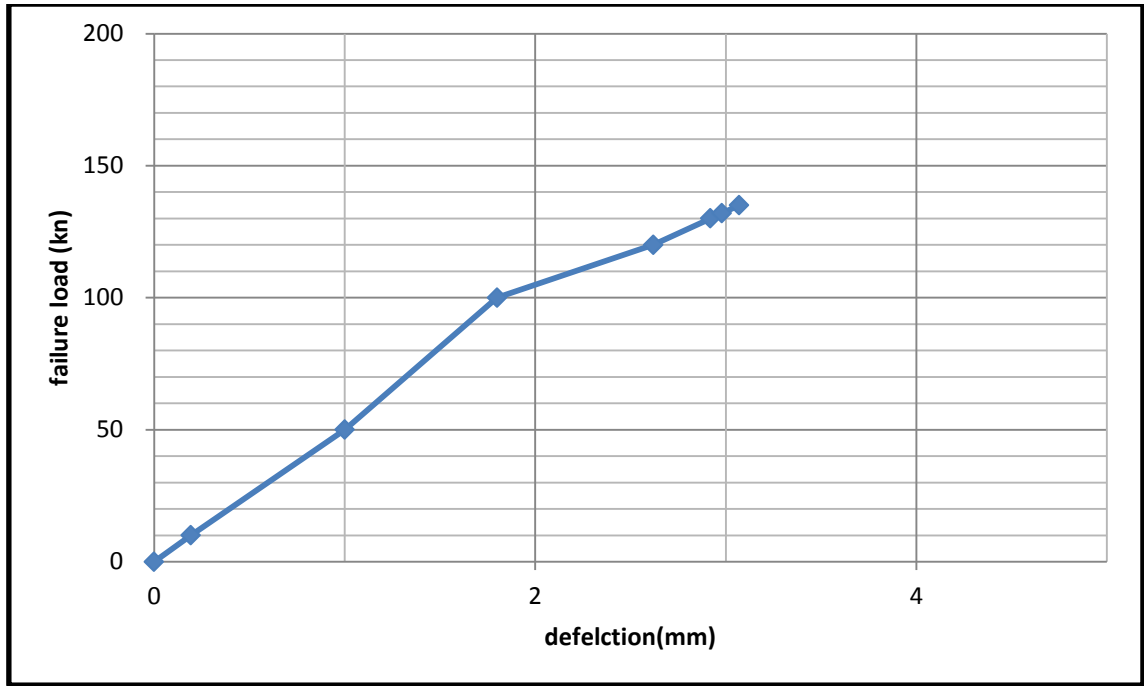
Fig (4.14). Load-Deflection Curve for Specimen (B-0).
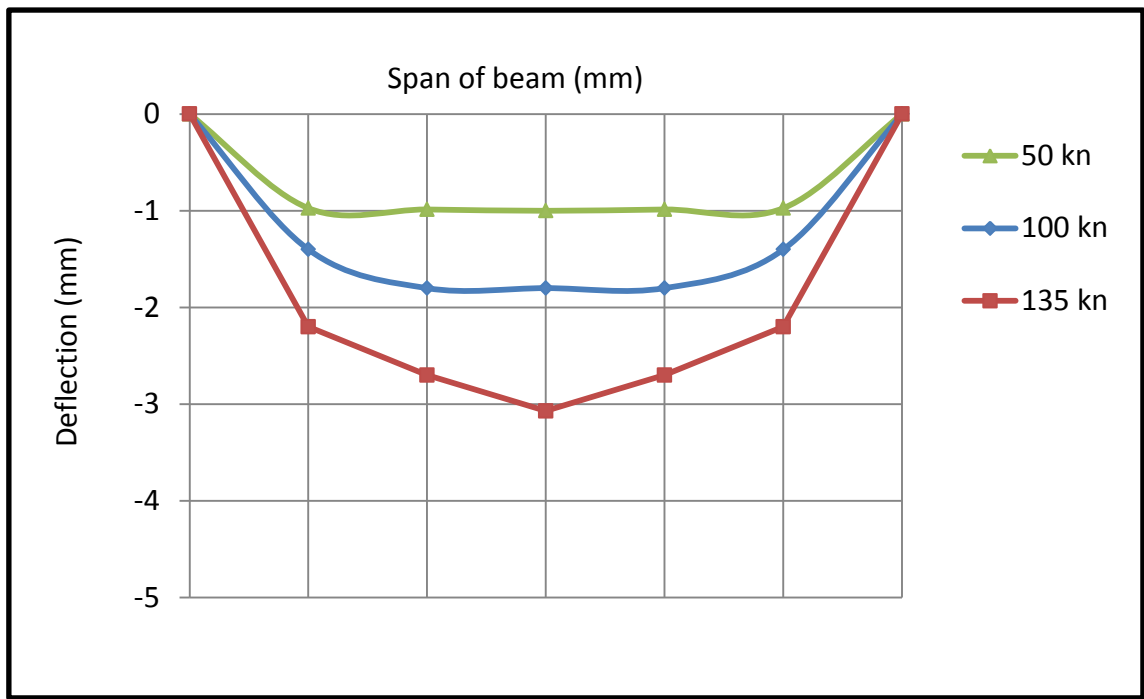
Fig (4.15). Deformed Shape for Specimen No (B-0)

4.2.2.2 Beam (B-1)

The beam has rectangular - section, of 250 mm in height and 120 mm width and its length was 1500 mm as mentioned before. The beam consisted of two 16 mm bars used as tension reinforcements and vertical stirrups 7ϕ8/m.

Shear span-to-depth ratio for this beam was 1.7, with fiber content (0.25%). The behavior of this beam can be summarized as follows:

    a- First shear cracks were initiated at 135 KN.

    b- At a load of about 145 KN another shear crack was initiated.

    c- The shear crack propagated until a load of about 155 KN which shear failure took place. This failure was sudden and loud. The crack patterns and load-deflection diagram of this beam are shown in Fig.   4.16 And Fig. 4.17 respectively.

    Fig 4.18 indicate the deformed shape of beam deflection along beam length at various values of loads 50 KN, 110 KN, and 145 KN.

Fig (4.16). Crack Patterns for specimen (B-1).

Fig (4.17). Load-Deflection Curve for Specimen (B-1).

Fig (4.18). Deformed Shape for Specimen No (B-1).

4.2.2.3 Beam (B-2)

The beam has rectangular - section, of 250 mm in height and 120 mm width and its length was 1500 mm as mentioned before The beam consisted of

two 16 mm bars used as tension reinforcements and vertical stirrups 7ϕ8/m. Shear span-to-depth ratio for this beam was 1.7, with fiber content (0.5%). The behavior of this beam can be summarized as follows:

    a- First shear cracks were initiated at 145 KN.

    b- At a load of about 148 KN first flexural crack was initiated with a small load drop.

    c- The shear crack propagated until a load of about 162 KN which the second flexural shear crack initiated, at this stage Propagation of flexural crack, and also initiation of eight minor flexural cracks was also observed.

    d- shear failure took place at a load of 170 KN. This failure was sudden and loud. The crack patterns and load-deflection diagram of this beam are shown in Fig. 4.19 and Fig. 4.20 respectively.

Fig 4.21 indicate the deformed shape of beam deflection along beam length at various values of loads 50 KN, 100 KN, and 130 KN.

Fig (4.19). Crack patterns for specimen (B-2).

Fig (4.20). Load-Deflection Curve for Specimen (B-2)
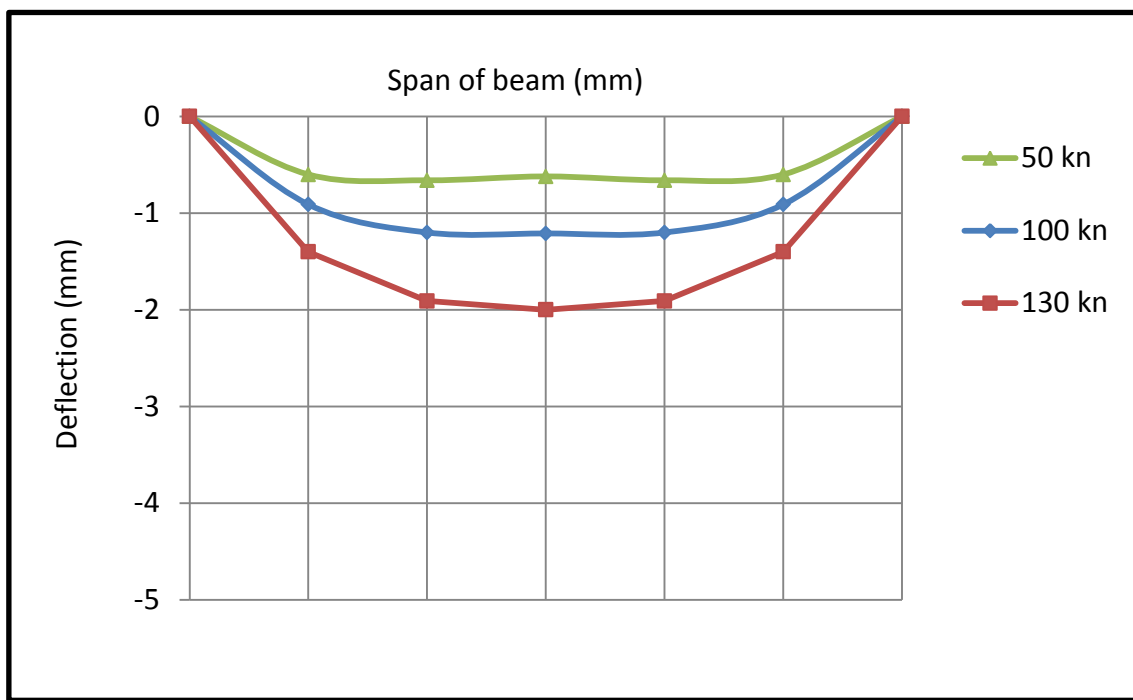
Fig (4.21). Deformed Shape for Specimen No (B-2)

4.2.2.4 Beam (B-3)

The beam has rectangular - section, of 250 mm in height and 120 mm width and its length was 1500 mm as mentioned before. The beam consisted of two 16 mm bars used as tension reinforcements and vertical stirrups 7ϕ8/m. Shear span-to-depth ratio for this beam was 1.7, with fiber content (0.75%). The behavior of this beam can be summarized as follows:

a- First shear cracks were initiated at 156 KN.

b- At a load of about 161 KN first flexural crack was initiated.

c- The shear crack propagated until a load of about 178 KN, which the second flexural shear crack initiated with drop in load, at thisstage propagation of flexural crack, and initiation of three minor flexural cracks was observed.

d- Shear failure took place at a load of 195 KN. This failure was sudden and loud. The crack patterns and load-deflection diagram of this beam are shown in Fig. 4.22 and Fig. 4.23 respectively.

Fig 4.24 indicates the deformed shape of beam deflection along beam length at various values of loads 50 KN, 130 KN, and 180 KN.


Fig (4.22). Crack Patterns for specimen (B-3).

Fig (4.23). Load-Deflection Curve for Specimen (B-3)
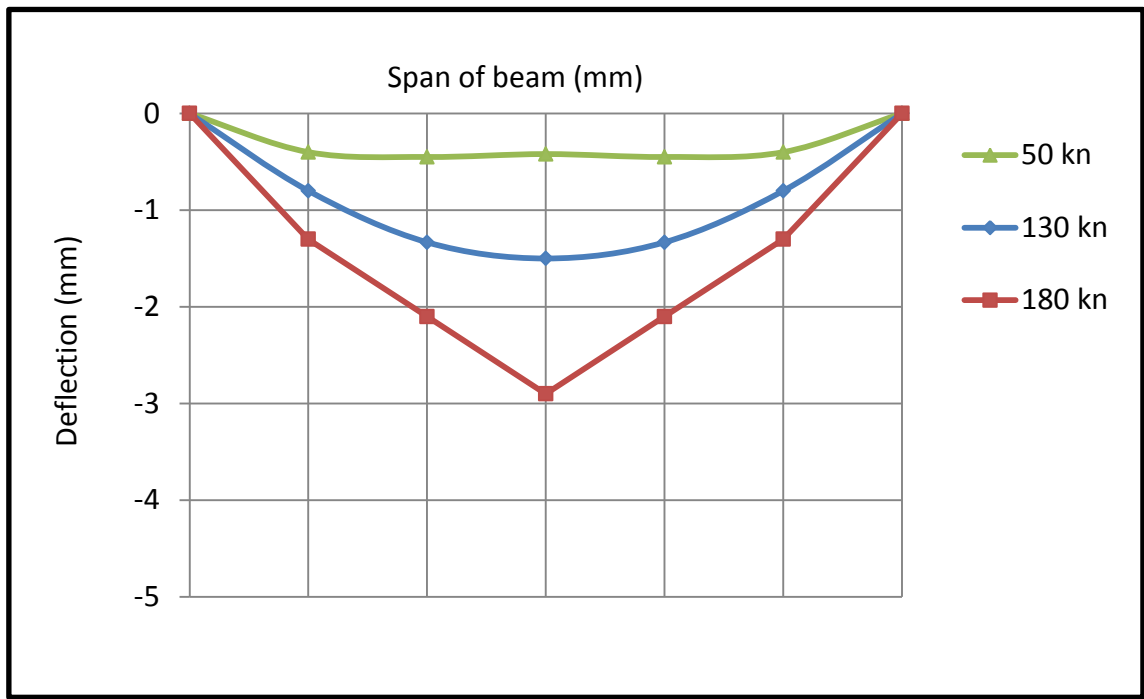
Fig (4.24) Deformed Shape for Specimen No (B-3)

4.2.3 GROUP C

4.2.3.1 Beam (C-0)

The beam has rectangular - section, of 250 mm in height and 120 mm width and its length was 1500 mm as mentioned before. The beam consisted of two 16 mm bars used as tension reinforcements and vertical stirrups 7ϕ8/m. Shear span-to-depth ratio for this beam was 2.2, with zero fiber content. The behavior of this beam can be summarized as follows:

a- First shear cracks were initiated at 80 KN.

b- At a load of about 105 KN small shear crack was initiated.

c- The shear crack propagated until a load of about 112 KN, which the second flexural shear crack initiated with a drop in load. At this stage, propagation of flexural, crack, flexural shear crack and initiation of six minor flexural cracks in st.4 was also observed.

d- Shear failure took place at a load of 115 KN. The crack patterns and load-deflection diagram of this beam are shown in Fig. 4.25 and Fig. 4.26 respectively.

Fig 4.27 indicates the deformed shape of beam deflection along beam length at various values of loads 50 KN, 100 KN, and 110 KN.
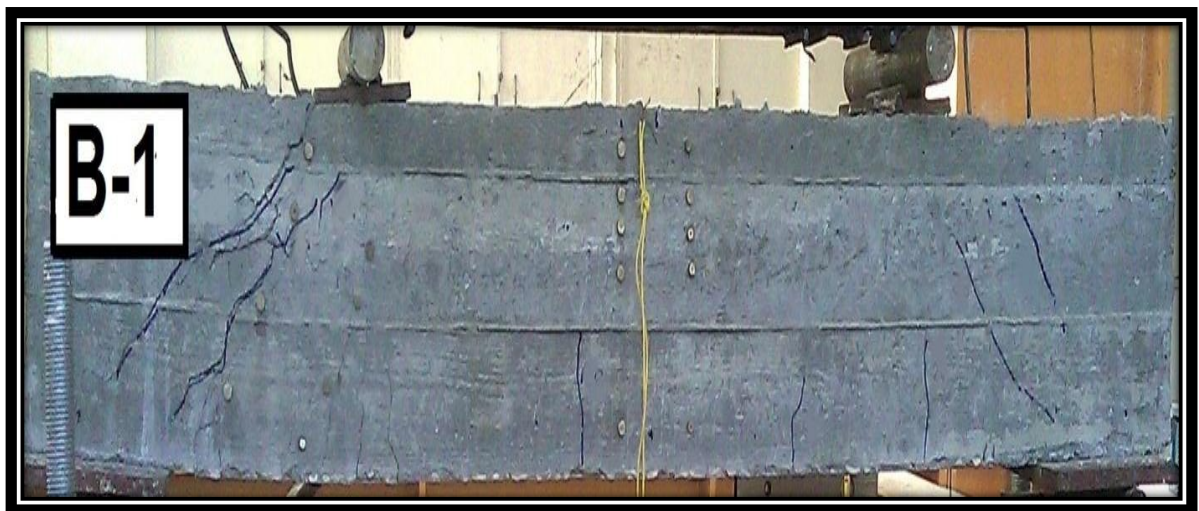

Fig (4.25) Crack Patterns for specimen (C-0).
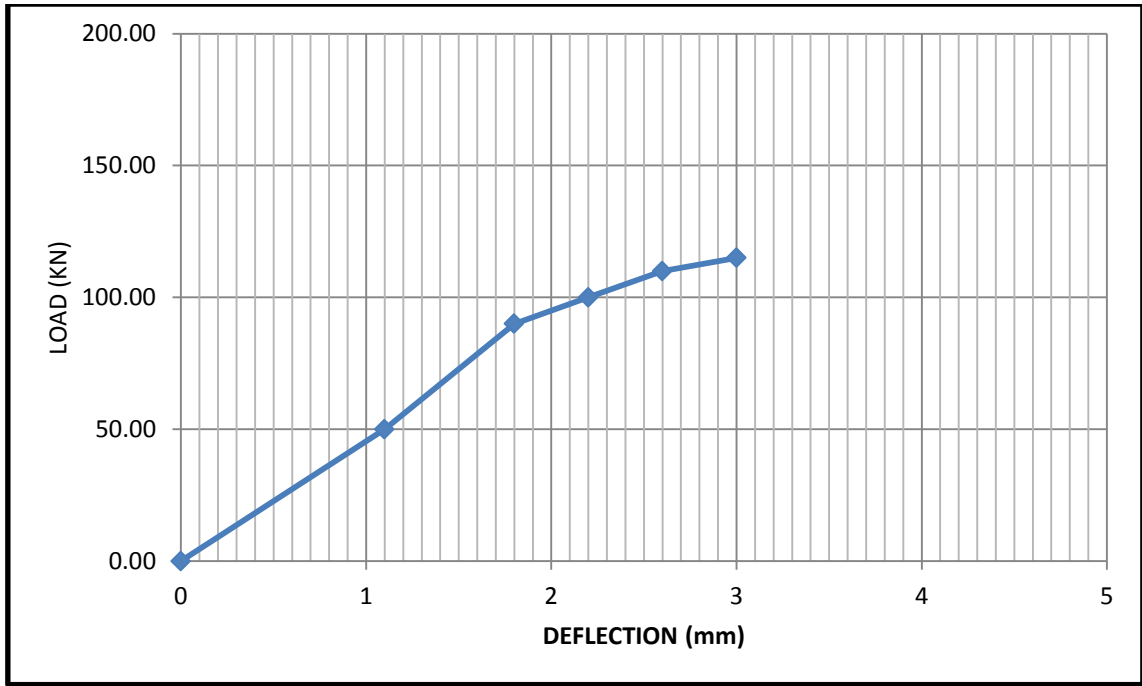
Fig (4.26) Load-Deflection Curve for Specimen (C-0).
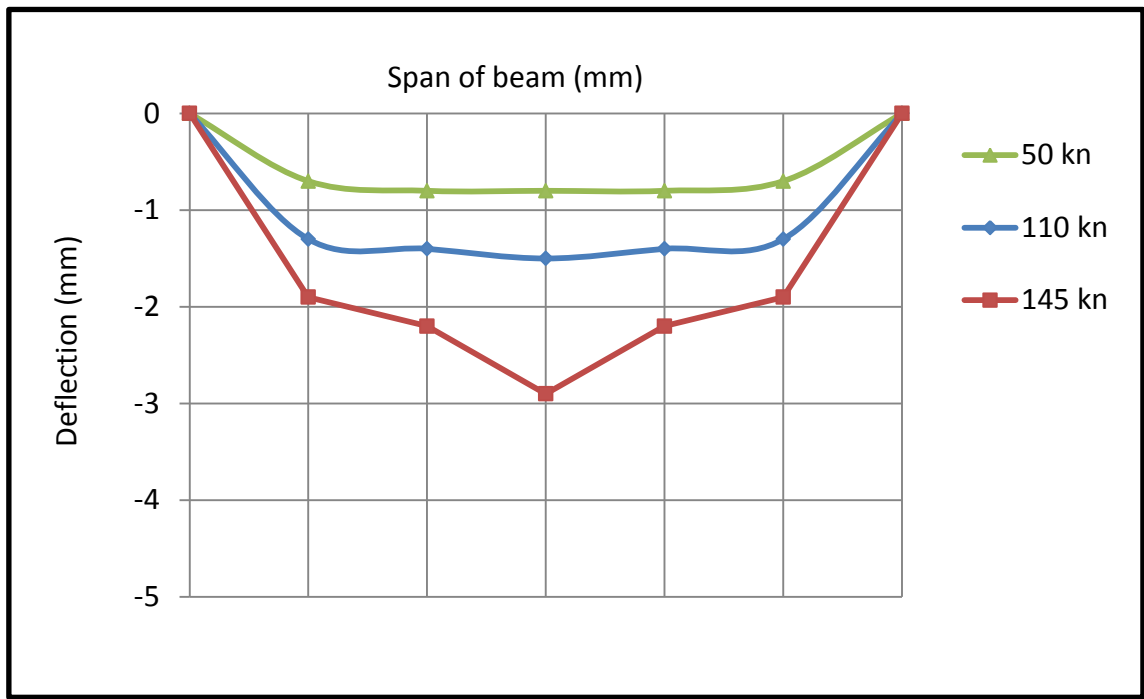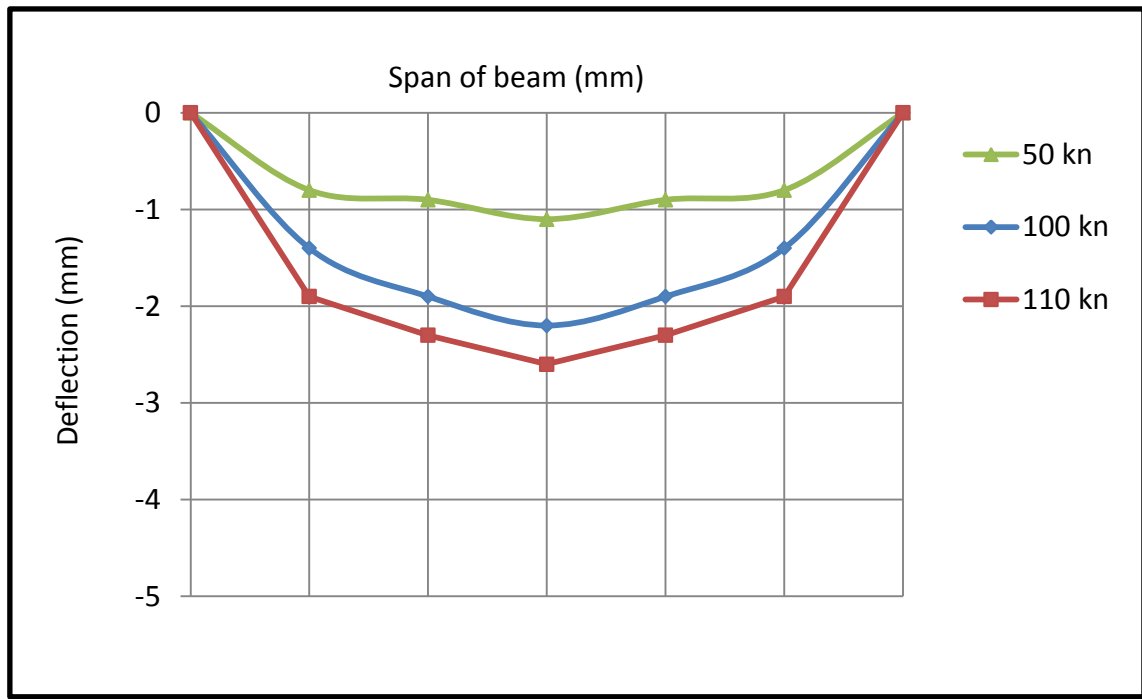

Fig (4.27). Deformed Shape for Specimen No (C-0).

4.2.3.2 Beam (C-1)

The beam has rectangular - section, consisted of 250 mm in thickness and 120 mm width and its length was 1500 mm as mentioned before. The

beam consisted of two 16 mm bars used as tension reinforcements and vertical stirrups 7ϕ8/m. Shear span-to-depth ratio for this beam was 2.2,with fiber content (0.25%).

The behavior of this beam can be summarized as follows:

a- First shear cracks were initiated at 111 KN.

b- At a load of about 119 KN flexure shear crack was initiated.

c- The shear crack propagated until a load of about 126 KN, which the second flexural shear crack initiated with a drop in load.

d- Shear failure took place at a load of 130 KN. The crack patterns andload-deflection diagram of this beam are shown in Fig.   4.28 And Fig. 4.29 respectively.

Fig 4.30 indicates the deformed shape of beam deflection along beam length at various values of loads 50 KN, 90 KN, and 130 KN.

Fig(4.28). Crack Patterns for specimen (C-1).
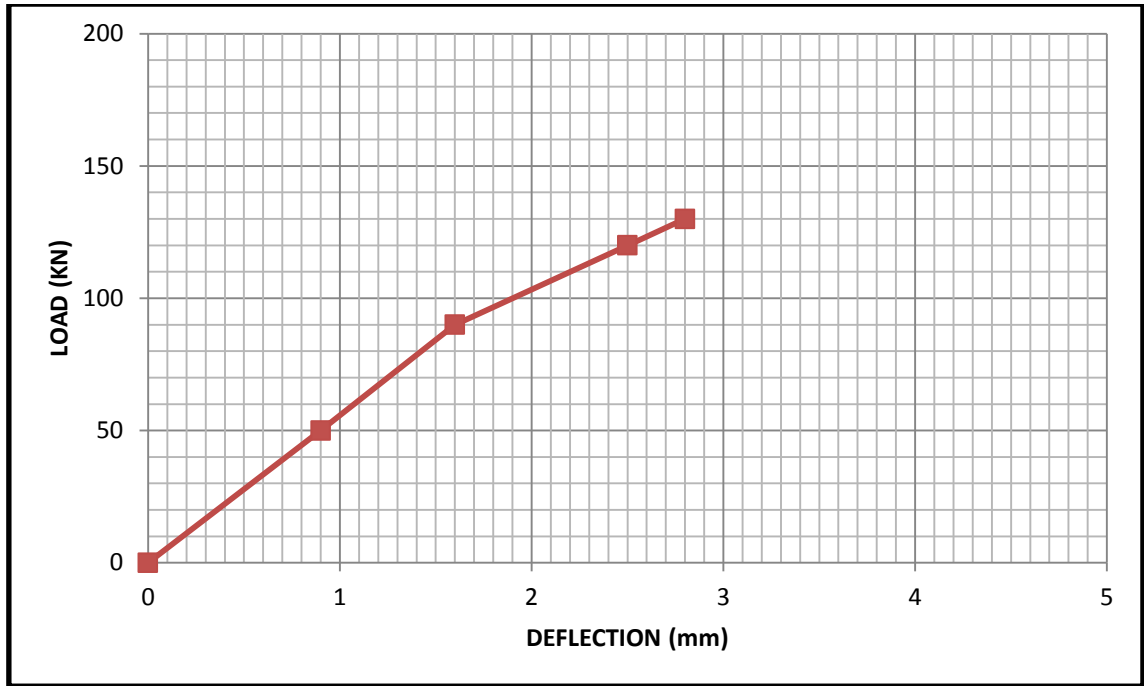
Fig (4.29.) Load-Deflection Curve for Specimen (C-1).
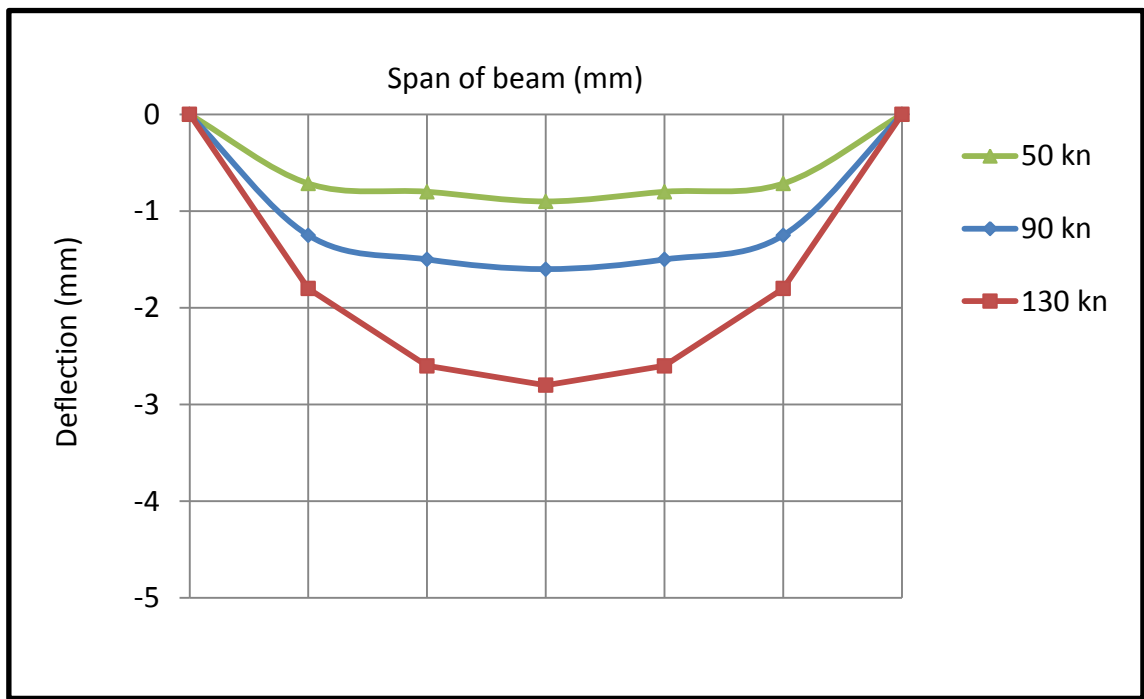
Fig (4.30). Deformed Shape for Specimen No (C-1).

4.2.3.3 Beam (C-2)

The beam has rectangular - section, consisted of 250 mm in thickness and 120 mm width and its length was 1500 mm as mentioned before. The

beam consisted of two 16 mm bars used as tension reinforcements and vertical stirrups 7ϕ8/m. Shear span-to-depth ratio for this beam was 2.2, with fiber content (0.5%). The behavior of this beam can be summarized as follows:

a- First shear cracks were initiated at 114 KN.

b- At a load of about 124 KN flexure crack was initiated.

c- At a load of about 133 KN shear crack was propagated.

d- diagonal shear failure took place at a load of 148 KN. This failure was sudden and loud. The crack patterns and load-deflection diagram of this beam are shown respectively in Fig. 4.31 and Fig. 4.32.

Fig 4.33 indicates the deformed shape of beam deflection along beam length at various values of loads 40 KN, 90 KN, and 148 KN.
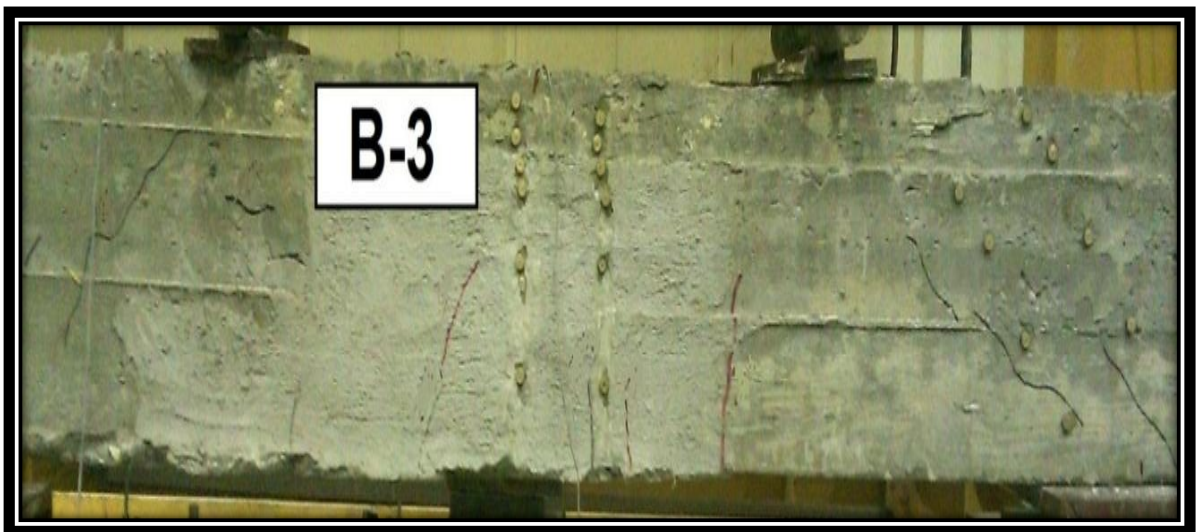

Fig (4.31). Crack Patterns for specimen (C-2).
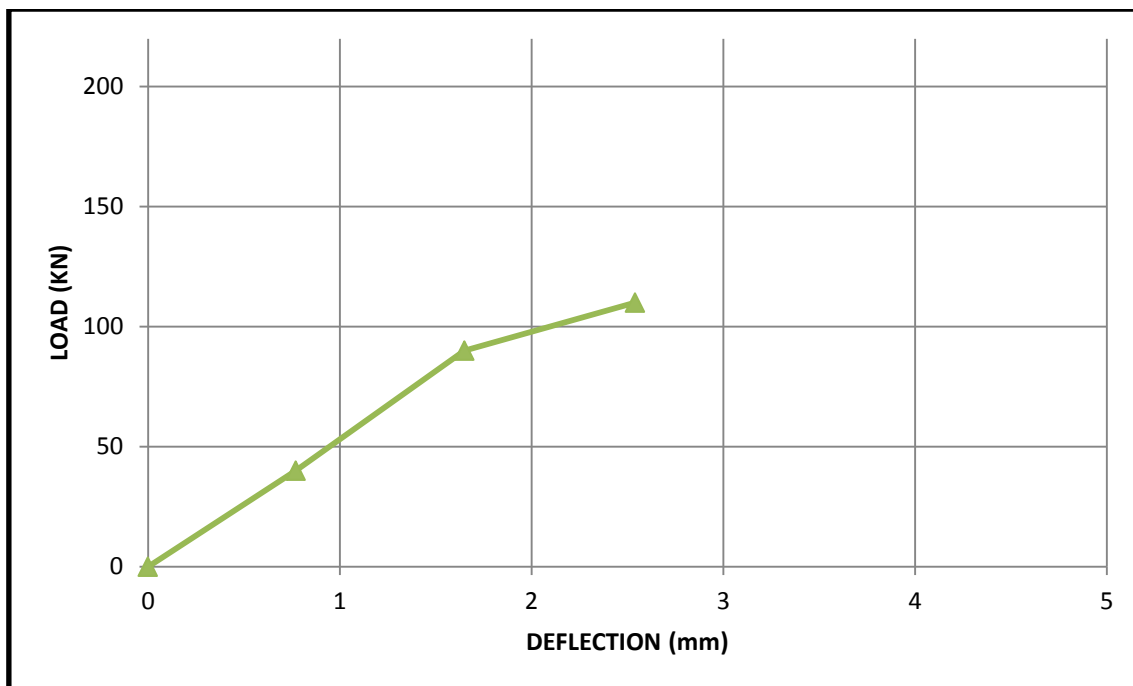
Fig (4.32). Load-Deflection Curve for Specimen (C-2).
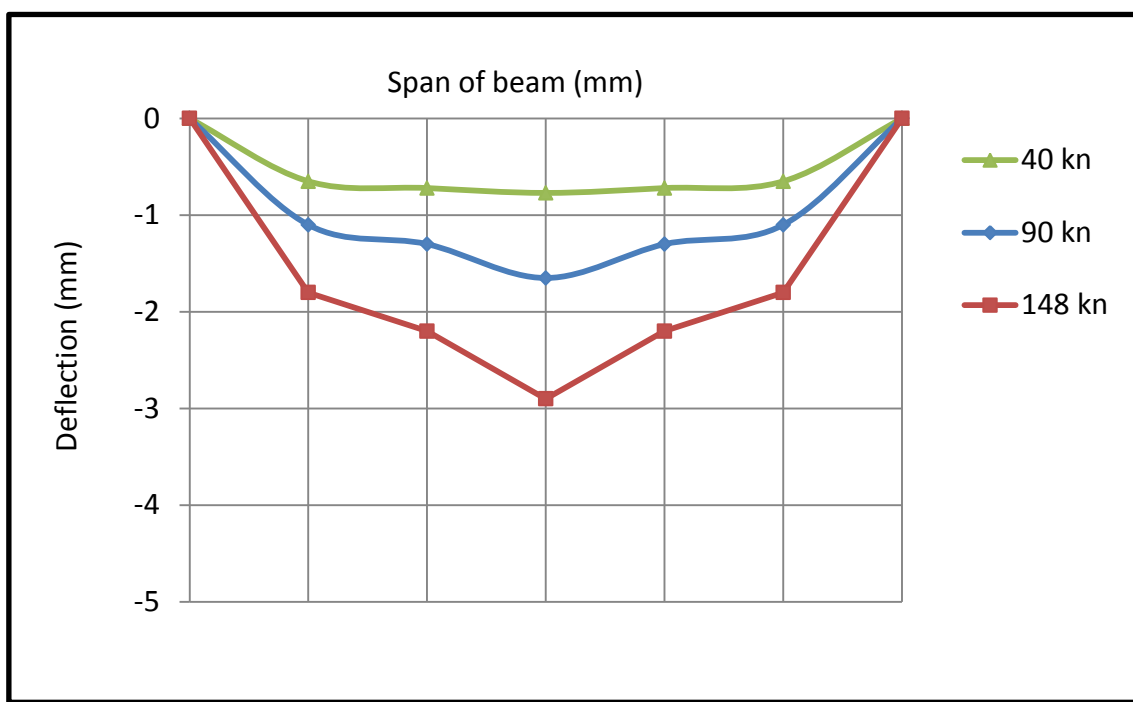
Fig (4.33). Deformed Shape for Specimen No (C-2).

4.2.3.4 Beam (C-3)

The beam has rectangular - section, consisted of 250 mm in thickness and 120 mm width and its length was 1500 mm as mentioned before. The beam consisted of two 16 mm bars used as tension reinforcements and vertical stirrups 7ϕ8/m. Shear span-to-depth ratio for this beam was 2.2, with fiber content (0.75%). The behavior of this beam can be summarized as follows:

a- First shear cracks were initiated at 122 KN.

b- At a load of about 133 KN flexure crack was initiated.

c- At a load of about 145KN flexure crack was propagated.

d- Diagonal shear failure took place at a load of 160 KN. This failure was sudden and loud. The crack patterns and load-deflection diagram of this beam are shown in Fig. 4.34 and Fig. 4.35 respectively.

Fig 4.36 indicates the deformed shape of beam deflection along beam length at various values of loads 40 KN, 90 KN, and 130 KN.


Fig (4.34). Crack Patterns for specimen (C-3).
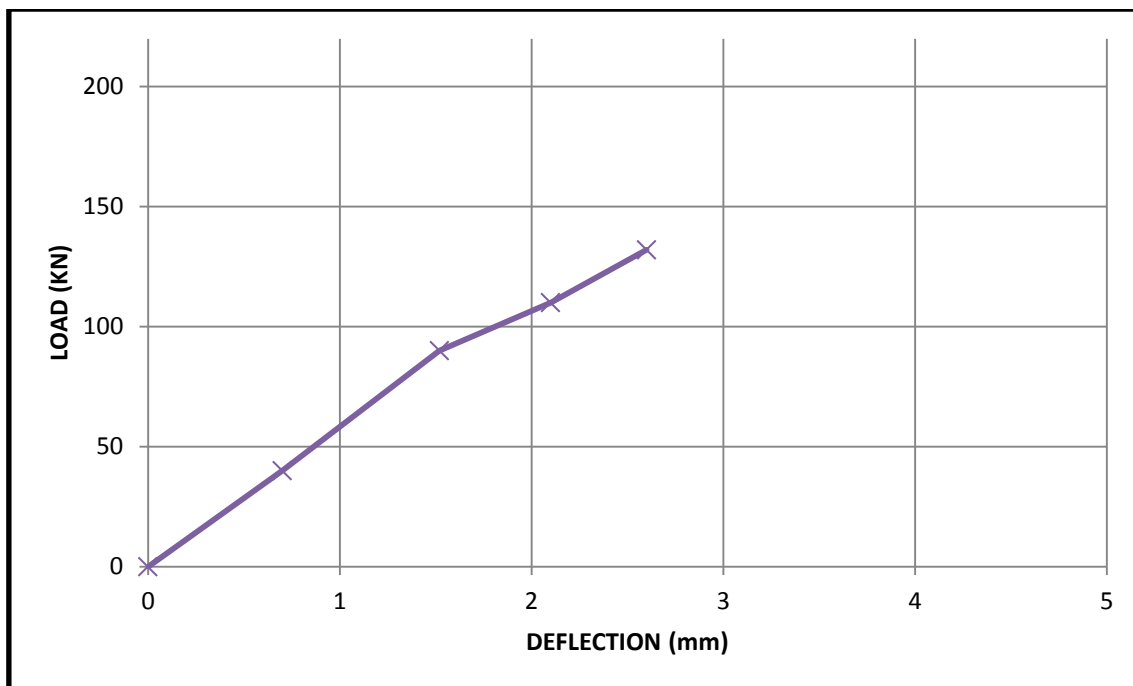
Fig (4.35). Load-Deflection Curve for Specimen (C-3).

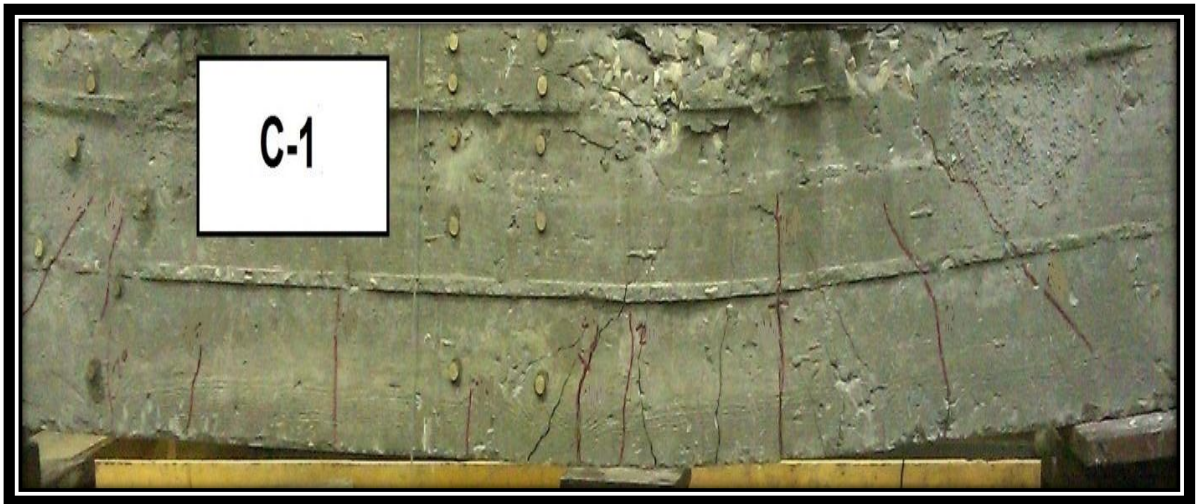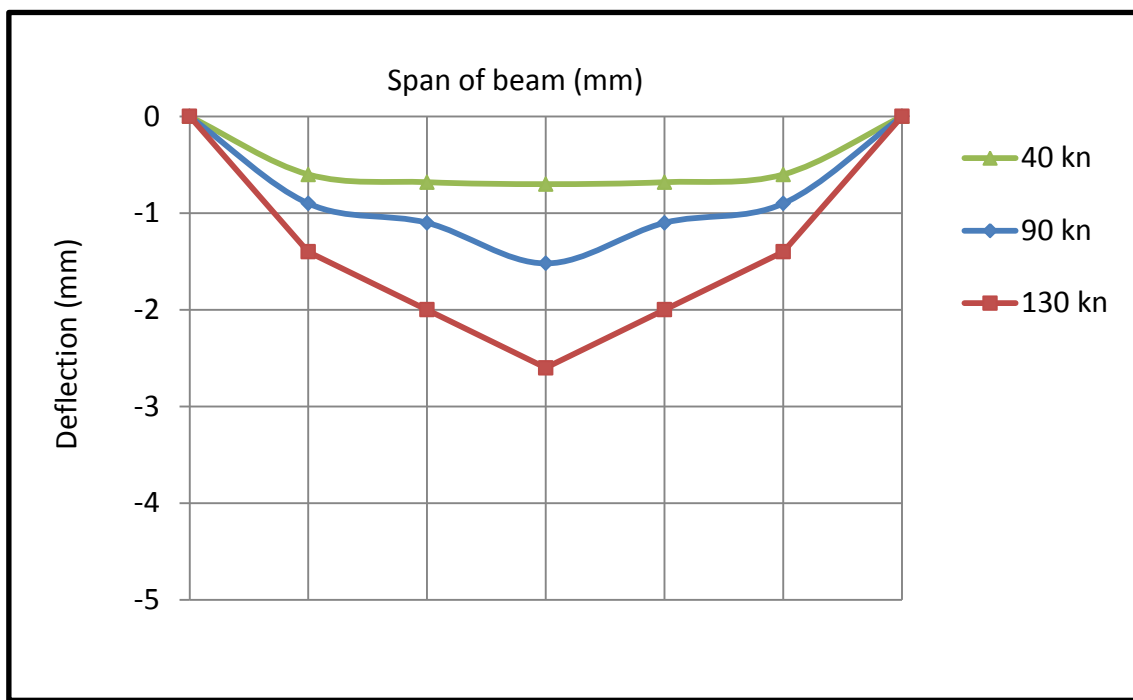Fig (4.36). Deformed Shape for Specimen No (C-3).

4.3 Failure Loads and Mode of Failure

Failure loads for all beams and failure modes are represented in Table(4.1).

Table (4.1). Failure Loads and Mode of Failure.

Group no.	Specimens	a/d	V_f	Failure Load (KN)	Mode of Failure
A	A-0	1.5	0.00%	145	(shear failure)
	A-1	1.5	0.25%	165	(shear failure)
	A-2	1.5	0.50%	180	(shear failure)
	A-3	1.5	0.75%	215	(shear failure)
B	B-0	1.7	0.00%	135	(shear failure)
	B-1	1.7	0.25%	155	(shear failure)
	B-2	1.7	0.50%	170	(shear failure)
	B-3	1.7	0.75%	195	(shear failure)
C	C-0	2.2	0.00%	115	(shear failure)
	C-1	2.2	0.25%	130	(shear failure)
	C-2	2.2	0.50%	148	(diagonal shear failure)
	C-3	2.2	0.75%	160	(diagonal shear failure)

4.4 Analysis of Experimental Results

We will discuss the comparison between the results to study the effect of two variables on shear strength of beams, mode of failure of beams, and deflection of beams these variables are,

1. The effect of variation of volume fraction of steel fibers (V_f).

2. The effect of variation of shear span to depth ratio (a/d).

4.4.1.1 Analysis the results of group (A) included beam (A-0), beam (A-1), beam (A-2) and beam (A-3):

All the beams failed as it was expected. The values of ultimate shear, failure modes, and percentage of load increase based on the ultimate load of control beam are given in Table (4.2). As shown in this Table, the discrete steel

fiber increased the ultimate capacity of R.C beams. The percentage of increase reached to about 48.2 % when the fiber ratio was increased to 0.75 % for the same span to depth ratio.

Crack pattern and failure mode for beams with and without steel fiber are shown in Table. The failure of concrete without steel fiber showed a brittle failure behavior compared to specimens with steel fiber. The higher the fibers ratio, the brisker failure of specimens.

The cracking pattern and failure mode of the beams were closely observed. When loads were applied to beams with steel fiber vertical cracks appeared in the mid span region. Initially the cracks were of small width and concentrated in the mid span region with angles vertical. However with further increase of load, the depth and width of cracks increased. The angles of cracks became small and turned diagonal. The change in the angle of cracks can be attributed to the cantilever action of the cracked concrete restrained by the longitudinal reinforcement in the tension zone. When load was further increased, the depth of some of the diagonal cracks further enhanced and crossed into the compression zone of the beams, which ultimately caused the failure of the beams as the cracks extended further towards the point of application of loads. This kind of failure is also called "diagonal tension" failure, which was observed in the beams having fiber of (0, 0.25) percent. For beams having fiber (0.5, 0.75) percent, the failure has been observed predominantly due to shear cracks, which are also called the shear failure. Here the flexural cracks are dominant in the middle third region and the angle of failure is large.

Table (4.2) Effect of Fiber on Specimens Group A.

Group	a/d	Specimen no.	v_f	Failure load(KN)	Increase ratio	Mode of failure
A	1.5	A-0	0%	145	CONTROL	Shear failure
		A-1	0.25%	165	13.80%	Shear failure
		A-2	0.5%	180	24.13%	Shear failure
		A-3	0.75%	215	48.20%	Shear failure

4.4.1.2 Load Deflection Curves for group A

Figure 4.37 shows the relationship between the applied load and mid-span deflection for different steel fiber ratio (group A). While increase ratio of steel fiber enhances the stiffness of beam when beam (A-0) start cracking at load equal 118 KN the deflection of beam at this load equal 1.8mm while beam (A-3) cracks at load 165 the deflection was 1.5mm. Moreover, it is clear that the increase of steel fiber ratio decreases the ultimate deflection as shown in Fig. 4.37 and in turn, increases shear capacity of beams, and increase stiffness as shown on table (4.3).

Table (4.3) Initial Stiffness for Group A.

Group	a/d	Specimen No.	Stiffness(KN/mm)	Increase Ratio
A	1.5	A-0	65.56	CONTROL
		A-1	70.45	7.40%
		A-2	97.06	48.00%
		A-3	110.00	67.70%
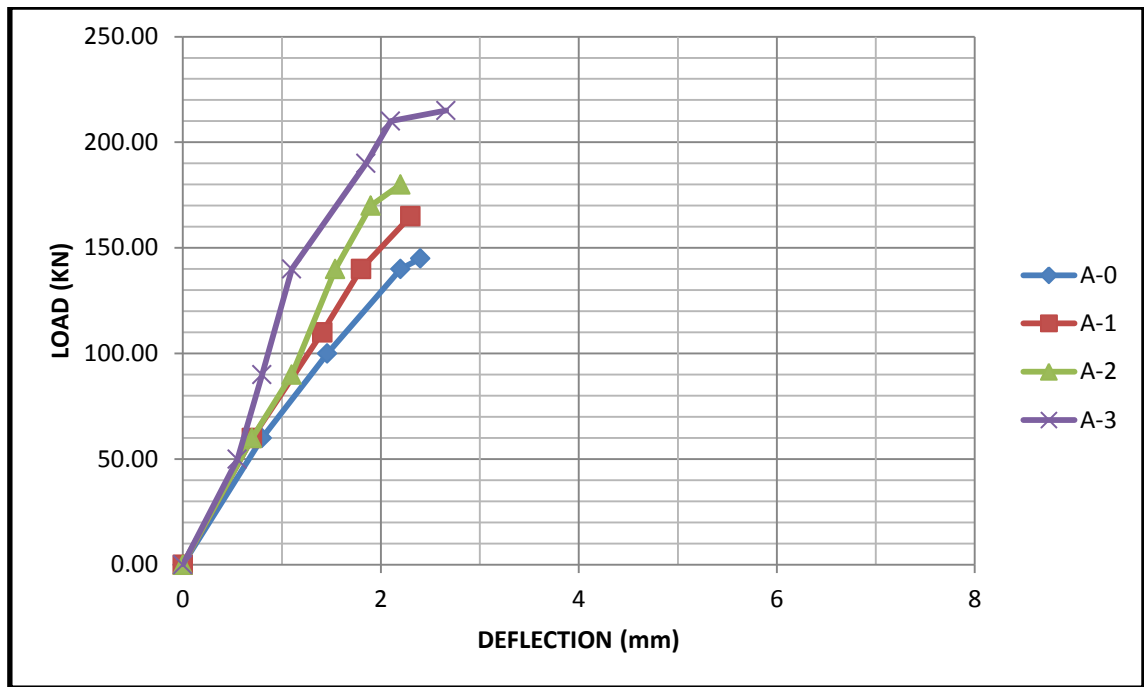
Fig (4.37). Load - Deflection Curves for Group A

4.4.1.3 Energy Absorption Capacity

Energy absorption capacity of all the specimens was calculated as area under load deflection curve. Table (4.4) shows the results and it can be observed that as fiber content increased, the energy absorption capacity increased and for 0.75% fiber, an increase of 42.6% was found. This can be attributed to the effect of fibers in bridging the crack and hence enhancement in energy absorption capacity.

Table (4.4) Energy Absorption Capacity for Group A.

Group No	Specimen No	v_f	Energy Absorption Capacity(KN-mm)
	A-0	0%	6.4×10^2
A	A-1	0.25%	8×10^2
	A-2	0.5%	8.6×10^2
	A-3	0.75%	11.2×10^2

4.4.2.1 Analysis the Results of Group (B) Included Beam (B-0), Beam (B-1), Beam (B-2) and Beam (B-3).

All the beams failed as it was expected. The values of ultimate shear, failure modes, and percentage of load increase based on the ultimate load of control beam are given in Table (4.5). As shown in this Table, the discrete steel fiber increased the ultimate capacity of R.C beams. The percentage of increase reached to about 44.5 % when the fiber ratio was increased to 0.75 % at the same span to depth ratio.

Crack pattern and failure mode for beams with and without steel fiber are shown in Table. The failure of concrete without steel fiber showed a brittle failure behavior compared to specimens with steel fiber. The higher the fibers ratio, the brisker failure of specimens.. When loads were applied to beams with steel fiber vertical cracks appeared in the mid span region. Initially the cracks were of small width and concentrated in the mid span region with angles being more or less vertical. However with further increase of load, the depth and width of cracks increased. The angles of cracks became small and turned diagonal. The change in the angle of cracks can be attributed to the cantilever action of the cracked concrete restrained by the longitudinal reinforcement in the tension zone. When load was further increased, the depth of some of the diagonal cracks further enhanced and crossed into the compression zone of the beams, which ultimately caused the failure of the beams as the cracks extended further towards the point of application of loads. This kind of failure is also called "diagonal tension" failure, which was observed in the beams having fiber of zero, 0.25 %. For beams having fiber 0.5, 0.75 % the failure has been observed predominantly due to shear cracks, which are also called the shear failure.

Here the flexural cracks are dominant in the middle third region and the angle of failure is large. These represent the values of a/d, where the beams are about to achieve the flexural strength before shear failure.

Table (4.5) Effect of Fiber on Specimens Group B.

Group	a/d	Specimen no.	v_f	Failure load(KN)	Increase ratio	Mode of failure
B	1.7	B-0	0%	135	Control	Shear failure
		B-1	0.25%	155	15%	Shear failure
		B-2	0.5%	170	25.90%	Shear failure
		B-3	0.75%	195	44.50%	Shear failure

4.4.2.2 Load Deflection Curves for group B

Figure 4.38 shows the relationship between the applied load and mid-span deflection for different steel fiber ratio (group B). While increase ratio of steel fiber enhances the stiffness of beam. when beam (B-0) start cracking at load equal 130 KN the deflection of beam at this load equal 2.8 mm while beam (B-3) cracks at load 156 the deflection was 3.1 mm. Moreover, it is clear that the increase of steel fiber ratio decreases the ultimate deflection as shown in Fig. 4.37 and in turn, increases shear capacity of beams. Moreover, it is clear that the increase of steel fiber ratio decrease the ultimate deflection as shown in Fig. 4.38 and in turn increases shear capacity of beams, and enhance the stiffness of beam as shown on table (4.6).

Table (4.6) Initial Stiffness for Group B.

| Group	a/d	Specimen No.	Stiffness(KN/mm)	Increase Ratio
B	1.7	B-0	46.43	control
		B-1	48.21	4%
		B-2	50.00	7.70%
		B-3	50.32	8.40%
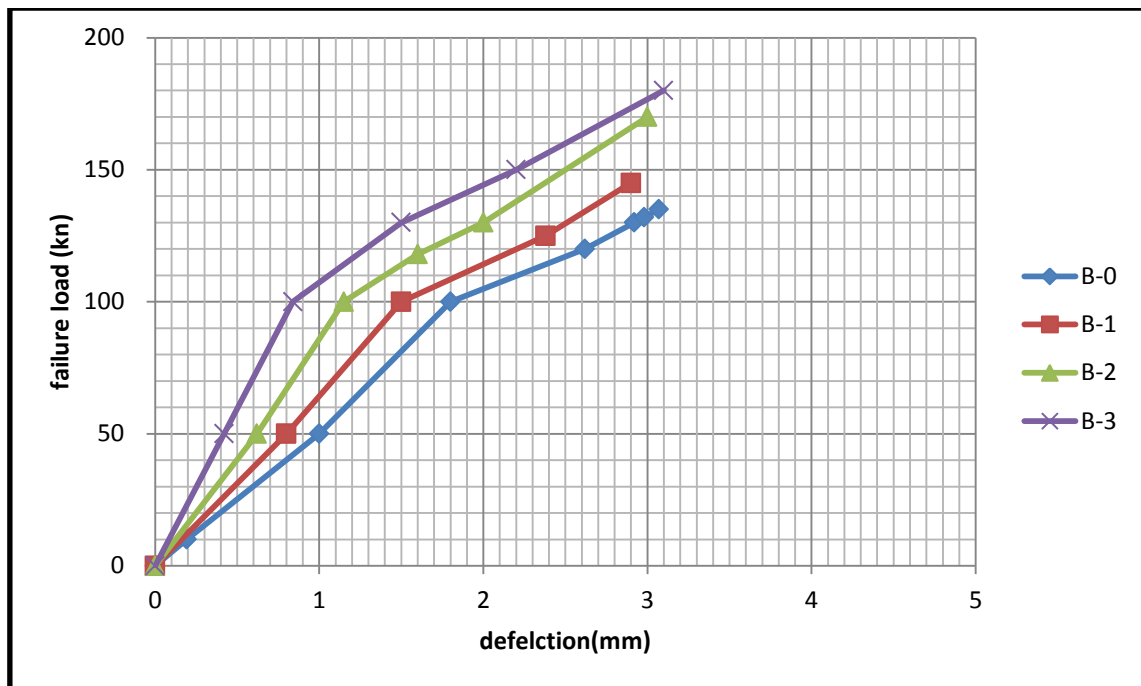
Fig (4.38). Load - Deflection Curves for Group B

4.4.2.3 Energy Absorption Capacity

Energy absorption capacity of all the specimens was calculated as area under load deflection curve. Table (4.7) shows the results and it can be observed that as fiber content increased, the energy absorption capacity increased and for 0.75% fiber, an increase of 34.4% was found. This can be attributed to the effect of fibers in bridging the crack and hence enhancement in energy absorption capacity.

Table (4.7) Energy Absorption Capacity for Group B.

Group No	Specimen No	v_f	Energy Absorption Capacity(KN-mm)
B	B-0	0%	4.2×10^2
	B-1	0.25%	4.8×10^2
	B-2	0.5%	5.6×10^2
	B-3	0.75%	6.4×10^2

4.4.3.1 Analysis the results of group (C) included beams (C-0), beam (C-1), beam (C-2), and beam (C-3).

All the beams failed as it was expected. The values of ultimate shear, failure modes, and percentage of load increase based on the ultimate load of control beam are given in Table (4.8). As shown in this table, the discrete steel fiber increased the ultimate capacity of R.C beams. The percentage of increase reached to about 39 %   when the fiber ratio was increased to 0.75 % at the same span to depth ratio.

Crack pattern and failure mode for beams with and without steel fiber are shown in Table. The higher the fibers ratio, the brisker failure of specimens.

The cracking pattern and failure mode of the beams was closely observed. For beams having fiber 0, 0.25 % the failure has been observed predominantly due to flexural cracks, which are also called the shear failure. Here the flexural cracks are dominant in the middle third region and the angle of failure is large. For beams having fiber 0.5, 0.75 percent the failure has been observed predominantly due to diagonal shear failure.

Table (4.8) Effect of Fiber on Specimens Group C.

Group	a/d	Specimen no.	v_f	Failure load(KN)	Increase ratio	Mode of failure
C	2.2	C-0	0%	115	Control	shear failure
		C-1	0.25%	130	13%	shear failure
		C-2	0.5%	148	28.70%	shear failure
		C-3	0.75%	160	39%	shear failure

4.4.3.2 Load Deflection Curves for group C

Figure 4.39 shows the relationship between the applied load and mid-span deflection for different steel fiber ratio (group C). While increase ratio of steel fiber enhances the stiffness of beam. when beam (C-0) start cracking at load equal 80 KN the deflection of beam at this load equal 1.7mm while beam (C-3) cracks at load 122 the deflection was 2.2 mm. Moreover, it is clear that the increase of steel fiber ratio decreases the ultimate deflection as shown in Fig. 4.37 and in turn, increases shear capacity of beams. Moreover, it is clear that the increase of steel fiber ratio decrease the ultimate deflection as shown in Fig. 4.39 and in turn increases shear capacity of beams, and enhance the stiffness of beam as shown on table (4.9).

Table (4.9) Initial Stiffness for Group C.

| Group	a/d	Specimen No.	Stiffness(KN/mm)	Increase Ratio
C	2.2	C-0	47.06	CONTROL
		C-1	48.26	3%
		C-2	51.82	10.00%
		C-3	55.45	18%
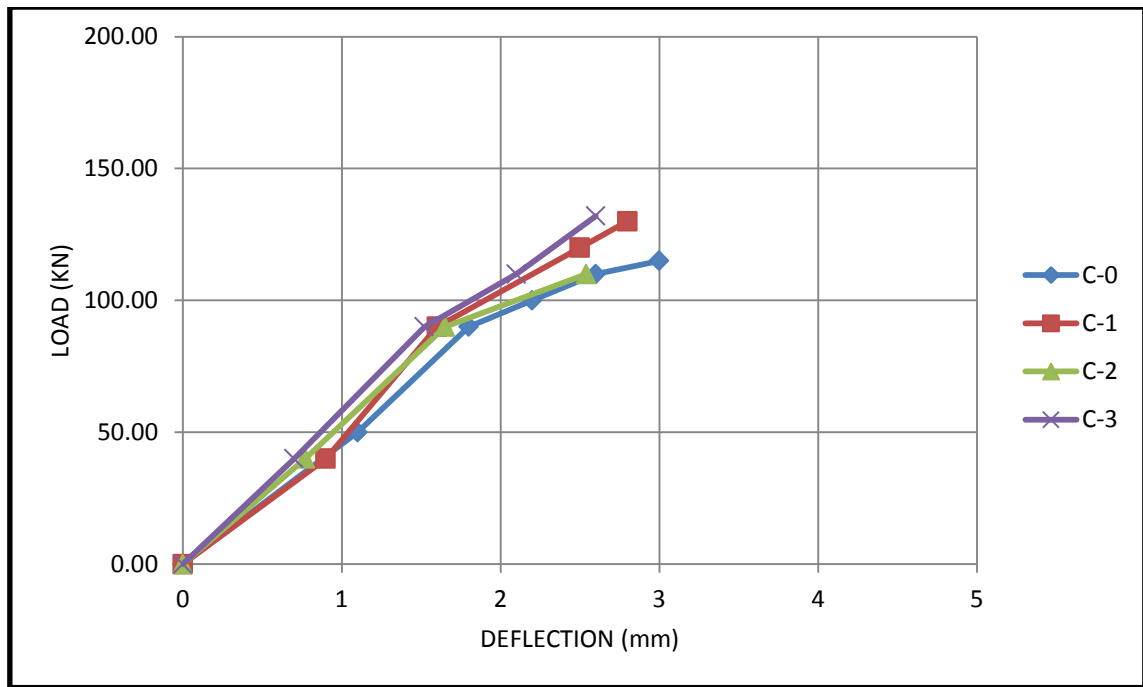
Fig (4.39). Load - Deflection Curves for Group C

4.4.3.3 Energy Absorption Capacity

Energy absorption capacity of all the specimens was calculated as area under load deflection curve. Table (4.10) shows the results and it can be observed that as fiber content increased, the energy absorption capacity increased and for 0.75% fiber, an increase of 20.6% was found. This can be attributed to the effect of fibers in bridging the crack and hence enhancement in energy absorption capacity.

Table (4.10) Energy Absorption Capacity for Group C.

Group No	Specimen No	v_f	Energy Absorption Capacity(KN-mm)
C	C-0	0%	3.1×10^2
	C-1	0.25%	3.32×10^2
	C-2	0.5%	3.63×10^2
	C-3	0.75%	3.9×10^2

4.5 Effect of Variable Changing of Volume of Fraction on Behavior of All Beams:

Table (4.11) shows the test result of ultimate load. It can be observed that as the fiber content increases the ultimate load gradually. ultimate load increased due to the addition of fibers, at the same shear span depth ratio of 1.5 ultimate load increased by 48.2 % from changing fiber ratio to 0.75 percent, when shear span depth ratio increased to 1.7 ultimate load increased by 44.5 percent, and when increasing shear span depth ratio to 2.2 the ultimate load increased by 39 percent. It was observed that using of steel discrete fiber is more effective in shear strength at lower shear span to depth ratio; the stiffness of beam was increase also with increase fiber content.

Fiber volume has a significant influence on plasticity and compression zone of the element. With small v_f, normal crack destroys compression zone in nearly the same manner as in the concrete element. With the increase of v_f, compression zone plastic hinge is formed like one in simple bending beam. Besides, fiber volume has significant influence on the height of compression

zone. Experiments show that the average height of compression zone for group A (a/d=1.5 was equal to 75– 84mm in conventional concrete element. In SFRC beams it was noticeably greater: the average height of compression zone, at fiber volume 0.75%, was equal to 95–102mm.

For group B (a/d=1.7) the average height of compression was equal to 86– 92 mm in conventional concrete element. In SFRC beams it was noticeably greater: the average height of compression zone, at fiber volume 0.75%, was equal to 104–110mm.

For group C (a/d=2.2) the average height of compression was equal to 120– 125 mm in conventional concrete element. In SFRC beams, it was noticeably greater: the average height of compression zone, at fiber volume 0.75%, was equal to 160–180mm.

In conclusion, the influence of shear stresses on principal stresses and fiber volume effect on the height of compression zone are the main factors determining load capacity.

The addition of fiber display an increased number of both flexural and shear cracks at closer spacing than the corresponding beams without fibers. As showed on beams (A-3),(B-3, and (C-3) clearly because of the fiber spacing is much closer, fibers bridging cracks like aggregate role.

Steel fibers beneficially and substantially improve the crack and deformational behavior as well as the ultimate strength because steel fibers enhance the post cracking behavior of beams. It can be noted that the fibers provide increased stiffness after cracking. Reduction of deflections is due to more effective control of cracking, regardless of the value of the modulus of elasticity which increased with addition of fibers.

The addition of fibres increases the work of fracture (represented by the area under the stress-crack opening curve) The fiber contributes to dissipate energy thanks to: (1) matrix fracture and matrix spalling, (2) fiber-matrix interface deboning, (3) post-deboning friction between fibre and matrix (fiber

pullout), (4) fiber fracture and (5) fiber abrasion and plastic deformation (or yielding) of the fiber.

Table (4.11) Effect of Fiber on All Specimens.

a/d	Specimen no.	v_f	Fcu (MPa)	Failure load(KN)	Increase ratio
a/d =1.5	A-0	zero	51	145	Control
	A-1	0.25%	53	165	13.80%
	A-2	0.5%	55.8	180	24.13%
	A-3	0.75%	68.9	215	48.20%
a/d=1.7	B-0	zero	51	135	Control
	B-1	0.25%	53	155	15%
	B-2	0.5%	55.8	170	25.90%
	B-3	0.75%	68.9	195	44.50%
a/d =2.2	C-0	zero	51	115	Control
	C-1	0.25%	53	130	13%
	C-2	0.5%	55.8	148	28.70%
	C-3	0.75%	68.9	160	39%

Figure 4.40 shows the influence of steel fiber content on the shear strength of beams with different shear span depth ratios. It can be seen that the shear strength increases with the increase of fiber content for each shear span depth ratio.
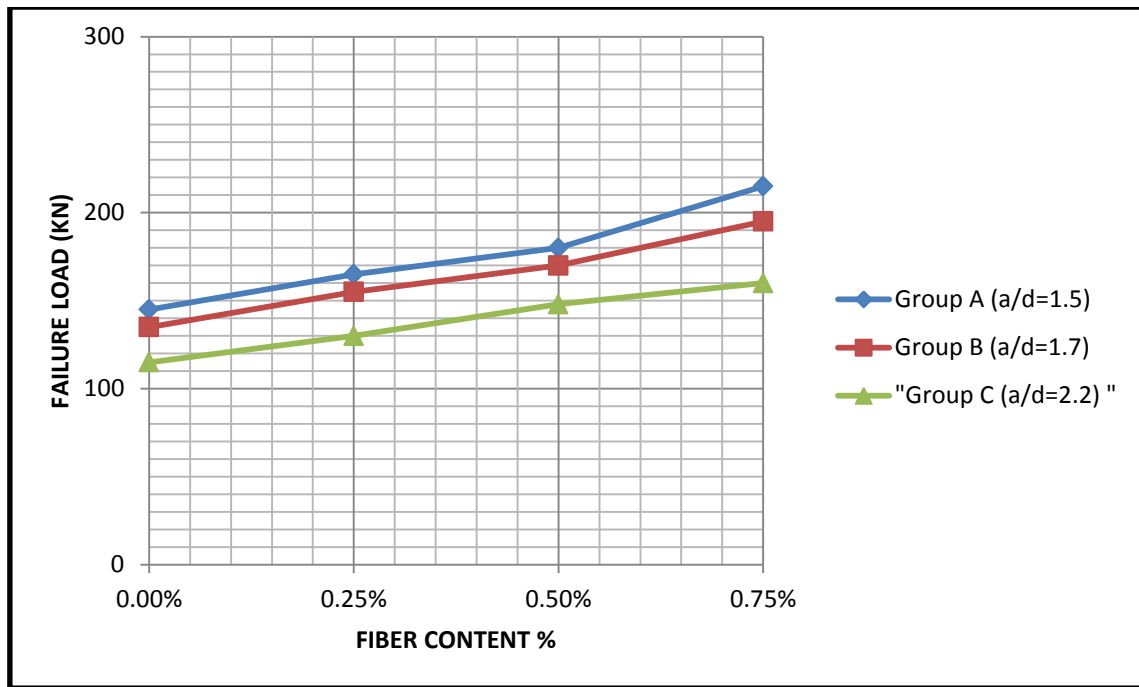
Fig (4.40) Effect of Fiber Content.

4.6 Effect of Variable Changing of Shear-Span Depth Ratio on Behavior of All Beams:

By comparing, the test results in this study The relation between the failure load and fiber content with different span to depth ratio will shown on the table (4.12) and figure 4.41.

In general, by change ratio of a/d from 1.5 to 2.2 the failure load decreased by 21 percent at the same fiber content 0, 0.25 percent. Moreover, by using discrete steel fiber with ratio 0.5% and 0.75% the load decreased by about 18 and 26 percent, respectively. By comparing between the strength for span to depth ratio 1.5 and 2.2 it found that, the shear strength in a/d=1.5 is more than that in a/d=2.2. The ratio between shear strength for a/d =1.5 to a/d=2.2 in the case of not used fiber is less than that in the case of used fiber From studding the effect of span to depth ratio on the shear failure and using discrete steel fiber it was found that, by increasing span to depth ratio the efficiency of used discrete steel fiber decreased. The shear strength decreases with the increase of a/d values for the same longitudinal steel.

Table (4.12) Effect of Shear Span Depth on All Specimens.

fiber content	specimen no.	Fcu(MPa)	a/d	failure load	decrease ratio
$V_{F0.0\%}$	A-0	51	1.5	145	Control
	B-0	51	1.7	135	6.70%
	C-0	51	2.2	115	21%
$V_{F0.25\%}$	A-1	53.	1.5	165	Control
	B-1	53	1.7	155	6.00%
	C-1	53	2.2	130	21%
$V_{F0.5\%}$	A-2	55.8	1.5	180	Control
	B-2	55.8	1.7	170	5.50%
	C-2	55.8	2.2	148	18%
$V_{F0.75\%}$	A-3	68.9	1.5	215	Control
	B-3	68.9	1.7	195	9.30%
	C-3	68.9	2.2	160	26%

Figure 4.41 shows the influence of shear span to depth ratio on the shear strength of beams with different volume fraction of steel fiber. Whenthe shear span increases, the deflection under external loads also increases and flexural cracks are formed at relatively lower values of external loads.
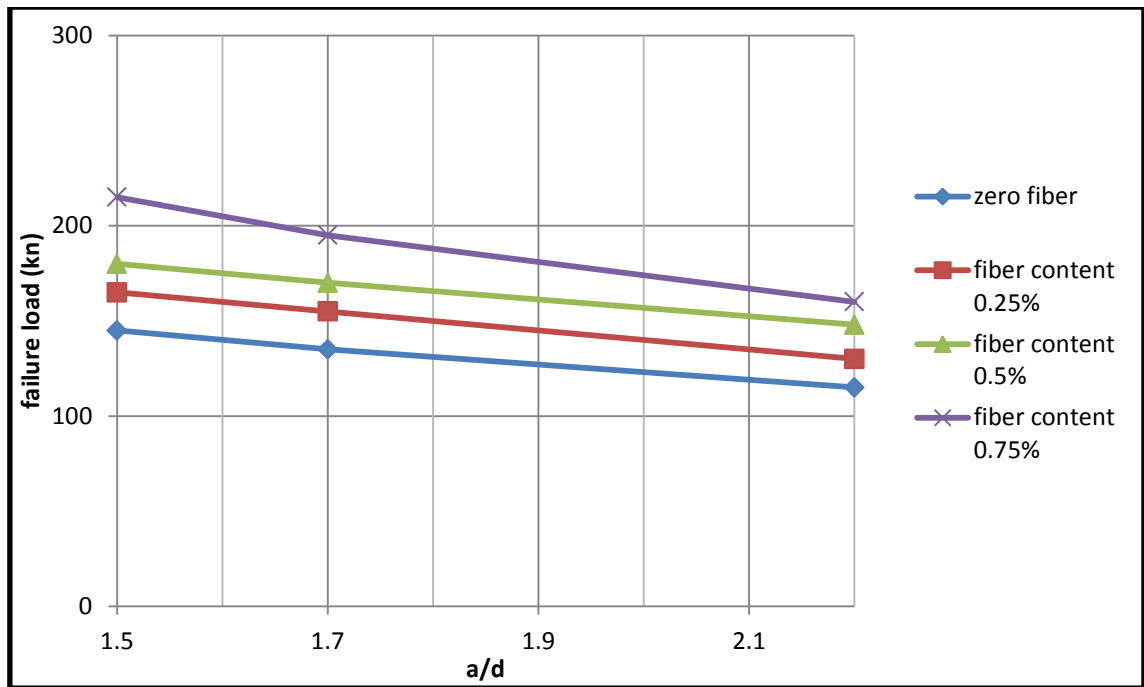
Fig. (4.41) Effect of Shear Span Depth on Ultimate Load

At lower shear span ratios (a/d =1.5,and 1.7) the behavior of beams without fiber were closer to deep beam which the concentrated load is resisted by two major inclined diagonal struts from compressive concrete at this zone which called disturbed region or (D-region). This means that resistance of concrete at this zone by arch action not beam action. We can also show that the effective compression strength at two ends of struts differs due to different bearing lengths. The strut was idealized as uniformly tapered strut as shown on figures (4.42and 4.43).
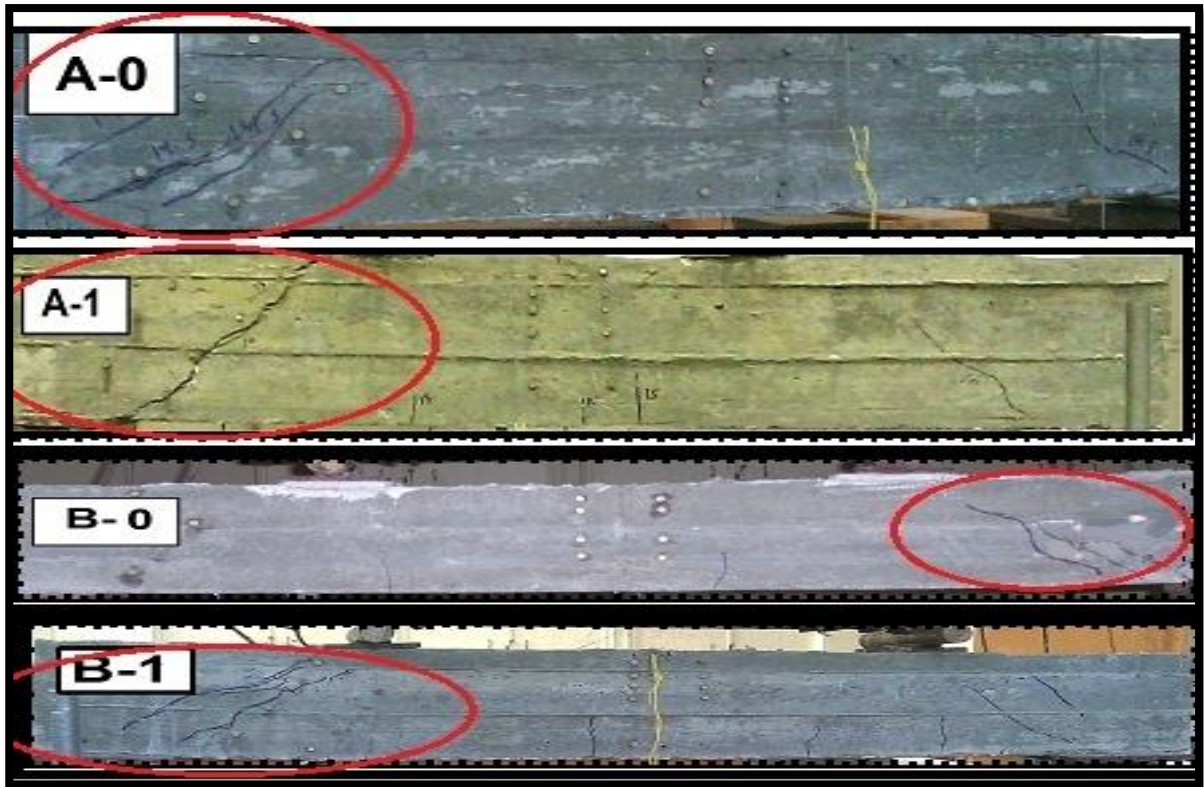
Fig. (4.42) Effect of Shear Span Depth on Ultimate Load at lower shear span ratios
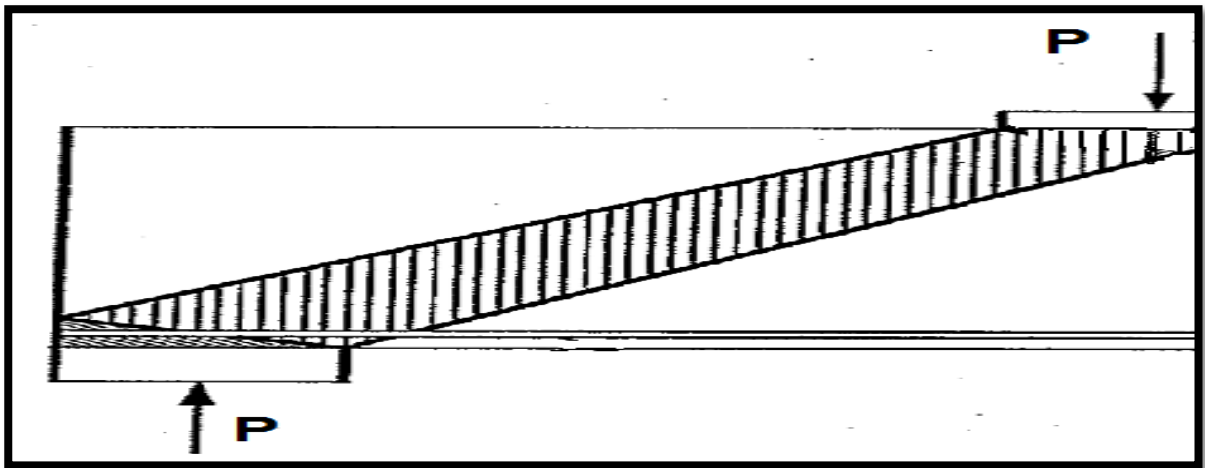
Fig. (4.43) Tappered strut model **(Ghoneim, M, And El-Mihimy, M) [47]**

At the same shear span ratios (a/d =1.5 and 1.7) the behavior of beams with fiber content equal 0.5,0.75% were closer also to deep beam which the concentrated load is resisted by two major inclined diagonal struts from compressive concrete at this zone, and resistance of concrete at this zone by arch action not beam action. However, we showed that the effective

compression strength at two ends of struts lookalike bottle shape and steel fibers acting as ties at this zone causes increase on shear strength and flexure cracks appears on these specimens as shown on figures (4.44 and 4.45).
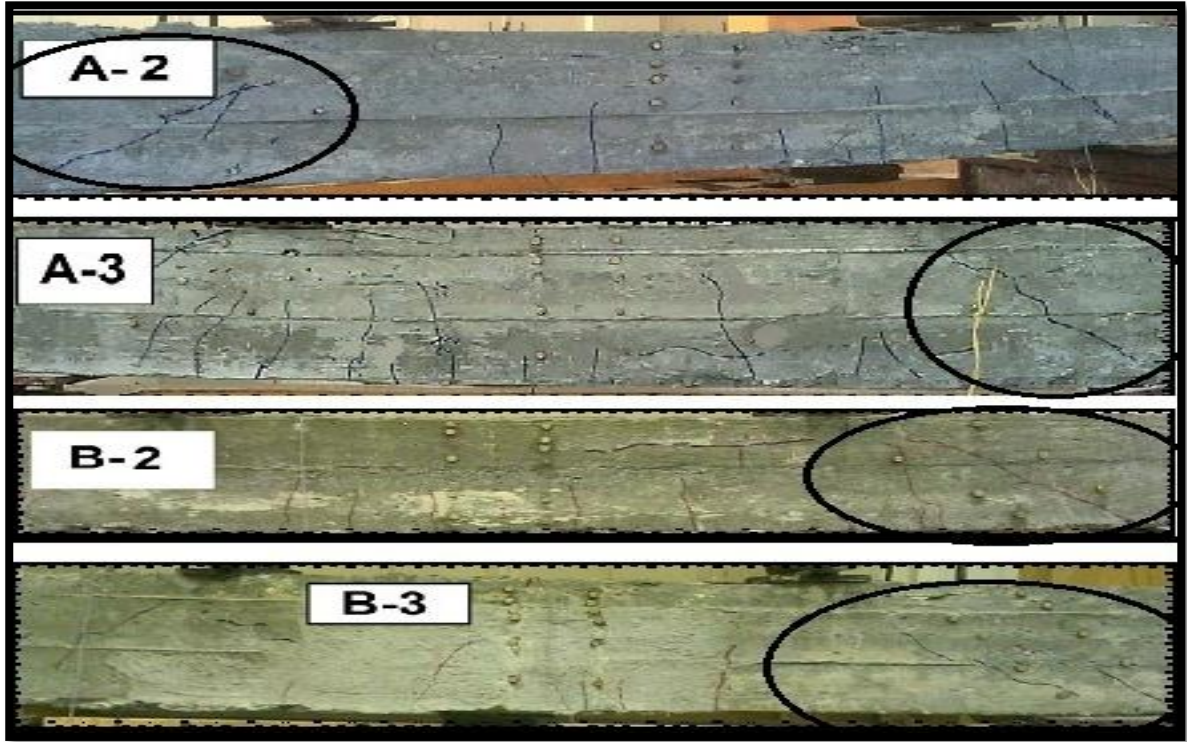
Fig. (4.44) Effect of Shear Span Depth on Ultimate Load
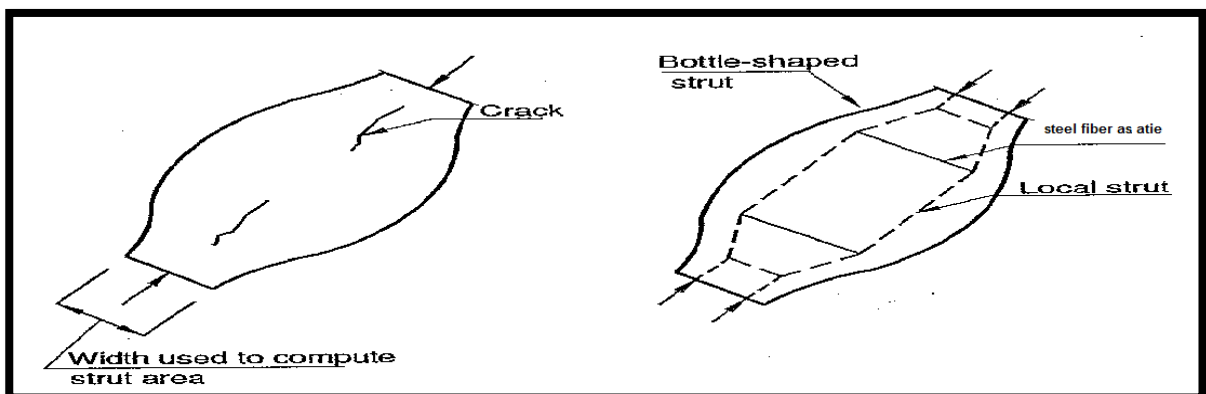
Fig. (4.45) Bottled Shape for Strut**(Ghoneim, M, And El-Mihimy, M) [47]**

When we increased shear span ratio bigger than 2 for group C (a/d =2.2) we showed that the beams were acted as beam action which having disturbed region and beam region as shown on figures (4.46 and 4.47).
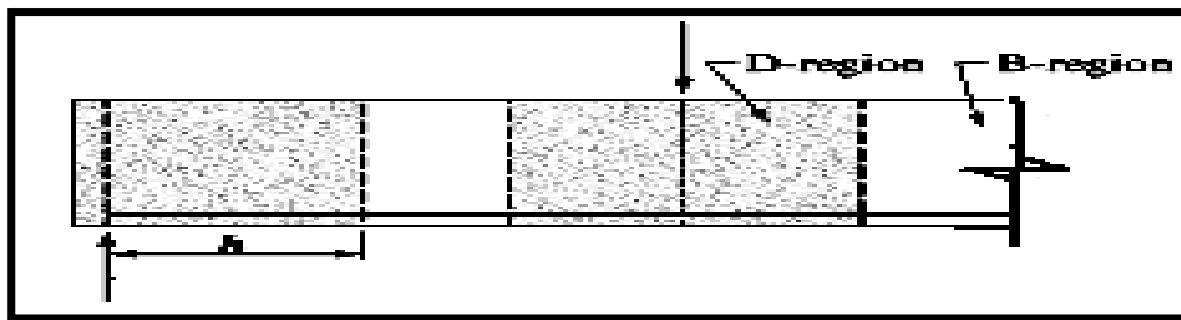
Fig. (4.46) B-Region and D- Region for Group C
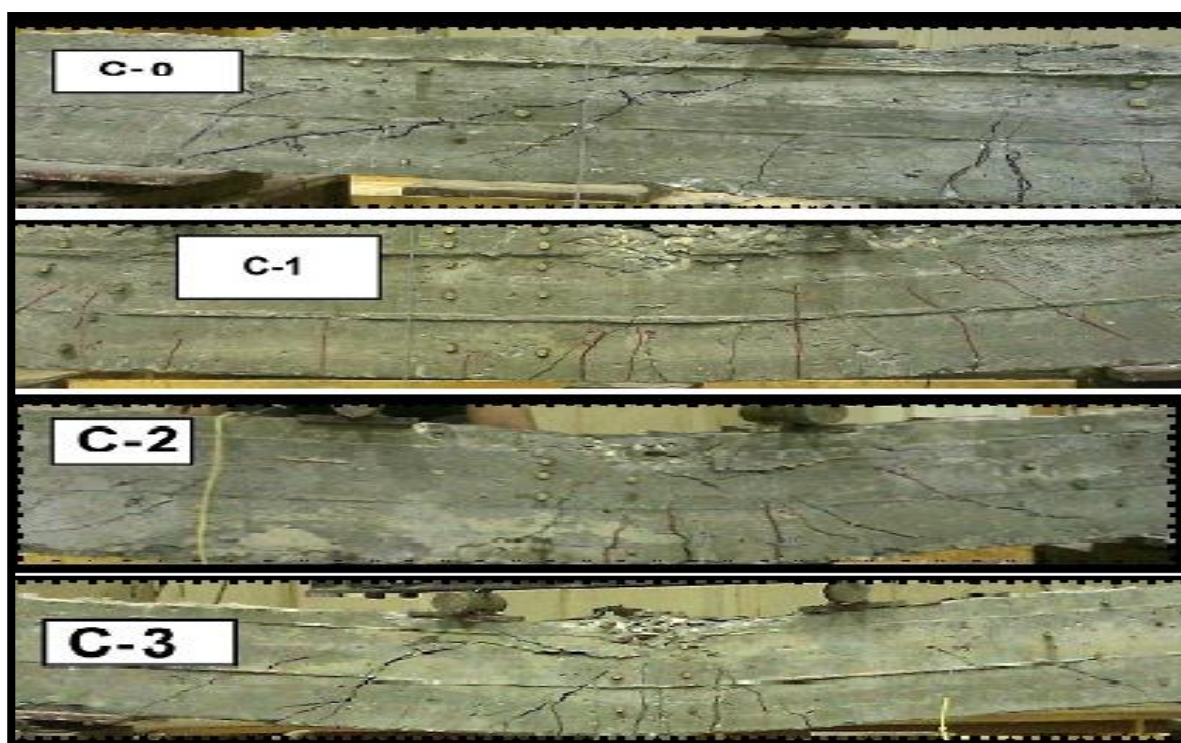
Fig. (4.47) Effect of Shear Span Depth on Ultimate Load Group C

We can showed that the increase of fiber enhance post cracking stiffness of beams at this shear span ratio, and increase energy absorption ratio due to fiber bridging of crack and very bond between fiber and matrix.

Chapter Five

THEORETICAL ANALSIS

5.1 Introduction

In this Chapter a comparison between the values of ultimate shear strength obtained by the experimental investigation ($v_u = v_u$.b.d , being $V_u=$ Pu/2) and the values deduced by using the expressions proposed in the literature, and codes are presented. Two expressions proposed in the literature (**shin [37], and ashour [32]**) where they take fiber effect into consideration..

The shear design of the high strength concrete beams is usually done by adopting the provisions of different codes based on various rationales. These provisions are expressed in the form of empirical equations. Some of the most commonly used design equations for the shear design of RC structures are as follows:

- ACI Code 318 (American Concrete Institute) **[1]**
- Egyptian code (ECP-206) **[46]**.
- European Code EC2-2003**[36]**.
- Chinese Code**[43]**.

Some of these codes take the fiber effect into consideration such as Chinese code, and others not take fiber effect. A proposed model is suggested within the range of the experimental results of this study, to take into account the effect of fiber percent v_f.

5.2 Review of Shin et al. (1994). [37]

The study reports the results of an investigation on the strength and ductility of fiber reinforced high strength concrete beams (with concrete compression

strength equal to 80 MPa) with and without steel fiber reinforcement, the diagonal cracking strength as well as the nominal shear strength of the beams were determined. 22 beam specimens were tested under monotonically increasing loads applied at mid-span. The major test parameters included the volumetric ratio of steel fibers, the shear-span-to depth ratio, the amount of longitudinal reinforcement, and the amount of shear reinforcement.

Empirical equations are suggested for evaluating the nominal shear strength of high strength concrete beams with steel fibers:

- For beam with a/d <3

$$v_n = 0.22\, f_{sp} + 217\rho.\frac{d}{a} + 0.34.\tau.\text{F}$$

f_{sp}-*Split* cylindrical strength.

a- Shear Span.

d - Effective depth.

d/a - Effective depth / Shear span.

ρ- Area of tensile reinforcement; ρ=As/bd.

τ - Average fiber matrix interfacial bond stress; τ=4.15.

F- Fiber factor given by: $F = \left(\frac{l}{d}\right) v_f\, d_f$

d_f -Bond factor; d_f=0.75 for crimped fiber.

v_f_ Fiber volume fraction.

$\left(\frac{l}{d}\right)$-Aspect ratio of fibre.

- The comparison of experimental and (Shin) results for shear strength of HSC beams with and without steel fiber has been given in Table 5.1.

Table (5.1). Comparison of the Shear Strength of Beams with the Provisions of Shin [37]

Beam title	a/d	F	f_{sp} MPA	V_{pre} (KN)	V_{exp} (KN)	V_{exp}/V_{pre}
A-0	1.5	0.00	27.5	132.86	145	1.09
A-1	1.5	0.15	28.6	145.69	165	1.13
A-2	1.5	0.30	30.1	158.86	180	1.13
A-3	1.5	0.45	37.2	176.32	215	1.22
B-0	1.7	0.00	27.5	131.78	135	1.02
B-1	1.7	0.15	28.6	144.61	155	1.07
B-2	1.7	0.30	30.1	157.78	170	1.08
B-3	1.7	0.45	37.2	175.24	195	1.11
C-0	2.2	0.00	27.5	129.94	115	0.89
C-1	2.2	0.15	28.6	142.77	130	0.91
C-2	2.2	0.30	30.1	155.94	148	0.95
C-3	2.2	0.45	37.2	173.40	160	0.92

The comparison of values given by the shin`s equation with the tested values of shear strength of HSC beams shows that the equation of shin gives very closer values for almost all level of steel fibers and shear-span depth ratios for this study

5.3 Review of Ashour. *(1992).* [32]

Two formulae (in MPa) were also proposed for the prediction of the shear capacity of HSFRC beams:

$$v_c = \left(0.7\sqrt{f_c'} + 7F \right)\frac{d}{a} + 17.2\, \rho\, \frac{d}{a} \quad \text{a/d} \le 2.5$$

$$v_c = \left(2.11\sqrt[3]{f_c'} + 7F \right) (\rho\, d/a)^{0.333} \quad \text{a/d} > 2.5$$

$$\boldsymbol{F} = \left(\frac{l}{d}\right) \boldsymbol{v_f}\, \boldsymbol{d_f} \quad \text{And} \quad d_f \text{ is the fiber effectiveness}$$

f_c' -Cube compressive strength of concrete.

The comparison of Ashour results for shear strength of HSC beams with and without steel fiber has been given in Table 5.2.

Table (5.2). Comparison of the Shear Strength of Beams with the Provisions of Ashour [32]

Beam title	a/d	F	V_{pre} (KN)	V_{exp} (KN)	V_{exp}/V_{pre}
A-0	1.5	0.00	136.298	145	1.06
A-1	1.5	0.15	157.806	165	1.05
A-2	1.5	0.30	179.99	180	1.00
A-3	1.5	0.45	210.575	215	1.02
B-0	1.7	0.00	124.731	135	1.08
B-1	1.7	0.15	143.709	155	1.08
B-2	1.7	0.30	163.279	170	1.04
B-3	1.7	0.45	190.27	195	1.02
C-0	2.2	0.00	105.015	115	1.10
C-1	2.2	0.15	119.68	130	1.09
C-2	2.2	0.30	134.802	148	1.10
C-3	2.2	0.45	155.659	160	1.03

The comparison of values given by the Ashour`s equation with the tested values of shear strength of HSC beams shows that the equation of Ashour gives very closer values for almost all level of steel fibers and shear-span depth ratios.

5.4 Review of ACI Code 318-06 (American Concrete Institute)

The ACI building code 318-06 is no doubt the most widely applied Code for the shear design of concrete. The nominal shear capacity of reinforced concrete beam v_u is given as the sum of concrete contribution v_c, and contributions of stirrups v_s.i.e.

$$v_u = v_c + v_s$$

$$v_c = \left[0.158\sqrt{f_c'} + 17.24\rho\left(\frac{V_u.d}{M_u}\right) \right] b.d \quad \leq 0.29\sqrt{f_c'}\, b.d \qquad MPa$$

V_u, M_u :   Shear force and moment at the critical section.

  ρ : Longitudinal tension steel ratio.

ACI allows the following simplification assuming that the term $\frac{V_u.d}{M_u}$ is small;

$$v_c = 0.166\lambda\sqrt{f_c'}\ b.d \quad MPa$$

$$v_s = \frac{A_{sv}\, f_{ysv} d_v\, (\cot\theta_v + \cot\alpha)\, \sin\alpha}{S}$$

Where

A_{sv}: Area of shear reinforcement within spacing S;

f_{ysv}: Yield strength of shear reinforcement;

d_v : Lever arm resisting flexural moment (usually =0.9d);

θ_v : Angle of inclination (which varies between 30 and 60 degrees) of the

       diagonal compressive stress to the longitudinal axis of the beam;

α : Angle of inclined stirrups to the longitudinal axis of the beam.

Table (5.3). Comparison of the Shear Strength of Beams with the
Provisions of the ACI with No Fiber Effect

beam title	a/d	b mm	d mm	fc' MPA	Vs (N)	V_{pre} (KN)	V_{exp} (KN)	V_{exp}/V_{pre}
A-0	1.5	120	250	40.8	37981.44	123.68	145	1.17
A-1	1.5	120	250	42.4	37981.44	124.60	165	1.32
A-2	1.5	120	250	44.64	37981.44	125.87	180	1.43
A-3	1.5	120	250	55.12	37981.44	131.42	215	1.64
B-0	1.7	120	250	40.8	37981.44	123.68	135	1.09
B-1	1.7	120	250	42.4	37981.44	124.60	155	1.24
B-2	1.7	120	250	44.64	37981.44	125.87	170	1.35
B-3	1.7	120	250	55.12	37981.44	131.42	195	1.48
C-0	2.2	120	250	40.8	37981.44	123.68	115	0.93
C-1	2.2	120	250	42.4	37981.44	124.60	130	1.04
C-2	2.2	120	250	44.64	37981.44	125.87	148	1.18
C-3	2.2	120	250	55.12	37981.44	131.42	160	1.22

Comparison of actual test results of shear strength of HSC beams with
the results given by ACI-318 in Table 5.3, comparison gives the following
general observations;

The ACI-318 provisions for shear strength of HSC beams is   more
conservative for small values of shear-span depth ratios both for
beams with and without steel fiber because the fiber effect not taken
into consideration on ACI.

5.5 Review of European Code EC2-2003.

Expresses the ultimate strength for HSC concrete in shear v_c by the following equation:

$$v_c = 0.035 f_{ck}{}^{2/3} k(1.2 + 40\rho) b.d \quad \text{Mpa}$$

$$k = (1.6 - d) \ > 1$$

The comparison of actual and euro code results for shear strength of HSC beams with and without steel fiber has been given in Table 5.4.

Table (5.4). Comparison of the Shear Strength of Beams with the Provisions of the Euro Code with No Fiber Effect

beam title	b mm	d mm	f_{ck}	k	Vs (N)	V_{pre} (KN)	V_{exp} (KN)	V_{exp}/V_{pre}
A-0	120	250	51	1.35	37981.44	141.80	145	1.02
A-1	120	250	53	1.35	37981.44	143.51	165	1.15
A-2	120	250	55.8	1.35	37981.44	145.89	180	1.23
A-3	120	250	68.9	1.35	37981.44	156.48	215	1.37
B-0	120	250	51	1.35	37981.44	141.80	135	0.95
B-1	120	250	53	1.35	37981.44	143.51	155	1.08
B-2	120	250	55.8	1.35	37981.44	145.89	170	1.17
B-3	120	250	68.9	1.35	37981.44	156.48	195	1.25
C-0	120	250	51	1.35	37981.44	141.80	115	0.81
C-1	120	250	53	1.35	37981.44	143.51	130	0.91
C-2	120	250	55.8	1.35	37981.44	145.89	148	1.01
C-3	120	250	68.9	1.35	37981.44	156.48	160	1.02

Comparison of actual test results of shear strength of HSC beams with the results given by EC2-2003 in Table 5.4, comparison gives the following general observations;

The Euro Code provisions for shear strength of HSC beams is more conservative for beams with and without steel fiber because the fiber effect not taken into consideration on Code.

5.6 Evaluation According to Egyptian Code (ECP-206):

Shear force is present in beams at sections where there is a change in bending moment along the span. An exact analysis of shear strength in reinforced concrete beam is quite complex. Several experimental studies have been conducted to understand the various modes of failure that could occur due to possible combination of shear and bending moment. Despite the great research efforts, however, there is still not a simple. In addition, many of the factors that influence the determination of the required minimum amount of shear reinforcement are not yet known. The shear strength of R.C. beams depends on the strength of concrete, the percentage of the longitudinal reinforcement and the span-to-depth ratio or stiffness of the beam. From shear force, diagram find that the shear force is equal to support reaction that equal to haft of vertical load. And the theoretical shear force is equal to the force for allowable concrete shear strength, plus the force from carrying shear strength by vertical stirrups.

$$q_{cu} = 0.214\sqrt{f_{cu}} \quad MPa$$

$$q_{sus} = A_{st}f_y/s \quad MPa$$

Where fcu is characteristic cube compressive strength of concrete in N/mm2, A_{st} is the area of stirrups, b is the section width, S is the spacing between stirrups. Then, the theoretical shear force can be calculated as the following equation:

$$v_{the} = [q_{cu} + q_{sus}]xbd \quad (N)$$

- The comparison of actual and ECP results for shear strength of HSC beams has been given in Table 5.5.

Table (5.5) Comparison of the Shear Strength of Beams with the Provisions of
the ECP with No Fiber Effect.

beam title	b mm	d mm	q_{sus}	q_{cu}	V_{pre} (KN)	V_{exp} (KN)	V_{exp}/V_{pre}
A-0	120	250	2.34	1.53	118.8	145	1.22
A-1	120	250	2.34	1.56	119.7	165	1.38
A-2	120	250	2.34	1.59	120.8	180	1.49
A-3	120	250	2.34	1.78	125.8	215	1.71
B-0	120	250	2.34	1.53	118.8	135	1.14
B-1	120	250	2.34	1.56	119.7	155	1.29
B-2	120	250	2.34	1.59	120.8	170	1.41
B-3	120	250	2.34	1.78	125.8	195	1.55
C-0	120	250	2.34	1.53	118.8	115	0.97
C-1	120	250	2.34	1.56	119.7	130	1.09
C-2	120	250	2.34	1.59	120.8	148	1.22
C-3	120	250	2.34	1.78	125.8	160	1.27

Comparison of actual test results of shear strength of HSC beams with
the results given by ECP-206 in Table 5.5, comparison gives the following
general observations;

The ECP code provisions for shear strength of HSC beams is more
conservative for beams with and without steel fiber because the fiber
effect not taken into consideration on Code.

5.7 Proposed Theoretical Equation:

The ratios between experimental results and theoretical results of Egyptian
code were from 0.97 to 1.71 without fiber effect. From this we will included
that steel fiber has obvious effect on the shear strength of beams.

The recommended theoretical equation will be as the following;

$$Vc = v_c + v_s + v_f \quad (N)$$

$$\text{Where } v_c = 0.214\sqrt{f_{cu}} \;.b.d \quad (N),$$

$$v_s = A_{st}f_y.b.d/s \quad (N), \text{ and}$$

$$V_f = \left(\frac{l}{d}\right).v_f.\beta.b.d \quad (N).$$

To consider fiber effect we will adding the term V_f to shear strength from the
Egyptian code where;

$\left(\dfrac{l}{d}\right)$: The aspect ratio for steel fiber.

v_f: The volume of fraction for steel fibers.

β : Fiber factor.

By analytically we find that the fiber factor β is equal (2.68).

Table no (5.6) showed the comparison of the shear strength of beams with fiber effect into consideration according to our equation.

Table (5.6) Comparison of the Shear Strength of Beams with the Provisions of Our Equation with Fiber Effect.

beam title	b mm	d mm	q_{sus}	q_{cu}	V_{pre} (KN)	V_{exp} (KN)	V_{exp}/V_{pre}
A-0	120	250	2.34	1.53	118.89	145	1.2
A-1	120	250	2.34	1.56	142.51	165	1.15
A-2	120	250	2.34	1.59	166.43	180	1.08
A-3	120	250	2.34	1.78	194.21	215	1.1
B-0	120	250	2.34	1.53	118.89	135	1.13
B-1	120	250	2.34	1.56	142.51	155	1.08
B-2	120	250	2.34	1.59	166.43	170	1.02
B-3	120	250	2.34	1.78	194.21	195	1.004
C-0	120	250	2.34	1.53	118.89	115	0.96
C-1	120	250	2.34	1.56	142.51	130	0.91
C-2	120	250	2.34	1.59	166.43	148	0.88
C-3	120	250	2.34	1.78	194.21	160	0.82

Comparison of actual test results of shear strength of HSC beams with the results given in Table 5.6, equations gives the following general observations:

1. The shear strength given by suggested equation for a/d =1.5 and 1.7 are however reasonably good and not more conservative for a/d=2.2.

2. The increase in shear strength of HSC beams due to addition of steel fibers in all beams is not same, as given by results.

3. The increase in shear strength of HSC beams due to addition of steel fibers is shown clear fully for small values of a/d , as given by results.

5.8 Review of Chinese Code for Design of Concrete Structure, GB50010–2002:

Expresses the ultimate strength for HSC with steel fiber in shear V_u by the following equation:

$$V_{uf} = \frac{1.75}{\lambda+1} f_t bd (1 + \beta_v \lambda_f) + f_{yst} \frac{A_{st}.d}{S} \quad \text{N}$$

$$v_{uf} = \frac{V_{uf}}{b.d} \quad \text{MPa}$$

Where V_{uf} is the shear load of the fiber reinforced RC member, β_v is the influence coefficient of the steel fibers=0.75, λ_f is fiber factor, $\lambda_f = v_f l_f / d_f$, $f_t = 0.54 \sqrt{f_c'}$, and v_{uf} is shear strength of fiber reinforced RC member.

The comparison of actual and Chinese code results for shear strength of HSC beams with and without steel fiber has been given in Table 5.7.

Table (5.7) Comparison of the Shear Strength of Beams with the Provisions of the Chinese Code

beam title	b mm	d mm	f_t MPa	λ_f	V_{pre} (KN)	V_{exp} (KN)	V_{exp}/V_{pre}
A-0	120	250	3.86	0.2	113.74	145	1.27
A-1	120	250	3.93	0.2	130.86	165	1.26
A-2	120	250	4.03	0.2	149.16	180	1.21
A-3	120	250	4.48	0.2	179.20	215	1.20
B-0	120	250	3.86	0.2	108.30	135	1.25
B-1	120	250	3.93	0.2	123.90	155	1.25
B-2	120	250	4.03	0.2	140.93	170	1.21
B-3	120	250	4.48	0.2	168.72	195	1.16
C-0	120	250	3.86	0.2	97.30	115	1.18
C-1	120	250	3.93	0.2	110.50	130	1.18
C-2	120	250	4.03	0.2	124.84	148	1.19
C-3	120	250	4.48	0.2	148.30	160	1.08

Comparison of actual test results of shear strength of HSC beams with the results given by GB50010–2002 in Tables 5.7, equations gives the following general observations;

1. The GB50010–2002 provision for shear strength of HSC beams
is conservative for small values of shear-span depth ratios
both for beams with and without steel fiber.

2. The shear strength given by GB50010–2002 for a/d =2.2 are
however reasonably good and becomes more conservative for
a/d=1.5 and a/d=1.7.

3. The increase in shear strength of HSC beams due to addition of
steel   fibers in all beams is not same, as given by GB50010–2002.

5.9 Comparison between Results

The overall comparison of V_{exp}/V_{pre} for proposed equation, GB50010–2002,
shin`s, and ashour`s equations have been shown in Table 5.8.

Table 5.8 Comparison of V_{exp}/V_{pre} for, (Equation, Gb50010–2002, SHIN`S, AND ASHOURS)
EQUATIONS for BEAMS with VARIABLE FIBER`S RATIOS.

	beam title	V_f	V_{exp}/V_{pre}			
			Suggested eq.	GB50010	Shin	Ashour
Group A a/d=1.5	A-0	0.00%	1.22	1.27	1.09	1.06
	A-1	0.25%	1.16	1.26	1.13	1.05
	A-2	0.50%	1.08	1.21	1.13	1.00
	A-3	0.75%	1.11	1.20	1.22	1.02
	Mean		1.14	1.24	1.14	1.03
	standard dev		0.06	0.04	0.06	0.03
Group B a/d=1.7	B-0	0.00%	1.14	1.25	1.02	1.08
	B-1	0.25%	1.09	1.25	1.07	1.08
	B-2	0.50%	1.02	1.21	1.08	1.04
	B-3	0.75%	1.00	1.16	1.11	1.02
	Mean		1.06	1.21	1.07	1.06
	standard dev		0.06	0.04	0.04	0.03
Group C a/d=2.2	C-0	0.00%	0.97	1.18	0.89	1.10
	C-1	0.25%	0.91	1.18	0.91	1.09
	C-2	0.50%	0.89	1.19	0.95	1.10
	C-3	0.75%	0.82	1.08	0.92	1.03
	Mean		0.90	1.16	0.92	1.08
	standard dev		0.06	0.05	0.03	0.03

From the comparison of Vexp/Vpre given in Table 5.8, the following general comments can be made;

1. All the equation of various codes and methods discussed in the study are safe for the shear design of tested HSFRC beams with and without steel fibers.

2. For beams with fibers, the corresponding values Vexp/Vpre have increased for a/d=1.5 and a/d=1.7 for all equations hence the equations given by most of the codes and methods discussed are conservative for HSC beams with a/d=1.5,a/d=1.7, and a/d=2.2 for both the cases with and without discrete steel fibers.

3. The equations are giving reasonably good predictions of the shear strength of HSC beams for a/d=1.5 and 1.7.

4. The shear design of HSC beams at low-level shear span to depth ratios by all the methods and equations considered need further work and verification of the improvement of the equations.

5. The shear strength of HSC beams with steel fibers is generally Considered as the sum of the individual contributions of the concrete and steel fibers but in fact is more complicated phenomena as their roles are not independent.

6. The our proposed equation gives reasonably good estimate of the HSC beams with steel fibers as shown on figure (5.1).
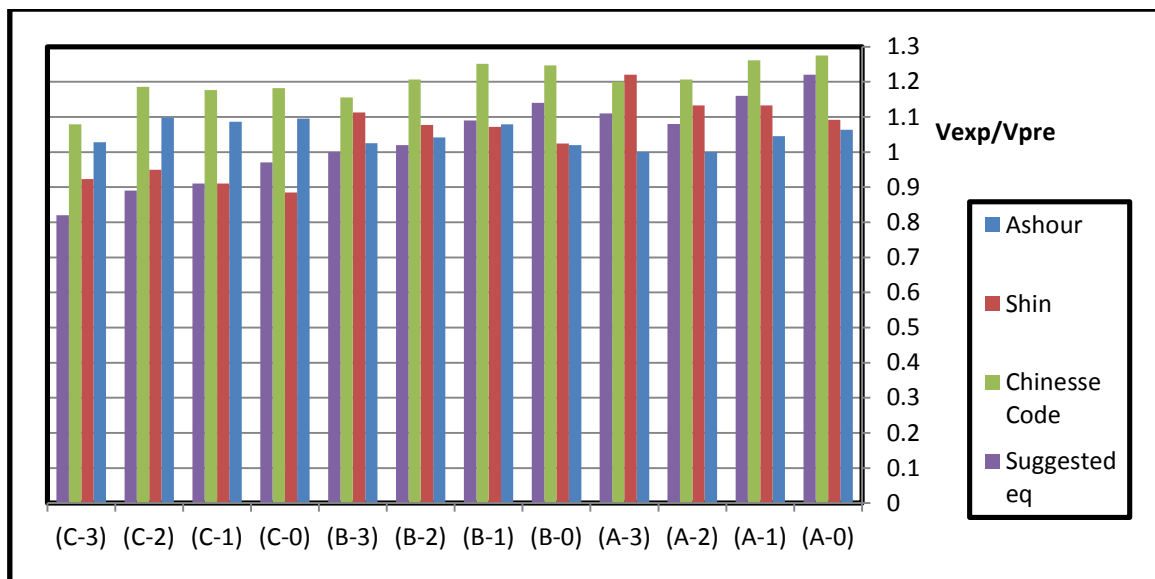
Fig(5.1) Comparison of V_{exp}/V_{pre} for, (Our equation, (Gb50010–2002), Shin, and Ashours).

Chapter Six
SUMMARY, CONCLUSIONS, AND RECOMMENDATIONS

6.1 Summary

In the experimental program of this research study, the behavior of HSFRC beams was studied where different values of a/d and vf were taken into consideration. In the theoretical program, an existing codes and purposed equations were used in order to incorporate the effect of steel fiber, and shear span depth ratio, where a comparison are presented between the values of proposal equation and different researches and codes.

6.2 Conclusions

6.2.1 Effect of Steel Fibers on Shear Strength of HSC Beams:

- Adding of fibers to high strength concrete increases the first crack load and ultimate load. For 0.75% volume fiber the ultimate load increased by 48.2% at a/d=1.5, for 0.75% fiber the ultimate load increased by 44.5% at a/d=1.7. In addition, for 0.75% volume fiber the ultimate load increased by 39% at a/d=2.2.

- Adding of steel fibers to the concrete mix improves the shear strength of RC beams and tends to increase initial and post cracking stiffness of beam.

- For each a/d ratio, increasing the volume fraction of steel fibers can increased the ultimate loads, the shear strength, and decreased ultimate deflections.

- The combination of stirrups and steel fibers demonstrates a positive hybrid effect on the mechanical behavior, and is one of the optimal choices for improving the shear capacity.

- Test results show that plasticity, cracks propagations and load capacity of elements are greatly influenced by steel fiber volume added.

- Steel fibers work as splice, which help the matrix to exhibit less cracks, and increase the stiffness.

6.2.2 Effect of Shear Span-Depth Ratio on Shear Strength of HSC Beams:

The shear span to depth a/d ratio has a strong influence on the shear strength of HSRC beams like NSRC beams.

- The shear strength decreases with the increase of a/d values for the same longitudinal steel.

- The increase in shear span ratio increases the number of cracks formed and as result more cantilever force applied at the cracked concrete, reducing the shear strength of concrete to greater extent.

- In general, by change ratio of a/d from 1.5 to 2.2 the failure load decreased by 21 percent at the same fiber content 0, 0.25 percent, by comparing between the strength for span to depth ratio 1.5 and 2.2 it found that, the shear strength in a/d=1.5 is more than that in a/d=2.2 because of arch action performed on lower shear span ratio.

- From studding, the effect of span to depth ratio on the shear failure and using discrete steel fiber it was found that, by increasing span to depth ratio the efficiency of used discrete steel fiber decreased.

From the discussion presented in Chapter 5, the following conclusions are drawn:

- The experimental variations in *a/d,* and v_f were performed in order to validate the proposed equation. It is seen that the equation offer very satisfactory predictions for these various cases. It

should, however, be noted that the model and equations do not provide good estimates for *a/d* >**(1.7).**

- The suggested equation applicable to take effect of steel fiber on shear strength of high strength concrete beams.

- The shear strength form ACI code and ECP code not take effect of fiber on strength into consideration.

- we found that differences of experimental values and predicted values from ACI and ECP codes up to 64% and 71% respectively, but the suggested equation given mean values up to 14% and the equation is valid for shear span ratio equal (1.7).

6.3 Recommendations for Further Study

Several areas may be identified which need further study in order for a more complete understanding of the behavior of HSFRC beams to be attained :

- The post-peak behavior of beam specimens needs to be modeled more accurately.

- More tests and studies are required towards a better understanding of the role of fibers in shear strengthening. Full-scale beam tests are also required to check the validity of the above findings and the proposed methods.

REFERENCES

1. ACI Committee 318, Building Code Requirements for Reinforced Concrete (ACI 318-06) and Commentary-ACI318RM-06, American Concrete Institute, Detroit, 2006.

2. Bickley, B.A and Mitchell, D., (2001) "A State of the Art Review of High Performance Concrete Structures built in Canada: 1990-2000" The Cement Association of Canada. Pp 122.

3. Zia .P., M. L. Leming., S. H. Ahmad, J. J. Schemmel, R. P. Elliott, and A. E. Naaman., (1993) "Mechanical Behavior of High-Performance Concretes, Volume 1: Summary Report". SHRP-C-361, Strategic Highway Research Program, National Research Council, Washington, D.C., xi, 98 pp.

4. Jose Miquel Albaine "Shear Strength of Reinforced Concrete Beams per ACI318-02 PDH course S153

5. Ritter, W. (1899). "Die bauweise hennebique". Shweizerische Bauzeitung, Vol. 33(7), pp. 59-61.

6. Kupfer,H., (1964). "Generalization of Mörsch Truss Analogy using the principles of minimum strain energy" Bulletin of Information CEB, Paris pp 44-57.

7. Collins, M.P., Mitchell, D., Adebar, P.E., and Vecchio, F.J. (1996)., "A general shear-Design method". ACI Structural Journal, Vol. 93, No. 1, January-February 1996, pp. 36-45.

8. Jose Miquel Albaine "Shear Strength of Reinforced Concrete Beams per ACI318-02 PDH course S153.

9. ASCE-ACI Committee 445 (1998). , "Recent approaches to shear design of structural concrete". Journal of Structural Engineering, v. 124, no. 12, December 1998, pp. 1375-1417.

10. National Cooperative Highway Research Program (NCHRP), Transport Research Board Washington DC-USA-2005.

11. Ritter, W. (1899). "Die bauweise hennebique". Shweizerische Bauzeitung, Vol. 33(7), pp. 59-61.

12. Kani, G.N.J. (1967). "How safe are our Large Reinforced Concrete Beams?" Proceedings of *ACI Structural journal* Vol 51.

13. Cladera.A., Mari.A.R., (2005), "Experimental study on high strength concrete beams failing in shear" *Engineering Structures (Elsevier)* Vol. 27 pp1519-1527

14. Ahmad, S. H., Khaloo, A. R. and Poveda, A., (1986). Shear Capacity of Reinforced High- Strength Concrete Beams". ACI Journal, Proceedings, Vol. 83, No 2, March-April 1986, pp. 297-305.

15. Duthlin., Dat, Carino; N.J., (1996). "Shear Design of High Strength Concrete Beams: A Review of State of the Art" Building and Fire Research laboratory NIST MD-USA.

16. Johnson,M.K and Rameriz,J.A., (1989) " Minimum Shear Reinforcement in beams with higher strength concrete" *ACI Journal* Vol86(4) Jul-Aug 1989 pp.378-382.

17. Balaguru, P. N. & Shah, S.P. (1992): *Fiber-Reinforced Cement Composites.* McGraw Hill, New York, USA, pp. 350.

18. Technical Report No. 63 (2007): *Guidance for the Design of Steel-Fibre-Reinforced Concrete*. Report of a Concrete Society Working Group. Camberley, UK.

19. Banthia, N. (2008): *Fiber Reinforced Concreye* [Online] Available at: http://www.watancon.com/technical.htm [Accessed on 25 March 2011].

20. ACI 544 (1996): *State-of-the-Art Report on Fiber Reinforced Concrete.* ACI Committee 544, Report 544.1R-96, American Concrete Institute, Detroit, USA.

21. CEN (2006): *EN 14889-1:2006 Fibres for Concrete - Part 1: Steel Fibres - Definitions, Specifications and Conformity*. Brussels, Belgium.

22. Löfgren, I. (2008): *Fibre-Reinforced Concrete for Industrial Construction - A Fracture Mechanics Approach to Material Testing and Structural Analysis*. Doctoral Thesis, Chalmers University of Technology, Department of Civil and Environmental Engineering, Structural Engineering, Göteborg, Sweden.

23. Minelli, F (2005): *Plain and Fiber Reinforced Concrete Beams under Shear Loading: Structural Behaviour and Design Aspects.* Doctoral Thesis, University of Brescia, Brescia, Italy, 429 pp.

24. Amlan, K. S. & Devdas, M. (2011): *Analysis for Shear.* [Online] Available at: http://ddenptel.thapar.edu/courses/Webcourse-contents/IITMADRAS/ Pre_Stre_Conc_Stru/pdfs/ [Accessed on 15 June 2011]

25. Cucchiara, C., La Mendola, L. & Papia, M. (2004): *Effectiveness of Stirrups and Steel Fibres as Shear Reinforcement*. Cement & Concrete Composites, Volume 26, No. 7, pp 777-786

26. Sharma, A.K. (1986): *Shear Strength of Steel Fiber Reinforced Concrete Beams*. ACI Journal, Volume 83, No. 4, pp. 624-628.

27. Batson, G., Jenkins, E. & Spatney, R. (1972): *Steel Fibers as Shear Reinforcement in Beams*. ACI Journal, Volume 69, No.10, pp. 640-644.

28. J. Son1, B. Beak1, C. Choi2* 1 Department of Sustainable Architectural Engineering, Hanyang University, Seoul, South Korea 2 Department of Architectural Engineering, Hanyang University, Seoul, South Korea * Changsik. Choi (ccs5530@hanyang.ac.kr) 'expreimental study of shear strength for ultra high performance concrete beams'

29. Divya S Nair Dr. Ruby Abraham Dr.Lovely K M,M.Tech Student Professor Professor,M A College of Engineering College of Engineering M A College of Engineering Kothamangalam Trivandrum Kothamangalam 'Shear Strength of High Strength Fibre Reinforced Concrete beams'

30. Remigijus Šalna, Gediminas Marčiukaitis *Dept of Reinforced Concrete and Masonry Structures, Vilnius Gediminas Technical University, Saulėtekio al. 11, LT-10223 Vilnius, Lithuania. E-mail: gelz@st.vtu.lt Received 23 June 2006; accepted 16 March 2007* 'THE INFLUENCE OF SHEAR SPAN RATIO ON LOAD CAPACITY OF FIBRE REINFORCED CONCRETE ELEMENTS WITH VARIOUS STEEL FIBRE VOLUMES'

31. *Lim, D.H. & Oh, B.H. (1999): Experimental and Theoretical Investigation on the Shear of Steel Fibre Reinforced Concrete Beams. Engineering Structures, Volume 21, No. 10, pp. 937-944.*

32. *Ashour, S.A., Hasanain, G.S. & Wafa, F.F. (1992): Shear Behavior of High-Strength Fiber Reinforced Concrete Beams. ACI Structural Journal Volume 89, No. 2, pp. 176-183.*

33. *Narayanan, R. & Darwish, I.Y.S. (1987): Use of Steel Fibers as Shear Reinforcement. ACI Structural Journal, Volume 84, No. 3, pp. 216-227.*

34. *Swamy, R. N., Mangat, P.S. & Rao, C. V. S. K. (1974): The Mechanics of Fiber-Reinforced in Cement Matrices. Fiber Reinforced Concrete, SP-44, American Concrete Institute, Detroit, USA, pp. 128.*

35. *Rilem TC 162-TDF (2003): Test and Design Methods for Steel Fibre Reinforced Concrete: Background and Experiences. Proceedings of the RILEM TC 162-TDF Workshop, eds. B. Schnütgen and L. Vandewalle. PRO 31, RILEM Publications S.A.R.L., Bagneaux.*

36. *EUROCODE 2 (2003): Design of Concrete Structures. European Committee for Standardization UNI-ENV 1992-1-2, Brussels, Belgium.*

37. *Shin, S.W., Oh, J.G. & Ghosh, S.K. (1994): Shear Behavior of Laboratory-Sized High Strength Concrete Beams Reinforced with Bars and Steel Fibers. Fiber Reinforced Concrete Developments and Innovations. ACI SP-142, Detroit, Michigan, pp. 181-200.*

38. *Ding, Y., You, Z. & Jalali, S. (2011): The Composite Effect of Steel Fibres and Stirrups on the Shear Behaviour of Beams Using Self-Consolidating Concrete. Engineering Structures, Volume 33, No. 1, pp. 107-117.*

39. *Lim, D.H. & Oh, B.H. (1999): Experimental and Theoretical Investigation on the Shear of Steel Fibre Reinforced Concrete Beams. Engineering Structures, Volume 21, No. 10, pp. 937-944.*

40. *Kwak, Y.K, Eberhard, M.O., Kim, W.S. & Kim, J. (2002): Shear Strength of Steel Fiber- Reinforced Concrete Beams without Stirrups. ACI Structural Journal, Volume 99, No.4, pp. 530-538.*

41. *Kearsley, E.P. & Mostert, H.F. (2004): The Effect of Fibres on the Shear Strength of Reinforced Concrete Beams. Proceedings of the Sixth RILEM Symposium on Fibre Reinforced Concrete (FRC). BEFIB 2004, Varenna, Italy. Volume 2, pp. 955-964.*

42. *British Standards Institution, Structural Use of Concrete. Part 1: Code of Practice for Design and Construction. BS8110, BSI, Milton Keynes, 1985*

43. *National Standard of the People's Republic of China. Code for Design of Concrete Structures (GB 50010–2002). China Architecture & Building Press; 2002 [in Chinese].*

44. *LI, V. C.; WARD, R.; HAMZA, A. M. Steel and Synthetic Fibres as Shear Reinforcement. ACI Material Journal, 1992, 89(5), p. 499–508.*

45. *Valle, M.O., Shear Transfer in Fiber Reinforced Concrete, M.S. Thesis, Department of Civil Engineering, Massachusetts Institute of Technology, 1991*

46. *Egyptian code of practice for design and construction of reinforced concrete structures; 2006.*

47. *Ghoniem, M, and El-Mihilmy, M ' Design of Reinforced Concrete Structures, Vol No3, PP.479,481.*

Appendix A

DESIGN OF H.S.C BEAMS

Flexure Analysis:

a) Bending moment diagram
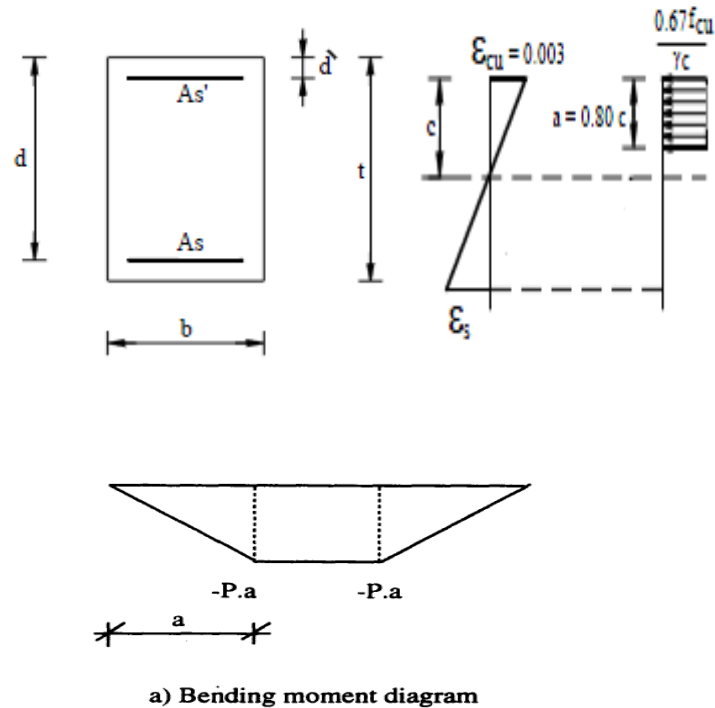
Step 1: calculation of the balanced compression zone depth c_b :

$$c_b = d.\frac{0.003}{0.003 + \varepsilon_s}$$

$\varepsilon_s = \dfrac{f_y}{E_s} = \dfrac{360}{(2*10^5)}$

$d = 225 \ mm$

We get $c_b = 140.6$ mm

Step 2: calculation of compression reinforcement stress $f_{s`}$:

$f_{s`} = E_s * \varepsilon_{s`}$

$f_{s`} = (2*10^5) * (0.003 * \frac{c-c`}{c})$

C`=15 mm

C = 1.25 a

$f_{s`} = 300 * a - 360$

Step 3: calculation of compression zone depth (c) :

At equilibrium C = T

$C_1 + C_2 = T$

0.67.* a * b+$A_{s`}$ * $f_{s`}$ = A_s* f_s

0.67 * 51 * a * 120 + (2 * 112) * (300 * a − 360) = (2 * 201) * f_s

Assume tension failure $f_s = f_y = 360\ MPa$

We get a = 20.8 mm c = 1.25*a = 26 mm

c < c_b ok (valid assumption)

Step 4: calculation of ultimate flexure moment (M_u):

$M_u = A_{s`} * f_{s`} * (d - d`) + 0.67 * f_{cu} * a * b * (d - \frac{a}{2})$

$M_u = 2 * 112 * (300 * a - 360) * (225 - 15) + 0.67 * 51 * a * 120 * (225 - \frac{a}{2})$

$M_u = 30755.6\ N.m = 30.7556$ KN.m

$M_u = P * \frac{a}{2}$ Where a (distance from load to support)

At a/d =1.5 and f_{cu} = 51 MPa

M_u =30.7556 KN.m and P = 164 KN

At a/d =1.5 and f_{cu} = 53 MPa

M_u =30.741 KN.m and P = 164.1 KN

At a/d =1.5 and f_{cu} = 55.8 MPa

M_u =32.4813 KN.m and P = 176 KN

At a/d =1.5 and f_{cu} = 68.9 MPa

M_u =36.7 KN.m and P = 195 KN

At a/d =1.7 and f_{cu} = 51 MPa

M_u =30.7556 KN.m and P = 144.9 KN

At a/d =1.7 and f_{cu} = 53 MPa

M_u =30.741 KN.m and P = 144.7 KN

At a/d =1.7 and f_{cu} = 55.8 MPa

M_u =32.4813 KN.m and P = 155 KN

At a/d =1.7 and f_{cu} = 68.9 MPa

M_u =36.7 KN.m and P = 172 KN

At a/d = 2.2 and f_{cu} = 51 MPa

M_u =30.7556 KN.m and P = 112 KN

At a/d = 2.2 and f_{cu} = 53 MPa

M_u =30.741 KN.m and P = 111.8 KN

At a/d = 2.2 and f_{cu} = 55.8 MPa

M_u =32.4813 KN.m and P = 120 KN

At a/d = 2.2 and f_{cu} = 68.9 MPa

M_u =36.7 KN.m and P = 133 KN

Shear Analysis:
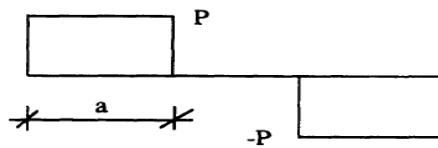
b) Shear force diagram

Step (1): Calculate the shear stress due to the ultimate shear force

$$q_u = [q_{cu} + q_{sus}] \quad \text{(N)}$$
$$q_{cu} = 0.214\sqrt{f_{cu}} \quad MPa$$
$$q_{sus} = n.\ A_{st}f_{yst}/s \quad MPa$$

Step (2): Calculate the ultimate shear load

For f_{cu}= 51 MPa

n = 2 , A_{sT} = 50.3 $mm2$, f_{yst} = 240 MPa , and S = 166.7 mm

Ultimate shear stress q_u = 293.4 MPa and ultimate shear load 103.2 KN

For f_{cu}= 53 MPa

n = 2, A_{sT} = 50.3 $mm2$, f_{yst} = 240 MPa , and S = 166.7 mm

Ultimate shear stress q_u = 293.4 MPa and ultimate shear load 104.4 KN

For f_{cu}= 55.8 MPa

n = 2 , A_{sT} = 50.3 $mm2$, f_{yst} = 240 MPa , and S = 166.7 mm

Ultimate shear stress q_u = 297.9 MPa and ultimate shear load 106 KN

For f_{cu}= 68.9 MPa

n = 2 , A_{sT} = 50.3 $mm2$, f_{yst} = 240 MPa , and S = 166.7 mm

Ultimate shear stress q_u = 317.6 MPa and ultimate shear load 113 KN

Beam no	Ultimate Flexure Load (KN)	Ultimate Shear Load (KN)
(A – 0)	164.3	103.2
(A – 1)	164	104.4
(A – 2)	176	106
(A – 3)	195	113
(B – 0)	144.9	103.2
(B – 1)	144.7	104.4
(B – 2)	155	106
(B – 3)	172	113
(C – 0)	112	103.2
(C – 1)	111.8	104.4
(C – 2)	120	106
(C – 3)	133	113

ملخص البحث

عنوان البحث

" سلوك القص للكمرات الخرسانية عالية المقاومة والمدعمة بالألياف في الخلطة الخرسانية. "

تعتبر الكمرات الرئيسية من أهم العناصر الانشائية الموجودة بالمنشأ حيث أنها تعمل على نقل الأحمال الأفقية والراسية من البلاطات والكمرات الثانوية وتتعرض لأحمال داخليه متنوعة وتعتبر احمال القص من الأحمال ذات التأثير عالي الخطورة على الكمرات حيث أنها من الممكن أن تؤدي إلى عملية انهيار قصف في الكمرات ومثل هـذا الانهيـار يسـبب كـوارث ويجـب تلافيـه وقـد ظهـرت فـي الاونـه الاخيـره مـواد تصـلح لتحسـين أداء العناصرالإنشائية ومن هذه المواد الالياف الفولاذية والتي يمكن استخدامها بإضافتها للخلطة الخرسانية أثنـاء الصب ومن هنا جاءت فكرة البحث وهي دراسة مدى تاثير إضافة الالياف الفولاذية بنسب مختلفة فـي الكمرات الخرسانية عالية المقاومة. وقد أوضحت النتائج العمليـة أنـه مـع زيادة نسب الألياف الفولاذيـة بالخلطـة تزيد مقاومة الكمرات للقص ويتغير نوع الانهيار وعدد وحجم الشروخ الناتجة وتم مقارنه النتائج بـالأكواد والدراسات السابقة.

شكر وتقدير

**HELWAN
UNIVERSITY**
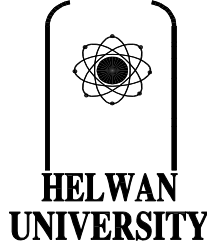
كليــة الهندســة بالمطرية
قسم الهندسة المدنية

"سلوك القص للكمرات الخرسانية المسلحة عالية المقاومة المدعمة بالألياف في الخلطة الخرسانية"

إعداد
المهندس/أحمد محمود يسري أحمد

بكالوريوس الهندسة المدنية

رسالة مقدمة كجزء من المتطلبات للحصول علي درجة الماجستير

في الهندسة المدنية

تحت إشراف

أ.م.د/ نصر زينهم حسن
أستاذ م. المنشآت الخرسانية

أ.م.د/ عطا الكريم شعيب	**أ.م.د/ مصطفي عبد المجيد عثمان**
أستاذ م.المنشآت الخرسانية	أستاذ م. المنشآت الخرسانية
كلية الهندسة بالمطرية-جامعة حلوان	كلية هندسة بالمطرية- جامعة حلوان

2014